SCIENTIFIC INNOVATION RESEARCH GROUP

Advanced Multidisciplinary Engineering Journal AMEJ

INTERNATIONAL JOURNAL

ISSN ONLINE:

ISSN PRINT:

Volume 1, November 2025

SIRG

Scientific Innovation Research Group

Advanced Multidisciplinary Engineering Journal (AMEJ)

ISSN: XXXX-XXXX

Journal Homepage

https://pub.scientificirg.com/index.php/AMEJ/en/index

Table of Contents

Published and typeset in Scientific Innovation Research Group (SIRG) is a USA academic publisher, established as an LLC company in 2025 at 2222 W. GRAND RIVER AVE STE A, Okemos, INGHAM COUNTY, MI 48864 USA. ***SIRG*** publishes online scholarly journals that are free of submission charges.

Scientific Innovation Research Group (SIRG) LLC,
Michigan, USA
Mailing Address: 2222 W. GRAND RIVER AVE STE A,
Okemos, INGHAM COUNTY, MI 48864 USA
e-mail: manager@pub.scientificirg.com
https://pub.scientificirg.com/index.php/index/en

Editorial Board

Aim and Scope

Advanced Multidisciplinary Engineering Journal (AMEJ) is an international, peer-reviewed journal dedicated to publishing high-quality research in all branches of engineering. The AMEJ provides a global platform for researchers, academics, industry experts, and innovators to present original contributions, cutting-edge advancements, and practical applications in engineering and applied sciences. The journal welcomes original research articles, review papers, short communications, and technical notes that introduce novel engineering solutions, modern methodologies, and practical implementations that address contemporary challenges in civil, mechanical, electrical, materials, chemical, industrial, environmental, and computational engineering.

As a multidisciplinary journal, the **AMEJ** serves as a global forum for researchers, engineers, scientists, and practitioners to share cutting-edge findings, emerging technologies, and impactful engineering innovations. The journal encourages submissions that bridge theory and application, promote engineering development, and contribute to sustainable and technological progress.

Researchers are welcome to submit papers to **AMEJ** after preparing them according to the SIRG template and **following the SIRG Publishing Ethics and Malpractice Statement** (See this page). **AMEJ *follows the* SIRG peer-review process in handling all submitted papers**. By submitting their paper to **AMEJ**, authors confirm their agreement to SIRG terms, conditions, and publication ethics (please check the author page) and (Copyrights page).

Topics of Interest

The AMEJ publishes high-impact research articles, review papers, case studies, technical reports, and short communications.
Topics

1) Civil & Structural Engineering
- *Concrete technology*
- *Construction materials*
- *Geotechnical engineering*
- *Transportation engineering*
- *Water resources & environmental engineering*
- *Structural analysis & design*

2) Mechanical Engineering
- *Thermofluids*
- *Heat transfer*
- *Manufacturing processes*
- *Dynamics & vibration*
- *Automotive & aerospace applications*

3) Electrical & Electronics Engineering
- *Power systems*
- *Renewable energy*
- *Control systems*
- *Electric machines*
- *Circuits, sensors & instrumentation*

4) Computer, Software & Systems Engineering
- *Algorithms & computational methods*
- *Embedded systems*
- *Networks & communication engineering*
- *Cyber-physical systems*

5) Materials & Metallurgical Engineering
- *Advanced materials*
- *Polymers & composites*
- *Nanotechnology*
- *Corrosion, failure analysis*

Advanced Multidisciplinary Engineering Journal (AMEJ)
ISSN: XXXX-XXXX

Journal Homepage:
https://pub.scientificirg.com/index.php/AMEJ/en

Cite this: AMEJ, xxxx (xx), xxx

Sustainable Ultra-High-Performance Concrete: Incorporating Nano-Eggshell Waste for Improved Strength and Durability

Sahar A. Mostafa[*1], and Ali H. AlAteah[2]

[*1] *Department of Civil Engineering, Faculty of Engineering, Beni-Suef University, Beni-Suef, Egypt,*
sahar_abdelsalam2010@yahoo.com

[2] *Department of Civil Engineering, College of Engineering, University of Hafr Al Batin, Hafr Al Batin 39524, Saudi Arabia,*
Ali.alateah@uhb.edu.sa

**Corresponding Author: sahar_abdelsalam2010@yahoo.com*

Abstract - This study examines the mechanical and microstructural properties of ultra-high-performance concrete (UHPC) incorporating nano-eggshell (NES) particles as a sustainable alternative to conventional nanofillers. Eggshell waste, consisting primarily of calcium carbonate, was processed through cleaning, calcination, and grinding to obtain nanosized particles. UHPC mixtures with varying NES contents (1-5%) were prepared and evaluated for compressive strength, splitting tensile strength, and sorptivity at different curing ages. The results indicate that the optimal NES dosage of 3% significantly enhanced the compressive strength of UHPC by 4.9%, 6.0%, and 4.5% at 7, 28, and 90 days, respectively, compared to the reference mixture. The splitting tensile strength at 28 days also improved by 16.9% with 3% NES. The sorptivity of UHPC was reduced by 28% at the optimal NES content, indicating its improved durability. XRD analysis revealed the presence of calcium carbonate and its interactions with the cementitious matrix. The performance improvements were attributed to the nanofiller effect, accelerated hydration, and microstructural refinement induced by NES particles. However, excessive NES addition beyond the optimal dosage led to slight reductions in the mechanical properties owing to agglomeration effects. The findings demonstrate the potential of nano-eggshell waste as a sustainable and performance-enhancing alternative in UHPC, contributing to the development of eco-friendly construction material.

Received: *20 July 2025*
Revised: *15 September 2025*
Accepted: *28 November 2025*
Available online: *25 December 2025*

Keywords:

-Ultra-high-performance concrete
-Nano-eggshell
-Mechanical properties
-Sorptivity

DOI: https://doi.org/XXXX.XXXX

Introduction

The incorporation of nanotechnology into cement-based materials has emerged as a transformative approach in modern construction engineering, driven by the need to overcome the inherent limitations of conventional concrete materials. Despite its widespread use, traditional concrete suffers from issues such as microcracking, high porosity, weak interfacial transition zones (ITZ), and limited durability under aggressive environmental conditions [1]. Nanomaterials, typically defined as materials with at least one dimension of less than 100 nm, offer unique physicochemical properties such as extremely high specific surface area, enhanced reactivity, and superior filler capability [2]. These characteristics enable nanomaterials to interact with cement hydration processes at the molecular and nanoscale levels, leading to substantial improvements in microstructural refinement and overall performance. Numerous experimental studies have demonstrated that the inclusion of nanomaterials, such as nano-silica, nano-alumina, nano-titania, and carbon-based nanostructures, significantly enhances the compressive strength, tensile strength, and fracture toughness while reducing permeability and shrinkage [3]. The improvement mechanisms are primarily attributed to accelerated cement hydration, nucleation effects, and densification of calcium–silicate–hydrate (C–S–H) gel [4]. As a result, nano-modified concrete exhibits superior mechanical and durability properties compared to conventional mixes. These advancements have positioned nanotechnology as a key enabler of next-generation high-performance concrete, including ultra-high-performance concrete (UHPC), self-compacting concrete, and multifunctional cementitious composites. A growing body of literature confirms that nanotechnology does not merely act as an additive enhancement but fundamentally alters the hydration kinetics and microstructural evolution of cement-based systems [5].

Extensive experimental investigations have consistently reported measurable performance improvements in nanomodified concrete systems, particularly when optimal dosage and dispersion techniques are employed [6]. One of the most significant outcomes of nanomaterial incorporation is the refinement of the pore structure, characterized by a reduction in capillary porosity and a shift toward finer gel pores. Mercury intrusion porosimetry (MIP) and scanning electron microscopy (SEM) analyses showed that nanomaterials effectively filled micro- and nanoscale voids, resulting in a denser cement matrix and improved load transfer mechanisms. In terms of mechanical performance, compressive strength increases of 15–40% have been widely reported, depending on the type and concentration of the nanomaterial used. Additionally, nano-modified concretes exhibit improved early age strength owing to accelerated hydration, which is particularly beneficial for fast-track construction and precast applications. Durability-related properties, including resistance to chloride ion penetration, sulfate attack, carbonation, and freeze–thaw cycles, were also significantly enhanced [7]. This is primarily due to the reduction in permeability and stabilization of hydration products. Furthermore, nanomaterials improve the interfacial transition zone between cement paste and aggregates, which is traditionally regarded as the weakest link in concrete. By reinforcing the ITZ at the nanoscale level, crack initiation and propagation are delayed, resulting in improved fatigue and impact resistance. Collectively, these outcomes demonstrate that nanotechnology provides a systematic and scalable pathway for improving concrete performance beyond the limits achievable through conventional mix design optimization alone [8].

Ultra-high-performance concrete (UHPC) is the most advanced class of cementitious materials, characterized by compressive strengths exceeding 150 MPa, extremely low permeability, and exceptional durability [9]. The role of nanotechnology in UHPC is particularly critical, as UHPC relies heavily on optimized particle packing across multiple length scales, from macro-aggregates to nano-sized fillers [10]. Nanomaterials are essential components in achieving this multiscale densification, ensuring minimal porosity and maximum matrix homogeneity. In UHPC systems, nanomaterials contribute to enhanced hydration kinetics, increased formation of C–S–H gel, and reduced calcium hydroxide content, collectively improving chemical stability and long-term durability. Research has demonstrated that nanoscale additives can significantly improve fiber–matrix bonding in fiber-reinforced UHPC, leading to superior tensile behavior and strain-hardening characteristics [11]. Additionally, nanomaterials enhance the resistance of UHPC to extreme conditions, including high temperatures, radiation exposure, and chemical attacks, making it suitable for critical infrastructure, military, and nuclear applications. However, the widespread application of UHPC is often constrained by its high material costs and environmental concerns associated with its high cement content [12]. Consequently, recent research efforts have focused on identifying alternative, cost-effective, and sustainable nanomaterials that can deliver comparable performance enhancements without increasing the environmental burden. This has opened new research avenues for bio-based and waste-derived nanomaterials [13].

DOI: https://doi.org/XXXX.XXXX

Eggshell waste has gained increasing attention as an environmentally sustainable and economically viable nanomaterial for cementitious composites. Generated in vast quantities by households, food processing industries, and commercial kitchens, eggshell waste poses significant disposal challenges owing to its organic content and slow biodegradation [14]. Eggshells consist of approximately 94–97% calcium carbonate ($CaCO_3$), along with minor amounts of magnesium carbonate, calcium phosphate, and organic matter [15]. When processed through controlled cleaning, calcination, and mechanical or chemical grinding, eggshells can be transformed into nanosized calcium carbonate particles with high purity and reactivity. The nano-eggshell powder exhibited properties comparable to commercially produced nano-$CaCO_3$, including a high surface area and excellent filler capability. From a sustainability perspective, the utilization of eggshell-derived nanoparticles aligns with circular economic principles by converting agricultural waste products into high-value construction materials. Numerous studies have confirmed that eggshell powder, particularly at the nanoscale, enhances cement hydration, reduces setting time, and improves microstructural compactness. Unlike conventional fillers, nano-eggshell particles actively participate in hydration reactions, contributing to the formation of stable carboalumination phases that improve the matrix integrity [16]. These characteristics make nano-eggshells a promising alternative nanomaterial for advanced concrete systems [17].

The incorporation of nano-eggshell particles into UHPC represents a novel and promising research direction that combines high-performance engineering with sustainable-material innovation. In UHPC matrices, the nano-eggshells function through synergistic physical and chemical mechanisms. Physically, their nanoscale dimensions enhance the particle packing density, effectively filling the nanovoids and reducing the total porosity [18]. Chemically, the high-purity calcium carbonate content promotes accelerated hydration and participates in secondary reactions that stabilize the hydration products. Experimental results reported in the recent literature indicate that the partial replacement of cement or micro-fillers with nano-eggshell powder can lead to noticeable improvements in compressive strength, flexural strength, and durability indicators, particularly at early curing ages [19]. Moreover, UHPC incorporating nano-eggshells exhibited reduced water absorption and enhanced resistance to chloride ingress, which are critical parameters for a long-term service life. Importantly, the use of eggshell-derived nanoparticles reduces the carbon footprint of UHPC by lowering cement consumption and diverting waste from landfills. This dual benefit of performance enhancement and environmental sustainability positions nano-eggshell-modified UHPC as a viable material for future infrastructure applications. As research continues to optimize processing techniques, dosage levels, and dispersion methods, nano-eggshells are expected to play a significant role in the development of next-generation sustainable UHPC [20].

The research on nano-eggshell-modified UHPC is significant due to its dual contribution to enhancing material performance and promoting environmental sustainability. By incorporating eggshell-derived nanoparticles, this approach not only improves the mechanical properties of UHPC but also reduces its carbon footprint through decreased cement consumption and waste diversion from landfills. Ongoing studies focusing on optimizing processing techniques, dosage levels, and dispersion methods are crucial for maximizing these benefits. As a result, nano-eggshells are poised to play a pivotal role in advancing next-generation sustainable UHPC, making it a viable and eco-friendly option for future infrastructure development.

Experimental program

A. Raw materials

The cement was characterized in accordance with the requirements of BS EN 197-1:2011. It exhibited a specific gravity of 3.15 and a Blaine specific surface area of 3960 cm^2/g and a chemical composition shown in **Tab. 1** The initial and final setting times were 135 and 195 min, respectively. Additionally, the cement achieved compressive strength values of 24.2 MPa after 7 days and 52.5 MPa after 28 days of curing. River sand was used as sand. Comprehensive physical and chemical characterizations were conducted to evaluate the properties of the processed waste glass. Eggshells were gathered, sanitized, and finely ground using a 90 µm sieve. **Fig.1** shows XRD for nano eggshell powder

Tab. 1. Chemical composition for cement and eggshell

Chemical Component	Cement (%)	Pulverized Eggshell (%)
SiO_2	25.75	–
Al_2O_3	9.88	–
Fe_2O_3	6.2	0.12
CaO	53.2	99.18
TiO_2	0.49	–
Na_2O	0.34	–
MgO	1.15	–

DOI: https://doi.org/XXXX.XXXX

SO_3	1.59	0.08
K_2O	0.17	0.3
Others	–	0.3
Loss on ignition (L.O.I)	1.23	0.02

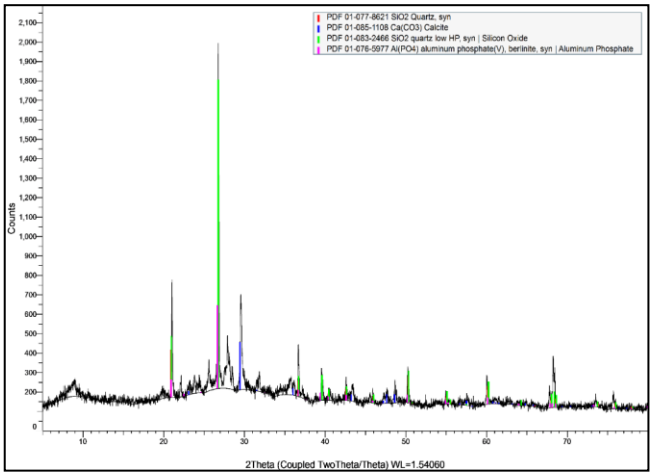

Fig.1. XRD for nano eggshell powder

B. Concrete mix design

The UHPC mixtures were designed by partially replacing cement with nano-eggshell (NES) at dosages of 0–5% by weight of cement, while maintaining constant contents of silica fume, sand, water, and superplasticizer, as summarized in **Tab. 2**. The reference mixture contained 900 kg/m³ of cement, whereas the cement content was gradually reduced with increasing NES content to ensure a constant total binder content. Silica fume was fixed at 90 kg/m³ to enhance matrix densification, and a low water-to-binder ratio was maintained to achieve the UHPC characteristics. A polycarboxylate-based superplasticizer was used at a constant dosage to ensure adequate workability for all mixtures.

Tab. 2. Mixing proportions

	Cement	NES	SF	Sand	SP	Water
Ref	900	0	90	1200	27	180
1 NES	891	9	90	1200	27	180
2 NES	882	18	90	1200	27	180
3 NES	873	27	90	1200	27	180
4 NES	864	36	90	1200	27	180
5 NES	855	45	90	1200	27	180

C. Mixing procedures

The mixing procedure was carefully controlled to ensure the homogeneous dispersion of nano-eggshell particles and prevent agglomeration. Initially, all dry constituents, including cement, silica fume, sand, and NES, were dry mixed for 2 min to achieve uniform distribution. Subsequently, approximately half of the mixing water was gradually added and mixed for 3 min to initiate hydration and improve the particle wetting.

The remaining water, which contained the dissolved superplasticizer, was then introduced, and mixing continued for an additional 5 min until a homogeneous and highly flowable UHPC mixture was obtained. Following mixing, the fresh UHPC was cast into steel molds in two layers with adequate compaction, covered to prevent moisture loss, and demolded after 24 h before curing under standard laboratory conditions until the designated testing ages [21].

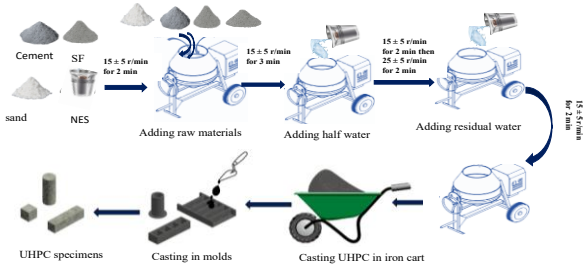

Fig. 2. Mixing procedures

D. Testing

The experimental program involved mechanical properties of compressive strength, splitting tensile strength, and sorptivity at different curing ages were tested in addition to XRD.

Results and discussion

A. Compressive strength

At the early curing age of 7 days, the reference UHPC mixture exhibited a compressive strength of 118.67 MPa. The incorporation of nano-eggshell (NES) resulted in a measurable enhancement in early age strength, with values increasing to 122.00, 123.91, and 124.54 MPa for the 1%, 2%, and 3% NES mixtures, respectively. These results correspond to strength improvements of approximately 2.8%, 4.4%, and 4.9% compared to the control mix, respectively. The

DOI: https://doi.org/XXXX.XXXX

enhancement in early-age compressive strength can be primarily attributed to the nucleation and nanofiller effects of NES particles, which accelerate cement hydration and improve the packing density within the UHPC matrix. However, further increasing the NES content to 4% and 5% led to a slight reduction in strength, indicating that excessive nano-eggshell content may hinder effective particle dispersion at early ages, as shown in **Fig. 3.**

At 28 days of curing, the reference mixture achieved a compressive strength of 137.67 MPa, whereas the UHPC mixtures containing NES demonstrated superior performance. The compressive strength increased to 141.44, 145.10, and 145.97 MPa for the 1%, 2%, and 3% NES mixtures, corresponding to improvements of approximately 2.7%, 5.4%, and 6.0%, respectively. This pronounced enhancement at the intermediate curing age suggests that NES contributes not only as a physical filler but also as a chemically active material. The calcium-rich nature of the nano eggshell particles facilitates additional hydration and promotes the formation of a denser C–S–H network, leading to reduced porosity and improved load-transfer capability [14]. Beyond the optimal dosage, the 4% and 5% NES mixtures exhibited marginally lower strength values, likely because of nanoparticle agglomeration and localized heterogeneity within the cementitious matrix [19].

At the later curing age of 90 d, the reference UHPC mixture reached a compressive strength of 149.48 MPa. The continued incorporation of NES resulted in sustained strength enhancement, with the 3% NES mixture attaining the highest value of 156.22 MPa, representing an increase of approximately 4.5% compared to the control. The strength gains observed at this stage reflect the long-term contribution of NES to microstructural refinement, including continued hydration, pore structure densification, and improved interfacial bonding within the UHPC matrix [22]. Nevertheless, UHPC mixtures containing higher NES contents (4% and 5%) showed a slight decline in compressive strength compared to the optimal mix, suggesting that excessive nano-eggshell addition may limit the long-term performance owing to agglomeration effects and reduced hydration efficiency. Overall, the results confirmed that an optimal NES dosage exists at which the UHPC exhibits enhanced compressive performance across all curing ages [23].

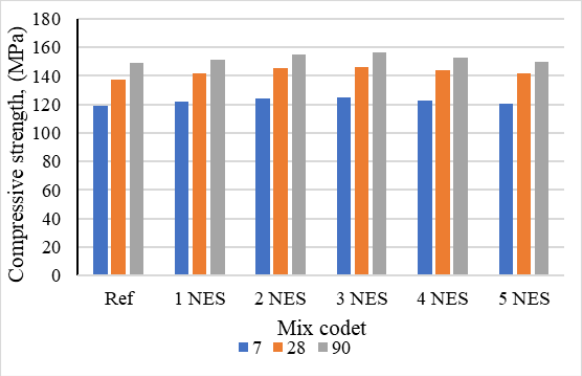

Fig. 3. Compressive strength of UHPC

b. ***Splitting tensile strength***

The splitting tensile strength results of the UHPC mixtures incorporating nano-eggshell (NES) at 28 d are presented in **Fig. 4.** The reference mixture exhibited a splitting tensile strength of 13.6 MPa. The incorporation of NES resulted in a notable improvement in tensile performance, with strength values increasing to 14.7, 15.4, and 15.9 MPa for the 1%, 2%, and 3% NES mixtures, respectively. These values correspond to enhancements of approximately 8.1%, 13.2%, and 16.9% compared with the control mix. The improvement in the splitting tensile strength can be attributed to the nanofiller and crack-bridging effects of the NES particles, which enhance matrix densification and improve stress transfer across microcracks. In addition, the calcium-rich composition of the nano-eggshell promotes improved interfacial bonding within the cementitious matrix, contributing to higher resistance to tensile cracking [24]. However, further increasing the NES content to 4% and 5% resulted in a slight reduction in splitting tensile strength to 14.7 and 15.1 MPa, respectively, although these values were higher than those of the reference mixture. This reduction is likely associated with nanoparticle agglomeration and reduced dispersion efficiency at higher dosages [25], which may introduce localized weak zones and limit the tensile performance. Overall, the results indicate that an optimal NES content of approximately 3% maximized the splitting tensile strength of UHPC at 28 days.

DOI: https://doi.org/XXXX.XXXX

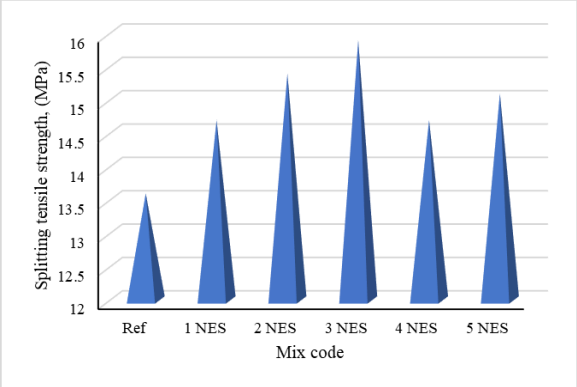

Fig. 4. Splitting tensile strength of UHPC

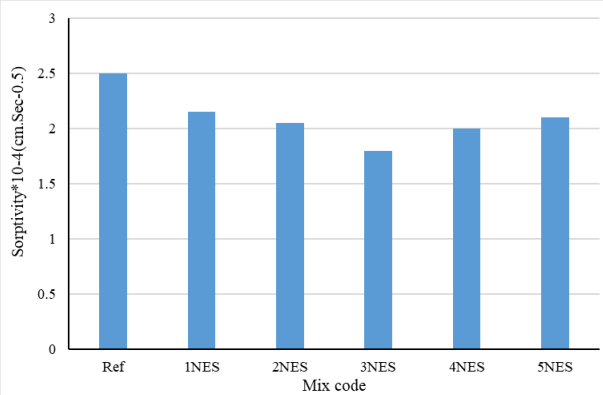

Fig. 5. Sorptivity of UHPC

C. Sorptivity

The sorptivity results of the UHPC mixtures incorporating nano-eggshell (NES) are presented in **Fig. 5**. The reference mixture exhibited a sorptivity value of 2.5 × 10^{-4} cm·$s^{-0.5}$, indicating a relatively high rate of capillary water absorption. The incorporation of NES resulted in a clear reduction in sorptivity, reflecting an improvement in the durability-related performance of the UHPC. The sorptivity values decreased to 2.15, 2.05, and 1.80 × 10^{-4} cm·$s^{-0.5}$ for the 1%, 2%, and 3% NES mixtures, corresponding to reductions of approximately 14.0%, 18.0%, and 28.0%, respectively, compared to the reference mixture. This significant reduction can be attributed to the nanofiller effect of NES, which enhances the particle packing density, refines the pore structure, and reduces the connectivity of capillary pores within the UHPC matrix. In addition, the calcium-rich composition of the nano-eggshell particles promotes the formation of additional hydration products, leading to a denser and less permeable microstructure [26]. However, further increasing the NES content beyond the optimal level resulted in a slight increase in the sorptivity values to 2.0 and 2.1 × 10^{-4} cm·$s^{-0.5}$ for the 4% and 5% NES mixtures, respectively. This behavior is likely associated with nanoparticle agglomeration at higher dosages, which may introduce microstructural heterogeneity and partially offset the beneficial pore-refining effects [27]. Overall, the results demonstrate that an optimal NES dosage of approximately 3% is effective in minimizing sorptivity and enhancing the resistance of UHPC to capillary-water ingress.

D. XRD analysis

XRD analysis was performed on six samples as the control mix and five mixes in the cases of 1, 2, 3, 4, and 5 % replacement of cement with eggshells. The XRD patterns of Series I at 91 days are shown in **Fig. 6**. Ultra-High-Performance Concrete (UHPC) undergoes X-ray Diffraction (XD) exhibits unique diffraction patterns corresponding to the crystalline phases found in the composite when subjected to X-ray Diffraction (XRD) examination. When UHPC is mixed with eggshell powder, the main crystalline phases typically consist of calcium carbonate (CaCO3) from the eggshell and different phases related to cementitious materials in the concrete matrix, such as calcium silicate hydrate (C-S-H) and calcium hydroxide ($Ca(OH)_2$). X-ray diffraction patterns exhibit distinct diffraction peaks at precise angles corresponding to the atomic arrangement within the crystal lattice. The positions and intensities of these peaks provide valuable insights into the composition and crystallinity of the present phases. The presence of these peaks in the UHPC composition that includes eggshell powder signifies the existence of CaCO3 and any possible chemical interplay between the eggshell and cementitious constituents [8,28]. By evaluating the XD patterns for different dosages, such as 1%, 2%, 3%, 4%, and 5% eggshell powder, the impact of varying dosage levels on the crystalline phases and peaks can be assessed [29]. In addition, an increase in dosage can result in more prominent $CaCO_3$ diffraction peaks, indicating a greater amount of eggshell-derived material in the UHPC. However, a

decrease in the highest intensity or changes in the placement of the highest levels may indicate possible interactions or phase changes within the crystalline structure of UHPC.

DOI: https://doi.org/XXXX.XXXX

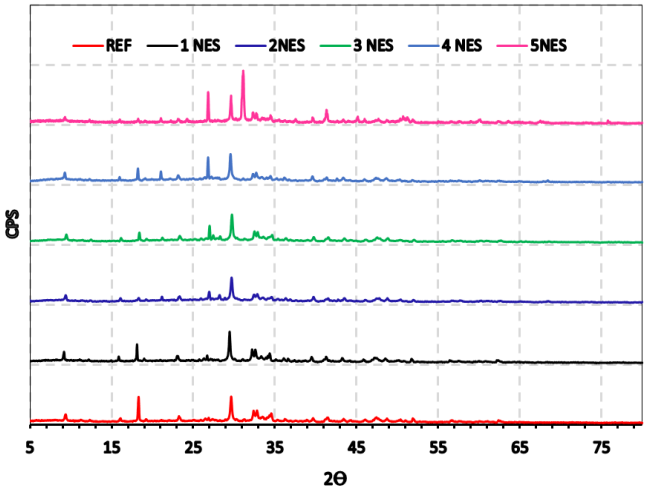

Fig. 6. XRD patterns of UHPC

Conclusions

Incorporating nano-eggshell (NES) particles into UHPC enhances its mechanical and durability performance, with an optimal dosage of approximately 3%. At 3% NES, the compressive strength improved by 4.9%, 6.0%, and 4.5% at 7, 28, and 90 days, respectively, compared to the reference mix. The splitting tensile strength at 28 days increased by 16.9% with 3% NES incorporation. Sorptivity was reduced by 28% at the optimal NES content, indicating improved resistance to capillary water absorption and enhanced durability of the bricks. XRD analysis confirmed the presence of calcium carbonate in NES and its interaction with the cementitious matrix, contributing to microstructural refinement. The performance improvements are attributed to the nanofiller effect, accelerated hydration, and improved particle packing induced by NES particles. Excessive NES content beyond 3% led to slight reductions in mechanical properties and durability, likely due to nanoparticle agglomeration and a reduced dispersion efficiency. Utilizing nano-eggshell waste in UHPC offers a sustainable and eco-friendly alternative to conventional nano-fillers, contributing to waste valorization and reduced environmental impact.

References

[1] S. Zhao, W. Sun, Nano-mechanical behavior of a green ultra-high performance concrete, Construction and Building Materials 63 (2014) 150-160.
[2] M. Heikal, H.A. Abdel-Gawwad, F.A. Ababneh, Positive impact performance of hybrid effect of nano-clay and silica nano-particles on composite cements, Construction and Building Materials 190 (2018) 508-516.
[3] Z. Wu, C. Shi, K.H. Khayat, L. Xie, Effect of SCM and nano-particles on static and dynamic mechanical properties of UHPC, Construction and Building Materials 182 (2018) 118-125.
[4] G. Xiaoyu, F. Yingfang, L. Haiyang, The compressive behavior of cement mortar with the addition of nano metakaolin, Nanomaterials and Nanotechnology 8 (2018) 184798041875559.
[5] G.F. Huseien, K.W. Shah, A.R.M. Sam, Sustainability of nanomaterials based self-healing concrete: An all-inclusive insight, Journal of Building Engineering 23 (2019) 155-171.
[6] P. Zhang, J. Wan, K. Wang, Q. Li, Influence of nano-SiO 2 on properties of fresh and hardened high performance concrete: A state-of-the-art review, Construction and Building Materials 148 (2017) 648-658.
[7] M. Eltaher, M. Khater, S. Park, E. Abdel-Rahman, M.J.A.i.n.r. Yavuz, On the static stability of nonlocal nanobeams using higher-order beam theories, 4(1) (2016) 51.
[8] S.A. Mostafa, A.S. Faried, A.A. Farghali, M.M. El-Deeb, T.A. Tawfik, S. Majer, M. Abd Elrahman, Influence of Nanoparticles from Waste Materials on Mechanical Properties, Durability and Microstructure of UHPC, Materials (Basel) 13(20) (2020).
[9] S.A. Mostafa, I.N. Fathy, A.A. Mahmoud, M.A. Abouelnour, K. Mahmoud, S.M. Shaaban, S.A. Elhameed, I.M.J.A.o.N.E. Nabil, Optimization of UHPC with basil plant ash: Impacts on strength, durability, and gamma-ray attenuation, 226 (2026) 111825.
[10] Z. Wang, X. Nie, J.-S. Fan, X.-Y. Lu, R. Ding, Experimental and numerical investigation of the interfacial properties of non-steam-cured UHPC-steel composite beams, Construction and Building Materials 195 (2019) 323-339.
[11] E. Ghafari, H. Costa, E. Júlio, Statistical mixture design approach for eco-efficient UHPC, Cement and Concrete Composites 55 (2015) 17-25.
[12] K. Liu, R. Yu, Z. Shui, X. Li, C. Guo, B. Yu, S. Wu, Optimization of autogenous shrinkage and microstructure for Ultra-High Performance Concrete (UHPC) based on appropriate application of porous pumice, Construction and Building Materials 214 (2019) 369-381.
[13] M. Ozawa, S. Subedi Parajuli, Y. Uchida, B. Zhou, Preventive effects of polypropylene and jute fibers on spalling of UHPC at high temperatures in combination

DOI: https://doi.org/XXXX.XXXX

with waste porous ceramic fine aggregate as an internal curing material, Construction and Building Materials 206 (2019) 219-225.

[14] Y. Zhang, Q. Zhang, A.H. AlAteah, A. Essam, S.A.J.C.S.i.C.M. Mostafa, Predictive modeling for mechanical characteristics of ultra high-performance concrete blended with eggshell powder and nano silica utilizing traditional technique and machine learning algorithm, 21 (2024) e04025.

[15] P. Murthi, V. Lavanya, K. Poongodi, Effect of eggshell powder on structural and durability properties of high strength green concrete for sustainability: A critical review, Materials Today: Proceedings (2022).

[16] R. Othman, B.W. Chong, R.P. Jaya, M.R. Mohd Hasan, M.M. Al Bakri Abdullah, M.H. Wan Ibrahim, Evaluation on the rheological and mechanical properties of concrete incorporating eggshell with tire powder, Journal of Materials Research and Technology 14 (2021) 439-451.

[17] Z. Quanwei, C. Qi, A.H. AlAteah, A.M. Alfares, S. Alinsaif, S.A.J.R.o.A.M.S. Mostafa, AI-based prediction for the strength, cost, and sustainability of eggshell and date palm ash-blended concrete, 64(1) (2025) 20250113.

[18] L.P. Singh, S.R. Karade, S.K. Bhattacharyya, M.M. Yousuf, S. Ahalawat, Beneficial role of nanosilica in cement based materials – A review, Construction and Building Materials 47 (2013) 1069-1077.

[19] H.K. Tchakouté, D.E. Tchinda Mabah, C. Henning Rüscher, E. Kamseu, F. Andreola, M.C. Bignozzi, C. Leonelli, Preparation of low-cost nano and microcomposites from chicken eggshell, nano-silica and rice husk ash and their utilisations as additives for producing geopolymer cements, Journal of Asian Ceramic Societies 8(1) (2020) 149-161.

[20] A.S. Aadi, N.H. Sor, A.A. Mohammed, The behavior of eco-friendly self – compacting concrete partially utilized ultra-fine eggshell powder waste, Journal of Physics: Conference Series 1973(1) (2021).

[21] Y. Zhu, H. Hussein, A. Kumar, G. Chen, A review: Material and structural properties of UHPC at elevated temperatures or fire conditions, Cement and Concrete Composites 123 (2021).

[22] J.L. García Calvo, G. Pérez, P. Carballosa, E. Erkizia, J.J. Gaitero, A. Guerrero, Development of ultra-high performance concretes with self-healing micro/nano-additions, Construction and Building Materials 138 (2017) 306-315.

[23] A.a.R. Al-Shamasneh, A. Mahmoodzadeh, M. Kewalramani, A. Alghamdi, J. Alnahas, M. Sulaiman, N. Ghazouani, I.J.S.R. Albaijan, Hybrid machine learning models for predicting the tensile strength of reinforced concrete incorporating nano-engineered and sustainable supplementary cementitious materials, 15(1) (2025) 35805.

[24] J. Xie, H. Zhang, L. Duan, Y. Yang, J. Yan, D. Shan, X. Liu, J. Pang, Y. Chen, X. Li, Y. Zhang,Effect of nano metakaolin on compressive strength of recycled concrete, Construction and Building Materials 256 (2020) 119393.

[25] A. Adesina, Durability Enhancement of Concrete Using Nanomaterials: An Overview, Materials Science Forum 967 (2019) 221-227.

[26] H. Du, S. Du, X. Liu, Durability performances of concrete with nano-silica, Construction and Building Materials 73 (2014) 705-712.

[27] H. Wu, J. Gao, C. Liu, Y. Zhao, S.J.J.o.B.E. Li, Development of nano-silica modification to enhance the micro-macro properties of cement-based materials with recycled clay brick powder, 86 (2024) 108854.

[28] W. Yonggui, L. Shuaipeng, P. Hughes, F. Yuhui, Mechanical properties and microstructure of basalt fibre and nano-silica reinforced recycled concrete after exposure to elevated temperatures, Construction and Building Materials 247 (2020) 118561.

[29] K. Nandhini, J. Karthikeyan, Sustainable and greener concrete production by utilizing waste eggshell powder as cementitious material – A review, Construction and Building Materials 335 (2022).

DOI: https://doi.org/XXXX.XXXX

Advanced Multidisciplinary Engineering Journal (AMEJ)
ISSN: XXXX-XXXX

Journal Homepage:
https://pub.scientificirg.com/index.php/AMEJ/en

Cite this: AMEJ, xxxx (xx), xxx

Optimizing Pelargonium Ash as a Partial Cement Replacement in High-Strength Self-Compacting Concrete: Mechanical and Durability Aspects

Sahar A. Mostafa[*1], and Mahmoud S. Hammad[2]

[*1]*Department of Civil Engineering, Faculty of Engineering, Beni-Suef University, Beni-Suef, Egypt,* sahar_abdelsalam2010@yahoo.com

[2]*Department of Civil Engineering, Faculty of Engineering, Beni-Suef University, Beni-Suef, Egypt.* mahmoud011312@eng.bsu.edu.eg

**Corresponding Author:* sahar_abdelsalam2010@yahoo.com

Abstract - This study investigates the effects of Pelargonium Ash (PGA) as a partial cement replacement on the mechanical and durability properties of High Strength-Self Compacting Concrete (HSSCC). PGA was incorporated at 5%, 10%, 15%, and 20% replacement levels, and its influence on setting time, compressive strength, splitting tensile strength, and resistance to sulfate and chloride attacks was evaluated. The results indicate that a 5% PGA replacement is optimal, leading to slight improvements in compressive strength at early and late curing ages without compromising self-compacting properties. Higher replacement levels (10%, 15%, 20%) adversely affect mechanical performance and durability due to rapid hardening, increased water absorption, and dilution of cementitious components. The 5% PGA mix exhibited enhanced resistance to sulfate and chloride attacks, attributed to pore refinement and pozzolanic activity. However, excessive PGA content beyond 10% negatively impacts durability and mechanical properties. Adjustments in water and superplasticizer dosages are necessary at higher PGA levels to maintain workability. In conclusion, PGA can be effectively used as a sustainable partial cement replacement in HSSCC at an optimal level of 5-10%, balancing mechanical performance, durability, and environmental benefits.

Received: 18 June 2025
Revised: 30
Accepted:
Available online:

Keywords:

-Pelargonium Ash
-High Strength-Self Compacting Concrete
-Mechanical properties
-durability

DOI: https://doi.org/XXXX.XXXX

Introduction

The current global trend toward resource conservation is primarily focused on the development of new technologies and the enhancement of existing ones, particularly through the utilization of industrial by-products and recyclable materials [1–3]. This approach is especially significant in the construction sector, where such materials can be effectively incorporated into composite building materials and concrete production [4–6]. Consequently, the cement industry has become one of the major contributors to greenhouse gas emissions, ranking after the energy and transportation sectors, with emissions ranging between 5% and 8%, mainly due to the combustion of Portland cement clinker [7–9]. Recent statistics indicate that the annual global cement production exceeds 4 billion tons, which is associated with carbon emissions exceeding 4 billion tons per year [10–11]. Furthermore, cement manufacturing has significantly increased atmospheric carbon dioxide concentrations, reaching approximately 380 ppm, with projections estimating an increase to nearly 800 ppm by the year 2100 [12]. The rapid growth in infrastructure demand has further intensified cement consumption, leading to excessive waste disposal in limited landfill areas and, consequently, increased greenhouse gas emissions [13–14]. It has been estimated that the production of one ton of cement releases approximately 800 kg of CO_2 into the atmosphere.

SCC performance is considered satisfactory when specific workability and flowability parameters comply with established SCC guidelines. Typically, SCC contains a relatively high cement content, reduced coarse aggregate (CA) content, and superplasticizers (SP) to lower the water-to-binder ratio, with a common CA-to-fine aggregate (FA) ratio of 1:1. The water-to-binder (W/B) ratio and SP dosage are optimized through mortar and concrete flow tests, followed by trial mixes to finalize the concrete composition.

Compared to conventional concrete, SCC offers several advantages, including the elimination of vibration during placement, enhanced flowability, superior workability and pumpability, and improved bonding in areas with congested reinforcement. SCC is produced using conventional concrete ingredients; however, stricter control over mix proportions is required to ensure stable fresh properties. A typical SCC mixture demands a high powder content, reduced coarse aggregate proportion, high-range superplasticizers, and viscosity-modifying agents to maintain stability and prevent segregation [15-16].

Agricultural waste (AW) has emerged as a promising sustainable material for partial replacement of cement in concrete production, addressing both environmental and economic challenges associated with conventional cement use. Large quantities of biomass ashes are generated globally, especially in developing countries. These wastes, when properly processed and ground to suitable fineness, exhibit high silica content (often exceeding 60%), which imparts pozzolanic properties beneficial for cementitious applications [17]. Utilizing AW ashes in concrete not only reduces the environmental burden of waste disposal but also mitigates the substantial CO_2 emissions linked to cement manufacturing, which accounts for 5–8% of global greenhouse gases. Incorporation of these ashes refines the microstructure of concrete, enhancing mechanical strength and durability. Studies have shown that AW ashes improve resistance to sulfate and chloride attacks, freeze-thaw cycles, and reduce porosity, thereby extending the lifespan of concrete structures. However, the effectiveness of AW ashes depends on their chemical composition, fineness, and optimal replacement levels, as excessive substitution can lead to dilution of cementitious components, adversely affecting workability and mechanical performance [18].

High Strength Self-Compacting Concrete (HSSCC) combines the benefits of high-strength concrete with the unique flowability and self-compacting properties of self-compacting concrete (SCC), offering significant advantages in modern construction. HSSCC eliminates the need for mechanical vibration during placement, which reduces labor costs, noise pollution, and the risk of improper compaction, thereby ensuring uniform density and minimizing voids [19-20]. Its superior flowability allows it to fill complex and heavily reinforced formwork efficiently, improving the quality and homogeneity of the concrete matrix. The high powder content, low water-to-binder ratio, and use of superplasticizers in HSSCC contribute to enhanced early-age strength, accelerated curing, and improved bonding between cement paste and aggregates. These characteristics enable faster construction timelines and earlier demolding of structural elements, which is particularly beneficial in projects with tight schedules or complex geometries. Moreover, HSSCC exhibits improved durability properties, including resistance to segregation, bleeding, and permeability, which enhances its performance against chemical attacks such as sulfate and chloride ingress [21]. The dense microstructure of HSSCC reduces porosity and refines the pore network, leading to increased resistance to environmental degradation and longer service life. Additionally, the improved surface finish achievable with HSSCC reduces the need for secondary treatments, lowering maintenance requirements and lifecycle costs. Its adaptability to incorporate supplementary cementitious materials and industrial by-products further enhances sustainability by reducing cement consumption and associated CO_2 emissions [22]. Overall, HSSCC represents a technologically advanced concrete type that optimizes mechanical performance, durability, and constructability, making it highly suitable for demanding structural applications and sustainable construction practices [23].

SCC enables faster concrete placement and construction timelines, particularly in complex structural elements. Its high fluidity and resistance to segregation contribute to improved homogeneity, reduced void content, and uniform strength

DOI: https://doi.org/XXXX.XXXX

distribution, which collectively enhance surface finish and durability. Additionally, SCC is often designed with a low water–cement ratio, allowing for higher early-age strength, accelerated demolding, and earlier utilization of structural elements. The incorporation of fine alternative materials alters certain concrete properties due to their chemical reactivity, which is a key aspect investigated in this study. From both economic and environmental perspectives, reducing cement consumption through the use of fine pozzolanic materials is strongly recommended [24]. Consequently, significant attention has been directed toward replacing cement with supplementary cementitious materials that enhance microstructure and improve durability and corrosion resistance [25-26]. The inclusion of materials such as silica fume (SF), metakaolin (MK), and fly ash (FA) has been shown to improve mechanical performance and resistance to freeze–thaw cycles compared to conventional concrete [27–28.

On the other hand, substantial quantities of industrial and agricultural waste are generated worldwide, particularly in developing countries. Agricultural waste (AW) ashes represent a promising alternative to conventional cement when properly processed and utilized [29]. It has been reported that rice and palm oil industries alone generate approximately 156 and 184 million tons of rice husk and palm oil residues annually, respectively [30]. Agricultural wastes such as rice straw ash (RSA), rice husk ash (RHA), and sugarcane bagasse ash (SCBA) are commonly used as biomass fuels in power plants; however, the disposal of the resulting ash poses serious environmental challenges. Therefore, incorporating these ashes into concrete production provides an effective strategy for waste management while simultaneously reducing cement consumption [31].

The high silica content (exceeding 60%) present in ashes such as palm leaf ash (PLA), palm oil fuel ash (POFA), RHA, and SCBA facilitates their application as pozzolanic materials once ground to suitable fineness [32]. Numerous studies have demonstrated that the use of agricultural waste ashes enhances the mechanical and durability properties of concrete by refining the microstructure through pozzolanic reactions. Overall, the partial replacement of cement with agricultural waste materials not only improves concrete performance but also significantly mitigates environmental issues related to waste disposal and CO_2 emissions from cement production. The use of such materials aligns with the principles of green and sustainable concrete. While some agricultural waste materials have yielded promising results, others require further investigation to determine their optimal utilization [33].

In this study, (HSSC) was investigated to evaluate the effect of Pelargonium Ash (PGA) as a partial cement replacement. The research aims to assess the influence of PGA on both fresh and hardened properties of HSSC. Mechanical properties, including compressive strength, splitting tensile strength, and flexural strength, were examined. Additionally, the performance of concrete exposed to sulfate and chloride attack conditions. This study seeks to expand the understanding of agricultural waste utilization in concrete and to identify the potential of PGA as a sustainable pozzolanic material for high-performance concrete applications.

Experimental program

Raw materials

Ordinary Portland cement (OPC) of type CEM I 52.5 N, conforming to the requirements of BS EN 197-1:2011, was used as the primary binder in this experimental investigation. The cement exhibited a specific gravity of 3.14, a specific surface area of 3450 cm^2/g, and a grey color, with its detailed chemical composition presented in Table 1. Silica fume (SF), supplied by Sika Egypt Company, was incorporated as a mineral admixture based on the cement mass. The utilized SF possessed a high specific surface area of 16.8×10^3 m^2/kg and a specific gravity of 2.15, and complied with ASTM C1240, indicating its highly siliceous nature; its physical properties and chemical composition are listed in Table 2. Dolomite aggregate was used as coarse aggregate in a saturated surface-dry condition, with a maximum particle size of 12.5 mm, specific gravity of 2.65–2.70, and water absorption of approximately 0.6–1.0%. Natural sand was employed as fine aggregate, characterized by a maximum particle size of 2.36–4.75 mm, specific gravity of 2.6–2.81, and water absorption of about 0.65%, with grading and physical properties. To achieve the required workability of SCC, a polycarboxylate-based superplasticizer (Sika ViscoCrete-3425) was utilized in accordance with ASTM C494/C494M-17. This admixture, with a density of 1.08 kg/L and a pH value of 8.0 ± 1.0, is suitable for concrete mixtures requiring high flowability and early strength development and was dosed as a percentage of the total binder content. Pelargonium waste was collected from an agricultural farm in the Beni-Suef region, Egypt, and initially burned in open air as shown in **Fig. 1.** The resulting ash was carefully cleaned to remove impurities, then calcined in a furnace at 700 °C for 2 h, followed by cooling at room temperature for 1 h. The ash was subsequently ground, and particles passing through a 75 µm sieve were used in this study. The processed Pelargonium ash satisfied the requirements of BS 3892: Part 1–1997 and relevant ASTM standards. Visual inspection and SEM analysis revealed that the Pelargonium ash particles were irregular in shape, predominantly micro-sized, and exhibited a morphology suitable for pozzolanic applications

DOI: https://doi.org/XXXX.XXXX

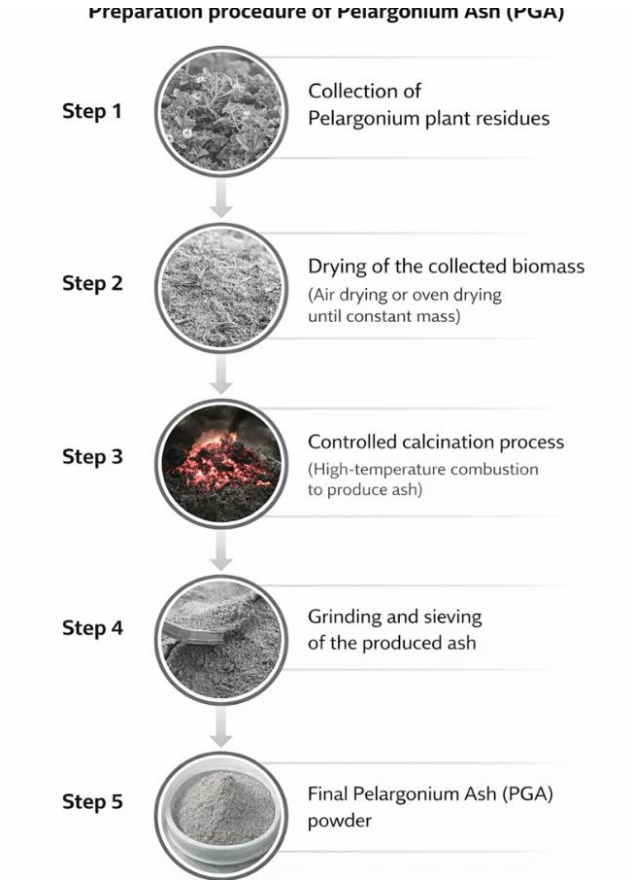

Fig. 1. Preparation steps

A. Concrete mix design

Mix proportions:

Make six (5) concrete mixes in total. In reference mix 1, the percentage of PGA was 0%. The remaining five mixes were created by partially substituting 5%,10%, 15%, and 20% of cement with PGA. **Tab. 1** represents mixing proportions

Tab. 1. Mixing proportions

Mix	PGA %	OPC Kg/m³	PGA Kg/m³	SF Kg/m³	CA Kg/m³	FA Kg/m³	Water g/m³	SP %	Water increasing	SP increasing %
HC0	0	550	-	27.5	762	762	184.8	1.25	-	-
HC5	5	550	27.5	27.5	762	762	184.8	1.25	-	-
HC10	10	550	55	27.5	762	762	184.8	1.25	0.33+0.03	-
HC15	15	550	82.5	27.5	762	762	184.8	1.25	0.33+0.04	0.1%
HC20	20	550	110	27.5	762	762	184.8	1.25	0.33+0.05	0.15%

B. Testing

The setting time of concrete was determined using the penetration resistance test in accordance with ASTM C403, which measures the initial and final setting times based on the penetration resistance of mortar sieved from fresh concrete with non-zero slump. Mechanical properties were evaluated through compressive, tensile, and elastic modulus tests. Compressive strength was measured on 100 × 100 × 100 mm cube specimens at curing ages of 7, 28, and 56 days following BS EN 12390-3, using a universal compression testing machine shown in **Fig. 2,** with the average value obtained from two specimens at each age. The modulus of elasticity in compression was determined in accordance with NS 3676, based on ISO 6784-1982, using 100 × 200 mm cylindrical specimens subjected to a controlled multi-cycle loading–unloading regime shown in **Fig. 3** with deformations recorded over a 120 mm gauge length using displacement transducers. Splitting tensile strength was assessed at 28 days on cylindrical specimens (100 mm diameter × 200 mm height) using the indirect tensile splitting method, where the tensile strength was calculated from the applied failure load. Additionally, uniaxial tensile strength was determined using Hansen's method, employing specially designed grips to ensure uniform stress transfer, with deformation measured over a 100 mm mid-gauge length to calculate the tensile modulus of elasticity. Durability performance was further investigated through chloride penetration resistance using the AASHTO T259 salt ponding test, in which concrete slabs were moist-cured, conditioned, and exposed to a 3% NaCl solution for 90 days to evaluate chloride ingress behavior.

DOI: https://doi.org/XXXX.XXXX

Fig. 2. Compressive strength

Fig. 3 Split tensile strength

Results and discussion

a. Setting

A test was conducted to demonstrate the problems encountered during mixing and casting. The objective of the test was to determine the water absorption percentage of a mixture. The VICAT apparatus was used to measure the initial and final setting times of the mixture. Firstly, the standard water-to-cement ratio (w/c) for Ordinary Portland Cement (OPC) without (PGA) was determined. The w/c ratio was 0.33, which means 128ml of water was used for every 400gm of cement. The initial and final setting times of the control mixture were then determined. Next, additional specimens were prepared with 5%, 10%, 15%, and 20% replacement of cement with PGA. The results showed that the addition of PGA reduced the initial and final setting times. Compared to the control mix, the 5% replacement resulted in a 10.31% decrease in the initial setting time and a 9.1% decrease in the final setting time. However, the 10% replacement had a more significant impact, reducing the initial and final setting times by 64% and 59.1% respectively, compared to the control mix, as shown in **Fig. 4.**

During the mixing process, it was observed that the mixture exhibited characteristics of normal concrete instead of SCC, which was at 10% replacement. Additionally, the specimens with 15% and 20% replacement did not pass the test, as their setting times decreased significantly. The initial setting time reduced from 145 minutes to 15 minutes, and the final setting time reduced from 220 minutes to 55 minutes. This indicates that the samples experienced rapid hardening due to a lack of water, which affected the setting process [34]. The inconsistent results and failure to pass the setting test indicate that the high-water absorption rate is caused by PGA. Therefore, it is necessary to increase the amount of water and plasticizer to compensate for this effect. The figure illustrates that the time interval between the final and initial setting times is shorter compared to the standard mixture. This observation aligns with the difficulties encountered during the casting process.

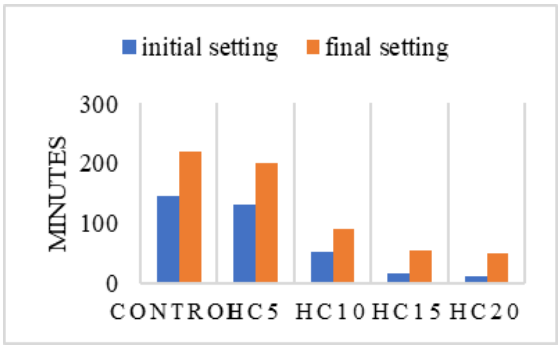

Fig.4: setting time of HSSCC

b. Compressive strength at 7 days

At the early curing age of 7 days shown in **Fig. 5** the compressive strength results clearly indicate that the incorporation of Pelargonium Ash (PGA) has a pronounced effect on the early hydration and strength development of HSSCC. The control mix (HC0) achieved a compressive strength of 49 MPa, which serves as the reference value. The addition of PGA at a low replacement level significantly enhanced early-age strength, as the HC5 mix recorded the highest compressive strength of 55.2 MPa, corresponding to an increase of approximately 12.7% compared to the control mix. This improvement can be attributed to the filler effect of fine PGA particles, which enhance particle packing density, reduce initial porosity, and promote early hydration. Similarly, the HC10 mix exhibited a compressive strength of 53.2 MPa, representing an improvement of about 8.6%, confirming that moderate PGA contents still contribute positively at early ages. However, further increases in PGA content resulted in diminished benefits, with HC15 and HC20 showing only slight increases of about 2.2% and 0.6%, respectively. This reduction in early-age performance at higher replacement levels is mainly associated with the dilution effect, where excessive replacement of cement reduces the amount of clinker phases responsible for early strength development, thereby limiting the hydration rate during the first curing period [35].

DOI: https://doi.org/XXXX.XXXX

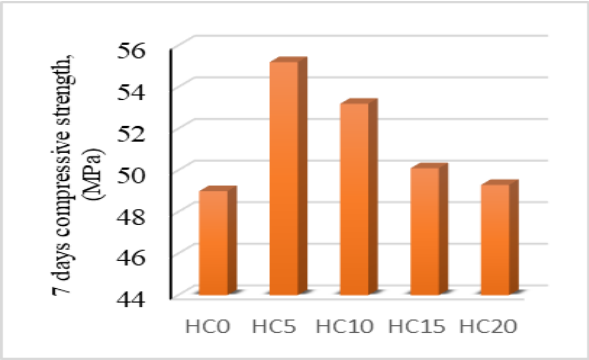

Fig. 5. 7 days compressive strength

C. Compressive strength at 28 days

At the standard curing age of 28 days shown in **Fig. 6** a more pronounced influence of PGA on compressive strength was observed, reflecting the contribution of pozzolanic reactions to the concrete matrix. The control mix (HC0) achieved a compressive strength of 50 MPa, while all PGA-modified mixes exhibited higher strength values. The HC5 mix again demonstrated superior performance, reaching 65 MPa, which corresponds to a substantial increase of approximately 30% compared to the control. This significant enhancement confirms the effectiveness of an optimized PGA content in improving the mechanical properties of concrete through secondary hydration reactions between the amorphous silica in PGA and calcium hydroxide released during cement hydration, leading to the formation of additional calcium silicate hydrate (C–S–H) gel [36-37]. The HC10 mix recorded a compressive strength of 56 MPa, showing an improvement of 12%, while HC15 and HC20 achieved values of 54 MPa and 52 MPa, corresponding to increases of 8% and 4%, respectively. Although these improvements are lower than those of HC5, they still indicate a positive contribution of PGA at moderate replacement levels. The gradual decrease in strength enhancement with increasing PGA content highlights the balance between beneficial pozzolanic activity and the adverse dilution effect associated with reduced cement content.

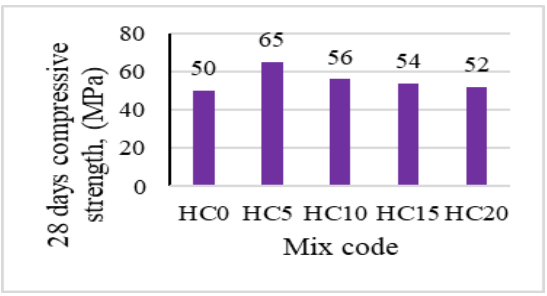

Fig. 6. 28 days' compressive strength

D. Compressive strength at 56 days

At the later curing age of 56 days shown in **Fig.7**, the compressive strength results reveal the long-term influence of PGA on strength development and durability-related performance. The control mix achieved a compressive strength of 66.5 MPa, indicating continuous hydration of cement over time. The HC5 mix maintained the highest compressive strength of 68 MPa, exceeding the control by approximately 2.3%, which confirms the sustained pozzolanic contribution of PGA at an optimal replacement level. In contrast, higher PGA contents resulted in noticeable reductions in compressive strength relative to the control mix, with HC10, HC15, and HC20 exhibiting decreases of approximately 9.8%, 12.8%, and 21.8%, respectively. Despite these reductions, it is important to note that the strength gain between 28 and 56 days for mixes containing higher PGA contents was relatively significant, indicating delayed pozzolanic activity and gradual microstructure densification at later ages. Nevertheless, the results clearly demonstrate that excessive replacement levels negatively affect long-term compressive strength due to insufficient cementitious material, despite ongoing pozzolanic reactions. Overall, the findings confirm that a PGA replacement level of 5% provides the most favorable balance between early-age strength enhancement and long-term performance, while higher replacement ratios lead to strength deterioration primarily due to cement dilution effects [38-39].

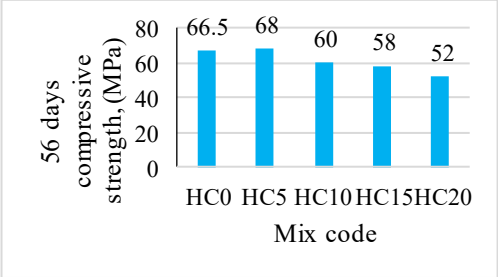

Fig. 7. 56 days compressive strength

E. Splitting tensile strength

Fig. 8 illustrates the effect of incorporating Pelargonium Ash (PGA) on the splitting tensile strength of HSSCC at the curing age of 28 days. The results clearly indicate that the addition of PGA has a noticeable influence on the tensile behavior of concrete, which is generally more sensitive to microstructural changes than compressive strength. The control mix (HC0) exhibited the highest splitting tensile strength, reaching approximately 3.52 MPa, reflecting the intact cementitious matrix and adequate bonding between the cement paste and

DOI: https://doi.org/XXXX.XXXX

aggregates. This value serves as a reference for evaluating the performance of PGA-modified mixtures.

The HC5 mixture recorded a splitting tensile strength of about 3.41 MPa, representing a slight reduction of approximately 3% compared to the control mix. This marginal decrease suggests that a low replacement level of PGA does not significantly impair the tensile performance of concrete. The slight reduction may be attributed to the partial replacement of cement with PGA, which initially reduces the availability of primary hydration products responsible for tensile resistance. However, at this replacement level, the filler effect and the gradual pozzolanic reaction of PGA may compensate for this reduction by refining the pore structure and improving the interfacial transition zone (ITZ) between the aggregates and the cement matrix [40].

In contrast, higher PGA replacement levels resulted in more pronounced reductions in splitting tensile strength. The HC10 mixture exhibited a tensile strength of approximately 3.00 MPa, corresponding to a reduction of about 13.5% compared to the control mix. Similarly, HC15 and HC20 showed further decreases to 2.80 MPa and 2.65 MPa, representing reductions of approximately 19.7% and 24.7%, respectively. This progressive decline in tensile strength with increasing PGA content can be primarily attributed to the dilution effect caused by excessive cement replacement, which reduces the formation of calcium silicate hydrate (C–S–H) gel, the main contributor to tensile resistance. Additionally, higher PGA contents may adversely affect workability and homogeneity, leading to increased entrapped air and microcracking, which are particularly detrimental to tensile performance [41].

Moreover, splitting tensile strength is highly influenced by the quality of the interfacial transition zone and the concrete's ability to resist crack initiation and propagation. The observed reductions at higher PGA levels suggest a weaker ITZ and less effective stress transfer across the matrix. Although PGA exhibits pozzolanic potential, its reaction rate is relatively slow, and at higher replacement ratios, the pozzolanic contribution at 28 days may not be sufficient to compensate for the reduced cement content. Overall, the results indicate that while a low PGA replacement level (5%) maintains acceptable tensile performance with only a negligible reduction, higher replacement ratios significantly compromise the splitting tensile strength of HSSCC. These findings highlight the importance of optimizing PGA content to achieve a balance between sustainability and mechanical performance.

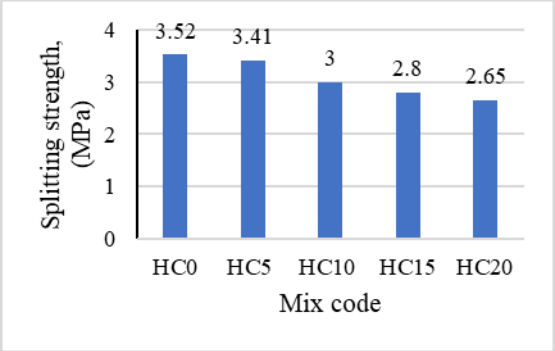

Fig.8: Splitting tensile strength of HSSCC

F. Sulfate attack

Sulfate attack was found to have a more severe impact on the compressive strength of HSSCC compared to chloride exposure, as shown in **Fig. 9** due to the aggressive nature of sulfate ions and their ability to form expansive products such as ettringite and gypsum. The control mix (HC0) exhibited a reduction in compressive strength from 50 MPa before exposure to 45.4 MPa after sulfate attack, corresponding to a loss of approximately 9.2%, accompanied by a mass loss of about 1.7%. This deterioration reflects the vulnerability of ordinary cementitious systems to sulfate-induced expansion and cracking, which progressively weakens the concrete matrix. The incorporation of PGA at a low replacement level significantly improved sulfate resistance, as evidenced by the performance of the HC5 mixture. This mix showed a reduction in compressive strength from 65 MPa to 62 MPa, corresponding to the lowest reduction rate of approximately 4.6%, along with a relatively low mass loss of 1.4%. The enhanced sulfate resistance of HC5 can be attributed to the pozzolanic reaction of PGA, which consumes calcium hydroxide and reduces the availability of reactive aluminates, thereby limiting the formation of expansive sulfate reaction products. In contrast, the HC10 mixture exhibited a strength reduction from 56 MPa to 50.5 MPa, corresponding to a decrease of about 9.8%, which is comparable to that of the control mix. This indicates that moderate PGA contents may not significantly improve sulfate resistance beyond a certain threshold. More severe deterioration was observed in mixes with higher PGA contents, as HC15 and HC20 showed substantial strength losses of 20.4% and 23.7%, respectively, with corresponding mass losses reaching up to 3.8% for HC20. These pronounced reductions suggest that excessive PGA replacement adversely affects sulfate resistance due to increased porosity and reduced cementitious content, which facilitates sulfate ion penetration and accelerates chemical degradation. Overall, the results confirm that sulfate attack is more detrimental than chloride attack for all mixtures; however, an optimal PGA replacement level of 5% markedly enhances

DOI: https://doi.org/XXXX.XXXX

sulfate resistance by improving microstructural densification and reducing the susceptibility of concrete to expansive chemical reactions, whereas higher replacement ratios lead to significant strength deterioration and reduced durability.

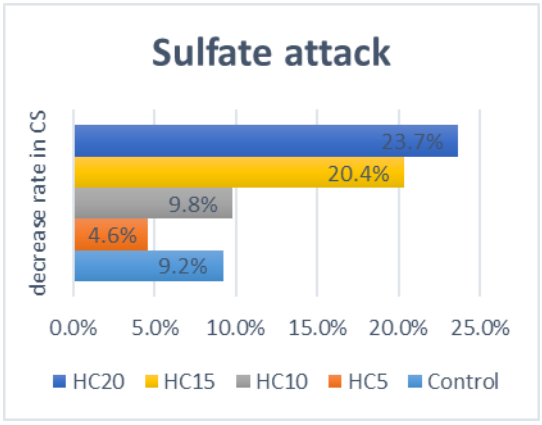

Fig. 9. Residual compressive strength of HSSCC after sulfate attack

G. Chloride attack

The influence of chloride attack on the compressive strength of HSSCC incorporating Pelargonium Ash (PGA) was evaluated by comparing the strength values before and after exposure to a chloride environment. The results shown in **Fig.10** indicate that chloride ingress caused a measurable reduction in compressive strength for all concrete mixtures; however, the extent of deterioration was strongly dependent on the PGA replacement level. The control mix (HC0) exhibited a reduction in compressive strength from 50 MPa before exposure to 47 MPa after chloride attack, corresponding to a strength loss of approximately 6.0%, with a relatively low mass loss of about 0.4%. This moderate reduction reflects the inherent susceptibility of conventional concrete to chloride penetration, which can disrupt the cementitious matrix and weaken the bond between hydration products. In contrast, the HC5 mixture, which contained 5% PGA, showed a compressive strength decrease from 65 MPa to 56.3 MPa, corresponding to a reduction of 13.4%. Although the percentage reduction appears higher than that of the control mix, HC5 maintained the highest residual compressive strength among all mixes after chloride exposure, indicating superior structural integrity. This behavior can be attributed to the pozzolanic activity of PGA at low replacement levels, which leads to pore refinement, reduced permeability, and a denser microstructure that restricts chloride ion penetration. The HC10 mixture exhibited a reduction in compressive strength from 56 MPa to 49 MPa, corresponding to a decrease of approximately 12.5%, while HC15 and HC20 experienced more pronounced strength losses of 16.7% and 15.4%, respectively. These higher reductions are associated with excessive replacement of cement, which results in a dilution effect and reduced formation of calcium silicate hydrate (C–S–H) gel, thereby weakening the resistance of the concrete matrix to chemical attack. Furthermore, the increased mass loss observed with higher PGA contents (up to 1.7% for HC20) suggests greater material degradation and microstructural damage. Overall, the results demonstrate that while chloride attack negatively affects compressive strength, the incorporation of PGA at an optimal replacement level of 5% enhances the residual strength and durability of HSSCC by limiting chloride ingress and preserving the integrity of the cementitious matrix [42]

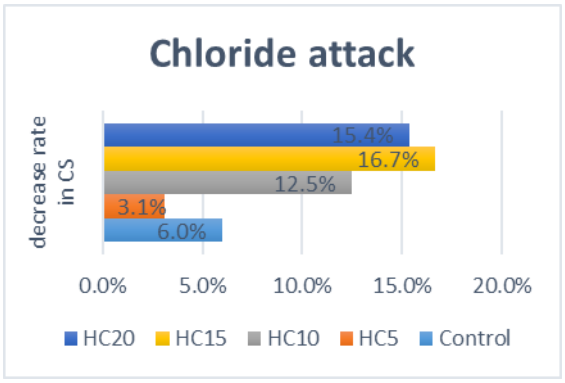

Fig. 10. Residual compressive strength of HSSCC after chloride attack

Conclusions

Partial replacement of cement with Pelargonium Ash (PGA) in High Strength- HSSCC reduces both initial and final setting times, with a significant reduction observed at 10% replacement. The optimum PGA replacement level for compressive strength is 5%, which showed slight improvements at early and late curing ages without compromising self-compacting properties. Higher PGA replacement levels (10%, 15%, 20%) lead to decreased compressive and split tensile strengths due to rapid hardening and increased water absorption, affecting workability and mechanical performance. Durability tests indicate that a 5% PGA replacement enhances resistance to sulfate and chloride attacks, attributed to pore refinement and pozzolanic activity improving the concrete microstructure. Excessive PGA content beyond 10% negatively impacts durability and mechanical properties, likely due to dilution of cementitious components and insufficient calcium hydroxide for secondary hydration. Adjustments in water and superplasticizer dosages are necessary at higher PGA levels to compensate for increased water absorption and maintain workability. Overall, PGA can

DOI: https://doi.org/XXXX.XXXX

be effectively used as a sustainable partial cement replacement in HSSCC at an optimal level around 5–10%, balancing mechanical performance, durability, and environmental benefits.

References

[1] A. Rajasekar, K. Arunachalam, M. Kottaisamy, V. Saraswathy, Durability characteristics of Ultra High Strength Concrete with treated sugarcane bagasse ash, Construct. Build. Mater. 171 (May 2018) 350–356,

[2]. Tang, L.V.; Bulgakov, B.; Aleksandrova, O.; Larsen, O.; Pham, A.N. Effect of rice husk ash and fly ash on the compressive strength of high performance concrete. E3S Web Conf. 2018, 33, 02030.

[3] Schmidt, M.; Fehling, E.; Geisenhanslüke, C. Ultra High Performance Concrete (UHPC). In Proceedings of the International Symposium on Ultra High Performance Concrete, Kassel, Germany, 13–15 September 2004.

[4] Wang, A.; Zhang, C.; Sun, W. Fly ash effects II. The active effect of fly ash. Cem. Concr. Res. 2004, 34, 2057–2060.

[5] Bui, D.D.; Hu, J.; Stroeven, P. Particle size effect on the strength of rice husk ash blended gap-graded Portland cement concrete. Cem. Concr. Compos. 2005, 27, 357–366.

[6] Stelmakh, S.A.; Shcherban, E.M.; Beskopylny, A.; Mailyan, L.R.; Meskhi, B.; Varavka, V. Quantitative and Qualitative Aspects of Composite Action of Concrete and Dispersion-Reinforcing Fiber. Polymers 2022, 14, 682.

[7] Scrivener, K.L.; Vanderley, M.J.; Gartner, E.M. Eco-efficient cements: Potential economically viable solutions for a low-CO2 cement-based materials industry. Cem. Concr. Res. 2018, 114, 2–26.

[8] Klemm, W.; Berger, R. Accelerated curing of cementitious systems by carbon dioxide: Part I. Portland cement. Cem. Concr. Res. 1972, 2, 567–576.

[9] McDonald, L.; Glasser, F.P.; Imbabi, M.S. A New, Carbon-Negative Precipitated Calcium Carbonate Admixture (PCC-A) for Low Carbon Portland Cements. Materials 2019, 12, 554.

[10] Olivier, J.G.J.; Peters, J.A.H.W.; Janssens-Maenhout, G. Trends in Global CO2 Emissions. 2012 Report; EU Publications: The Hague, The Netherlands, 2012.

[11] Yang, H.J.; Usman, M.; Hanif, A. Suitability of Liquid Crystal Display (LCD) Glass Waste as Supplementary Cementing Material (SCM): Assessment based on strength, porosity, and durability. J. Build. Eng. 2021, 42, 102793.

[12] Huntzinger, D.N.; Eatmon, T.D. A life-cycle assessment of Portland cement manufacturing: Comparing the traditional process with alternative technologies. J. Clean. Prod. 2009, 17, 668–675.

[13] Hanif, A.; Diao, S.; Lu, Z.; Fan, T.; Li, Z. Green lightweight cementitious composite incorporating aerogels and fly ash cenospheres— Mechanical and thermal insulating properties. Constr. Build. Mater. 2016, 116, 422–430.

[14] Kim, Y.; Hanif, A.; Usman, M.; Munir, M.J.; Kazmi, S.M.S.; Kim, S. Slag waste incorporation in high early strength concrete as cement replacement: Environmental impact and influence on hydration; durability attributes. J. Clean. Prod. 2018, 172, 3056–3065.

[15] D.M. Kannan, S.H. Aboubakr, A.S. El-Dieb, M.M.R. Taha, High performance concrete incorporating ceramic waste powder as large partial replacement of Portland cement, Constr. Build. Mater. 144 (2017) 35–41.

[16]. R. Gopalakrishnan, R. Jeyalakshmi, the effects on durability and mechanical properties of multiple nano and micro additive OPC mortar exposed to combined chloride and sulfate attack, Mater. Sci. Semicond. Process. 106 (2020), 104772.

[17]. M.S. Meddah, M.A. Ismail, S. El-Gamal, H. Fitriani, Performances evaluation of binary concrete designed with silica fume and metakaolin, Constr. Build. Mater. 166 (2018) 400–412.

[18]. A. Pandey, B. Kumar, A comprehensive investigation on application of microsilica and rice straw ash in rigid pavement, Constr. Build. Mater. 252 (2020), 119053.

[19]. Q. Zhang, Y. Li, L. Xu, P. Lun, Bond strength and corrosion behavior of rebar embedded in straw ash concrete, Constr. Build. Mater. 205 (2019) 21–30.

[20]. M.S. Meddah, M.A. Ismail, S. El-Gamal, H. Fitriani, Performances evaluation of binary concrete designed with silica fume and metakaolin, Constr. Build. Mater. 166 (2018) 400–412.

[21]. A. Pandey, B. Kumar, A comprehensive investigation on application of microsilica and rice straw ash in rigid pavement, Constr. Build. Mater. 252 (2020), 119053.

[22]. M.S. Saif, M.O. El-Hariri, A.I. Sarie-Eldin, B.A. Tayeh, M.F. Farag, Impact of Ca+ content and curing condition on durability performance of metakaolin-based geopolymer mortars, Case Studies in Construction, Materials 16 (2022), e00922.

[23]Mechanical and durability properties of concrete incorporating silica fume and a high volume of sugarcane bagasse ash.

[24]Gursel, A. P., Maryman, H., & Ostertag, C., 2016. A life-cycle approach to environmental,mechanical, and durability properties of “green” concrete mixes with rice husk ash. Journal of Cleaner Production 112, 823-836.

[25]. Vargas, J., Halog, A., 2015. Effective carbon emission reductions from using upgraded fly ash in the cement industry. J. Clean. Prod. 103, 948–959.

[**26**]**.** Kannan, V., & Ganesan, K., 2014. Chloride and chemical resistance of self-compacting concrete containing rice husk ash and metakaolin. Construction and Building materials 51, 225-234.

[27] Chopra, Rafat , Kunal, Strength, permeability and microstructure of self-compacting concrete containing rice husk ash. Biosystems Engineering, Volume 130, February 2015, Pages 72-80

[28] N. Shafiq, A.A.E. Hussein, M.F. Nuruddin, H. al Mattarneh, Effects of sugarcane bagasse ash on the properties of concrete, Proc. Inst. Civ. Eng.: Eng. Sustain. 171 (3) (Aug. 2018) 123–132, https://doi.org/10.1680/jensu.15.00014.

[29] A.A.E. Hussein, N. Shafiq, M.F. Nuruddin, F.A. Memon, Compressive strength and microstructure of sugar cane bagasse

DOI: https://doi.org/XXXX.XXXX

ash concrete, Res. J. Appl. Sci. Eng. Technol. 7 (12) (2014) 2569–2577, https://doi.org/10.19026/rjaset.7.569.
[30] A. Tadjarodi, M. Haghverdi, V. Mohammadi, Preparation and characterization of nano-porous silica aerogel from rice husk ash by drying at atmospheric pressure, Mater. Res. Bull. 47 (9) (2012) 2584–2589.
[31] A. Serag Faried, Sahar A. Mostafa, Bassam A. Tayeh, Taher A. Tawfik, the effect of using nano rice husk ash of different burning degrees on ultra-high-performance concrete properties Construction and Building Materials 290 (2021)
[32] Ganesan, K., Rajagopal, K., Thangavel, K., 2008. Rice husk ash blended cement: assessment of optimal level of replacement for strength and permeability properties of concrete. Construct. Build. Mater. 22, 1675–1683.
[33] Taha Awadallah El-Sayed, Performance of Porous Slabs Using Recycled Ash. Polymers 2021, 13(19), 3319; Polymers | Free Full-Text | Performance of Porous Slabs Using Recycled Ash (mdpi.com)
[34] Mohamed Amin, Bassam A. Tayeh, Mohamed A. Kandil, Ibrahim Saad Agwa, Mohammad Farouk Abdelmagied, Effect of rice straw ash and palm leaf ash on the properties of ultrahigh-performance concrete, Case Studies in Construction Materials, Volume 17, 2022, e01266, ISSN 2214-5095,
[35] Șerbănoiu, A.A.; Grădinaru, C.M.; Muntean, R.; Cimpoeșu, N.; Șerbănoiu, B.V. Corn Cob Ash versus Sunflower Stalk Ash, Two Sustainable Raw Materials in an Analysis of Their Effects on the Concrete Properties. *Materials* 2022, *15*, 868.
[36] Neha Sharma, Prashant Sharma, Arun Kumar Parashar, Incorporation of Silica Fume and Waste Corn Cob Ash in Cement and Concrete for Sustainable Environment, Materials Today: Proceedings 62 (2022) 4151–4155
[37] S.N. Chinnu, S.N. Minnu, A. Bahurudeen, R. Senthilkumar, Influence of palm oil fuel ash in concrete and a systematic comparison with widely accepted fly ash and slag: A step towards sustainable reuse of agro-waste ashes, Cleaner Materials, Volume 5, 2022, 100122, ISSN 2772-3976,
[38] A.S.M. Abdul Awal, I.A. Shehu, Mohammad Ismail,Effect of cooling regime on the residual performance of high-volume palm oil fuel ash concrete exposed to high temperatures, Construction and Building Materials, Volume 98, 2015, Pages 875-883, ISSN 0950-0618,
[39] Taha A. El-Sayed, Performance of heavy weight concrete incorporating recycled rice straw ash as radiation shielding material, Progress in Nuclear Energy, Volume 135, 2021, ISSN 0149-1970,
[40] Divya Chopra, Rafat Siddique, Kunal, Strength, permeability and microstructure of self-compacting concrete containing rice husk ash, Biosystems Engineering, Volume 130, 2015, Pages 72-80, ISSN 1537-5110,

[41] Ibrahim Saad Agwa, Omar Mohamed Omar, Bassam A. Tayeh, Bassam Abdelsalam Abdelsalam, Effects of using rice straw and cotton stalk ashes on the properties of lightweight self-compacting concrete, Construction and Building Materials, Volume 235, 2020, 117541, ISSN 0950-0618,
[42] Kumar Gedela Santhosh, Sk M. Subhani, A. Bahurudeen, Recycling of palm oil fuel ash and rice husk ash in the cleaner production of concrete, Journal of Cleaner Production, Volume 354, 2022, 131736, iSSN 0959-6526.

DOI: https://doi.org/XXXX.XXXX

Advanced Multidisciplinary Engineering Journal (AMEJ)
ISSN: XXXX-XXXX

Journal Homepage:
https://pub.scientificirg.com/index.php/AMEJ/en

Cite this: AMEJ, xxxx (xx), xxx

Performance Evaluation of Sustainable Lightweight Concrete Incorporating Recycled Brick Aggregates

Sahar A. Mostafa[*1], *and Ahmed Essam[2]*

*[*1] Department of Civil Engineering, Faculty of Engineering, Beni-Suef University, Beni-Suef, Egypt,*
sahar_abdelsalam2010@yahoo.com

[2]Delta Higher Institute for Engineering & Technology, Mansoura, Egypt.
Ahmed.esam1523@gmail.com

**Corresponding Author:* sahar_abdelsalam2010@yahoo.com

Abstract - This study investigates the performance of lightweight concrete incorporating crushed waste bricks as a partial replacement for natural coarse aggregates, focusing on optimizing the mixing proportions and evaluating the influence of silica fume content and superplasticizer dosage. The experimental results demonstrated that replacing 25% of the natural aggregates with crushed bricks improved the 28-day compressive strength, with higher cement contents mitigating the adverse effects of increased brick incorporation. The optimal silica fume content for enhancing compressive strength was identified as 15%; beyond this, the strength decreased due to reduced workability and microstructural inefficiencies. The dosage of superplasticizer significantly affected the compressive strength, with an optimum range observed at 2.0%, whereas excessive dosages resulted in strength reduction. The study also revealed that the early age compressive strength is more sensitive to brick incorporation, particularly at lower cement contents. However, mixtures with higher cement contents exhibited superior early-age strength retention. The splitting tensile strength consistently improved with increasing normal aggregate content, highlighting the role of aggregate stiffness and bond quality in controlling the tensile behavior. These findings contribute to the development of sustainable, high-performance lightweight concrete utilizing recycled materials, with potential applications in structural and non-structural elements where reduced self-weight and enhanced mechanical properties are desired.

Received: *15 August 2025*
Revised: *30 September 2025*
Accepted: *15 December 2025*
Available online: *25 December 2025*

Keywords:

- *Lightweight concrete*
- *Recycled brick aggregates*
- *Compressive strength*
- *Silica fume*
- *Superplasticizer*
- *Early-age strength*
- *Splitting tensile strength*

DOI: https://doi.org/XXXX.XXXX

Introduction

Lightweight concrete (LWC) has attracted significant attention in modern construction engineering because of its ability to reduce the self-weight of structural elements while maintaining acceptable mechanical performance and durability. Unlike conventional concrete, which relies on dense natural aggregates, lightweight concrete incorporates low-density aggregates or engineered voids to achieve a reduced unit weight, typically ranging between 1400 and 2000 kg/m³ [1]. This reduction in density offers multiple structural and functional advantages, including lower dead loads, improved seismic performance, reduced foundation sizes, and enhanced thermal insulation [2]. These benefits make lightweight concrete particularly attractive for high-rise buildings, long-span structures, precast elements, and rehabilitation projects, where weight reduction is critical [3]. In addition, the increasing demand for sustainable construction materials has further reinforced the relevance of lightweight concrete, as it provides opportunities to incorporate alternative and recycled materials without compromising its performance. However, the reduction in density is often accompanied by challenges related to strength development, workability, and durability, necessitating careful mix design and material selection [4]. Consequently, extensive research has focused on optimizing lightweight concrete mixtures to balance weight reduction with the mechanical and durability requirements. The performance of lightweight concrete is highly dependent on the characteristics of its constituent materials, particularly the type, porosity, and grading of the lightweight aggregates, as well as the interaction between the aggregates and the cementitious matrix. Understanding these interactions is essential for developing lightweight concrete with predictable behavior and reliable performance in structural and nonstructural applications [5].

The construction industry is one of the largest consumers of natural resources worldwide, with natural aggregates accounting for a substantial portion of the concrete volume. Continuous sand and gravel extraction has severe environmental consequences, including the depletion of natural reserves, ecological degradation, and increased carbon emissions associated with quarrying and transportation processes [6]. In response to these concerns, sustainable construction practices have increasingly emphasized the reuse of recycled and waste materials as alternatives to conventional aggregate. The utilization of recycled aggregates derived from construction and demolition waste aligns with circular economy principles by diverting waste from landfills and reducing the reliance on virgin materials. Incorporating recycled aggregates into lightweight concrete is a promising strategy for achieving environmental sustainability and material efficiency [7]. However, recycled aggregates typically exhibit higher porosity, lower density, and greater water absorption than natural aggregates, which significantly influence the properties of fresh and hardened concrete. These characteristics can be advantageous in producing lightweight concrete but may also adversely affect its strength, stiffness, and durability if not properly controlled. Therefore, the successful replacement of natural aggregates with recycled materials requires a comprehensive understanding of their physical and chemical properties, as well as appropriate adjustments in the mix design, water demand, and admixture usage. Research efforts have increasingly focused on identifying suitable recycled aggregate sources and evaluating their performance in lightweight concrete applications to ensure compliance with the structural and durability requirements [8].

Among the various recycled materials, waste bricks generated from the construction, demolition, and

DOI: https://doi.org/XXXX.XXXX

ceramic industries have emerged as viable alternative aggregates for lightweight concrete production. Crushed waste bricks are characterized by a relatively low density, high porosity, and rough surface texture, which distinguishes them from conventional natural aggregates [9]. These properties make waste brick aggregates particularly suitable for lightweight concrete, as they contribute to density reduction while enhancing mechanical interlocking with cementitious matrices [10]. Additionally, waste bricks often contain residual amorphous and crystalline silica phases that may participate in secondary pozzolanic reactions under favorable conditions. Despite these advantages, the incorporation of crushed brick aggregates presents several technical challenges, including increased water absorption, reduced workability, and potential variability in the material quality [11]. The porous nature of brick aggregates can lead to rapid water uptake during mixing, thereby affecting the effective water-to-cement ratio and early age hydration. As a result, pretreatment methods, such as presoak or moisture conditioning, are often required to achieve consistent fresh properties. Furthermore, the replacement level of natural aggregates with crushed bricks plays a critical role in determining the balance between the weight reduction and mechanical performance. Excessive replacement ratios may result in significant strength loss, whereas optimized proportions can yield structurally viable lightweight concrete. Therefore, a systematic investigation of the waste brick aggregate content and its interaction with other mix constituents is essential for developing reliable lightweight concrete mixtures [12].

The performance of lightweight concrete incorporating recycled aggregates is strongly influenced by the adopted mixing proportions and the interactions between cementitious materials, aggregates, water, and chemical admixtures. Unlike conventional concrete, lightweight concrete mixtures require careful control of the paste volume, water content, and aggregate gradation to compensate for the higher porosity and lower stiffness of the lightweight aggregates [13]. The water-to-cement ratio plays a particularly critical role, as recycled and brick aggregates exhibit higher absorption capacities, which can significantly alter the effective water content during mixing. Improper control of the water content may lead to reduced workability, non-uniform mixing, or compromised strength development [14]. Additionally, the proportion of fine to coarse aggregates affects the particle packing density, internal curing behavior, and overall concrete homogeneity. The inclusion of supplementary cementitious materials, such as silica fume, can further modify the microstructure by refining the pore structure and improving the interfacial transition zone between aggregates and cement paste. High-range water-reducing admixtures are often necessary to maintain adequate workability at reduced water content, particularly in mixtures containing high volumes of fine or porous aggregates [12, 15]. Consequently, the optimization of mixing proportions is not only a matter of achieving the target density but also of ensuring adequate mechanical strength, durability, and consistency. Therefore, a systematic evaluation of different mixing proportions is essential to understand their combined effects on the fresh and hardened properties of lightweight concrete [16].

Despite the growing body of research on lightweight concrete and recycled aggregates, several gaps remain regarding the combined use of recycled aggregates, waste brick materials, and optimized mixing proportions of these materials. Many previous studies have focused on isolated parameters, such as single aggregate replacement levels or individual material properties, without fully addressing the synergistic effects of aggregate type, replacement ratio, and mix composition [17, 18]. In particular, limited attention has been given to

DOI: https://doi.org/XXXX.XXXX

understanding how different mixing proportions influence the lightweight characteristics, including the density, strength-to-weight ratio, and overall performance stability. Moreover, the variability in recycled material properties necessitates a comprehensive experimental approach to establish reliable correlations between the mix design parameters and concrete behavior [19]. Addressing these gaps is essential for promoting the practical adoption of lightweight concrete incorporating recycled aggregates in structural and nonstructural applications [20]. Therefore, this study aims to investigate lightweight concrete produced by replacing conventional natural aggregates with recycled aggregates and crushed waste bricks, while systematically examining the influence of different mixing proportions on the fresh and hardened properties. By providing a detailed evaluation of material interactions and performance outcomes, this study contributes to the development of sustainable, resource-efficient lightweight concrete with predictable and reproducible properties suitable for modern construction practices [21, 22].

The study investigates sustainable lightweight concrete using crushed waste brick aggregates as a partial replacement for natural coarse aggregates, focusing on optimizing mix proportions with silica fume and superplasticizer. This study fills gaps in understanding the synergistic effects of recycled aggregate type, replacement ratio, and mix design on lightweight concrete performance, providing a systematic experimental evaluation of these factors.

Experimental program

A. Raw materials

The raw materials used for producing lightweight concrete incorporating crushed brick as a partial replacement for natural coarse aggregate consisted of ordinary Portland cement, natural fine aggregate (sand), crushed brick aggregate, silica fume, and a high-range water-reducing agent. Ordinary Portland cement, conforming to the relevant ASTM specifications, was used as the primary binding material, as shown in **Fig. 1.** Natural river sand with appropriate grading and cleanliness was used as the fine aggregate to ensure adequate workability and packing density. Crushed brick waste, obtained from construction and demolition residues, was utilized as a lightweight coarse aggregate replacement owing to its lower density and rough surface texture, which enhances mechanical interlocking with the cement matrix. Silica fume, composed mainly of amorphous silicon dioxide (SiO_2), was incorporated as a highly reactive pozzolanic material to improve the microstructure, reduce porosity, and enhance the mechanical and durability properties of lightweight concrete. Its quality complies with the ASTM C1240 and AASHTO M 307 specifications. To compensate for the high-water demand associated with silica fume and crushed brick aggregates, a naphthalene sulfonate-based superplasticizer supplied by CMB under the trade name Addicrete BVF was used. This admixture meets the requirements of ASTM C494 Types F and G as well as BS EN 934-2:2001, and it was effective in achieving the desired workability at a reduced water-to-cement ratio without adversely affecting the setting characteristics of the concrete.

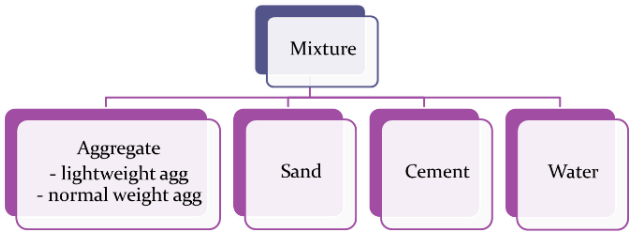

Fig. 1. Raw materials

B. Mixing procedures

The mixing procedure was conducted in a controlled and sequential manner to ensure proper homogeneity of the lightweight concrete mixture and mitigate the negative effects associated with the high porosity of the crushed brick aggregates and the ultra-fine nature of the silica fume. Before mixing, the crushed brick coarse

DOI: https://doi.org/XXXX.XXXX

aggregates were washed to remove adhered dust and then pre-soaked in water for 24 h to reduce excessive water absorption during mixing. Before use, the aggregates were brought to a saturated surface-dry (SSD) condition. The mixing was performed using a laboratory pan mixer. Initially, all dry constituents, including ordinary Portland cement, silica fume, and natural fine aggregate, were dry mixed for approximately 3 min to achieve uniform distribution and prevent agglomeration of silica fume particles. Subsequently, the crushed brick aggregates were added gradually and mixed for an additional 2 min to ensure even coating with the cementitious materials.

The mixing water was divided into two portions; approximately 70% of the total mixing water was added slowly while mixing continued for 2 min to initiate hydration and improve particle packing. The remaining 30% of the water was premixed with the naphthalene sulfonate-based superplasticizer and introduced gradually into the mixture to enhance dispersion and workability. The concrete was then mixed for an additional 3–5 min until a homogeneous, cohesive mixture with no visible segregation or bleeding was obtained. After mixing, the fresh concrete was allowed to rest for approximately 1 min before casting to allow air release and stabilization of the mixture. This mixing protocol ensured consistent fresh-state properties and reproducible hardened performance of lightweight concrete. **Tabs. 1-4** shows the designed experimental program and mixing proportions.

Tab. 1. Designed experimental program

w/c	cement	N.w / L.w aggregate	Super plasticizer	Silica fume + 0.2%SP
• 0.5 • 0.4	• 400 • 450 • 500	• 0% • 25% • 50% • 70% • 100%	• 0% • 0.5% • 1% • 1.5% • 2% • 2.5% • 3%	• 0% • 10% • 15% • 20% • 30%

Tab. 2. mixing proportions G1

Mix	Cement	W/C	Sand	N.w./L.w. (%)	Silica fume	S.P./C (%)
B40-5-0	400	0.5	583	0	0	0
B40-5-25				25		
B40-5-50				50		
B40-5-75				75		
B40-5-100				100		
B40-4-0		0.4	619	0		
B40-4-25				25		
B40-4-50				50		
B40-4-75				75		
B40-4-100				100		
B45-5-0	450	0.5	549	0	0	0
B45-5-25				25		
B45-5-50				50		
B45-5-75				75		
B45-5-100				100		
B45-4-0		0.4	588	0		
B45-4-25				25		
B45-4-50				50		
B45-4-75				75		
B45-4-100				100		
B50-5-0	500	0.5	512	0	0	0
B50-5-25				25		
B50-5-50				50		
B50-5-75				75		
B50-5-100				100		
B50-4-0		0.4	556	0		
B50-4-25				25		
B50-4-50				50		
B50-4-75				75		
B50-4-100				100		

Tab. 3. mixing proportions G2

Mix	Cement	W/C	Sand	N.w./L.w. (%)	Silica fume	S.P./C (%)
BA0	450	0.3	586	25	0	0.00%
BA0.5						0.50%
BA1						1%
BA1.5						1.50%
BA2						2%
BA2.5						2.50%
BA3						3%

DOI: https://doi.org/XXXX.XXXX

Tab. 4. mixing proportions G3

Mix	Cement	W/C	Sand	N.w./L.w. (%)	Silica fume	S.P./C (%)
BAF10	450	0.3	586	25	10%	2%
BAF15		0.3			15%	2%
BAF20		0.3			20%	2%
BAF30		0.3			30%	2%

Fig. 2. Testing procedures

Mixing procedures

All tests were conducted following relevant ASTM standards to ensure the accuracy and reliability of the experimental results. The concrete was cast into standard steel molds in accordance with ASTM specifications. For compressive strength testing, cubic or cylindrical specimens were prepared and compacted using mechanical vibration to eliminate entrapped air and ensure uniform density. After casting, the specimens were covered and kept at room temperature for 24 hours before demolding. The demolded specimens were then cured in water at a controlled temperature until the designated testing ages of 7 and 28 days. Compressive strength tests were carried out using a calibrated universal testing machine by applying a continuous and uniform load at the specified loading rate until failure occurred, and the maximum load was recorded. Splitting tensile strength tests were performed on cylindrical specimens following ASTM C496, where the load was applied diametrically until splitting failure was observed. For each mix, at least three specimens were tested at each curing age, and the average value was reported to ensure result consistency and minimize experimental variability. **Fig.2** shows some procedures during testing

Results and discussion

A. Effect of SF

The effect of the silica fume content on the compressive strength of the lightweight concrete mixtures is illustrated in **Fig.3** and summarized in the corresponding mix proportions shown in **Tab 4.** The results demonstrated a clear influence of the silica fume replacement level on both early- and later-age compressive strengths. At 7 and 28 d, the compressive strength exhibited a progressive increase with increasing silica fume content up to 15%, followed by a noticeable reduction at higher replacement levels. The reference mixture containing 10% silica fume (BAF10) showed moderate compressive strength values, whereas increasing the silica fume content to 15% (BAF15) resulted in the highest compressive strength at both curing ages. This improvement can be attributed to the high pozzolanic reactivity of the silica fume, which enhances the formation of additional calcium silicate hydrate (C–S–H) gel and refines the pore structure, particularly in the interfacial transition zone between the cement paste and the lightweight aggregate. However, further increasing the silica fume content to 20% and

DOI: https://doi.org/XXXX.XXXX

30% (BAF20 and BAF30) led to a reduction in compressive strength, despite maintaining a constant water-to-cement ratio and superplasticizer dosage. This decline is primarily associated with the excessive fineness of the silica fume, which increases the water demand and may result in inadequate dispersion and particle agglomeration when used in high proportions. Consequently, the effectiveness of silica fume in improving strength diminishes beyond the optimum replacement level. Moreover, although the 28-day compressive strength values were consistently higher than the corresponding 7-day results for all mixtures, the same trend of optimal performance at 15% silica fume was observed. These findings indicate that an optimal silica fume content exists for lightweight concrete incorporating recycled aggregates, beyond which the beneficial effects on compressive strength are outweighed by the adverse effects related to workability and microstructural inefficiencies.

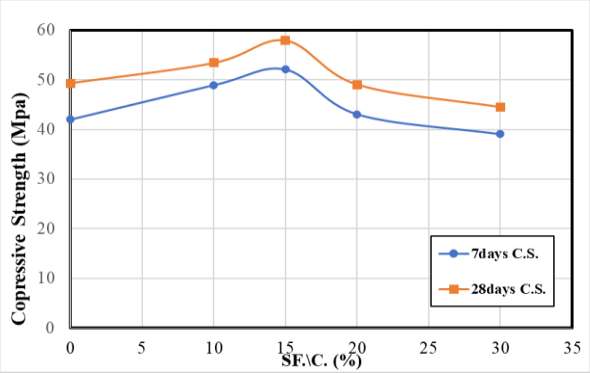

Fig. 3. compressive strength for G3

B. Effect of SP

Fig. 4 illustrates the influence of superplasticizer dosage (SP/C%) on the compressive strength of lightweight concrete mixtures at 7 and 28 days, with the corresponding mix proportions presented in **Tab. 3.** The results indicate that the compressive strength is significantly affected by the superplasticizer content, which exhibits a clear optimum range. At both curing ages, a gradual increase in compressive strength was observed with an increase in the SP/C ratio up to 2.0%, after which a noticeable reduction occurred at higher dosages. The control mixture without the superplasticizer (BA0) exhibited the lowest compressive strength, primarily owing to inadequate workability and incomplete compaction, which negatively affected the internal structure of the concrete. The introduction of small amounts of superplasticizer (0.5–1.5%) led to a marked improvement in compressive strength, which was attributed to enhanced workability, improved particle dispersion, and more efficient cement hydration at a constant water-to-cement ratio.

The optimum performance was achieved at a superplasticizer dosage of 2.0% (BA2), which recorded the highest compressive strength values at both 7 d and 28 d. This behavior can be explained by the ability of the superplasticizer to reduce internal friction, improve paste fluidity, and enhance the homogeneity of the lightweight concrete mixture, particularly when porous recycled aggregates are present. However, further increasing the superplasticizer content to 2.5% and 3.0% (BA2.5 and BA3, respectively) reduced the compressive strength. This decrease is likely due to excessive dispersion and segregation tendencies, as well as possible retardation effects that adversely influence the formation of dense cementitious matrices. Although the 28-day compressive strength values were consistently higher than those at 7 days for all mixtures, the same trend of optimal performance at 2.0% superplasticizer dosage was observed. These results confirm that the superplasticizer content must be carefully optimized in lightweight concrete mixtures to achieve a balance between workability enhancement and mechanical performance.

DOI: https://doi.org/XXXX.XXXX

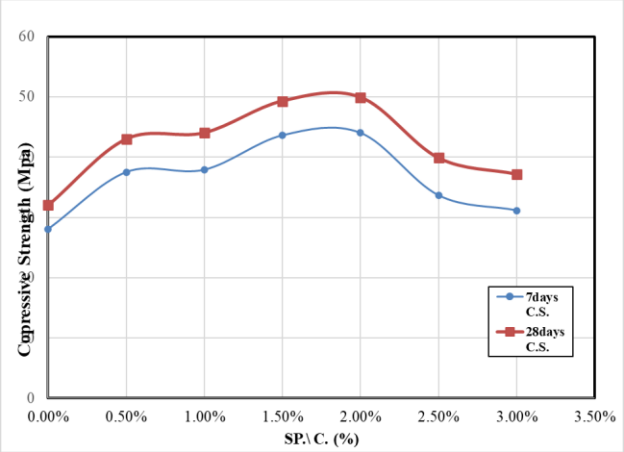

Fig. 4. compressive strength for G2

C. *Early compressive strength*

Fig. 5 illustrates the effect of the crushed brick replacement ratio on the 7-day compressive strength of the lightweight concrete mixtures with different cement contents (400, 450, and 500 kg/m³). For mixtures with a cement content of 400 kg/m³, replacing 25% of the natural aggregate with crushed bricks increased the compressive strength from 28.05 MPa to 30.27 MPa, corresponding to an improvement of approximately 7.9%. However, increasing the replacement level to 50% resulted in a reduction to 25.61 MPa, representing a strength loss of approximately 8.7% compared to the control mix. A more pronounced decrease of approximately 11.0% was observed at 75% replacement (24.97 MPa), whereas a slight recovery occurred at full replacement (100%), with a strength of 27.10 MPa, indicating a marginal reduction of 3.4% relative to the reference mixture.

A similar trend was observed for mixtures containing 450 kg/m³ of cement. The 7-day compressive strength increased from 36.35 MPa to 33.98 MPa at 25% replacement, showing a reduction of approximately 6.5%, indicating that early age strength development is more sensitive to brick incorporation at this cement content. Further increases in brick replacement led to strength reductions of approximately 9.2%, 19.1%, and 25.5% at 50%, 75%, and 100% replacement levels, respectively.

In contrast, mixtures with the highest cement content (500 kg/m³) demonstrated superior early age strength. A 25% crushed brick replacement increased the compressive strength from 37.93 MPa to 38.92 MPa, achieving an improvement of approximately 2.6%. At higher replacement levels, the strength reductions were limited to 9.3% at 50% replacement, 17.7% at 75% replacement, and 18.3% at 100% replacement. These results confirm that moderate crushed brick replacement ratios, particularly approximately 25%, can enhance or maintain early age compressive strength, whereas higher cement contents effectively mitigate the adverse effects of increased brick aggregate incorporation at early curing ages.

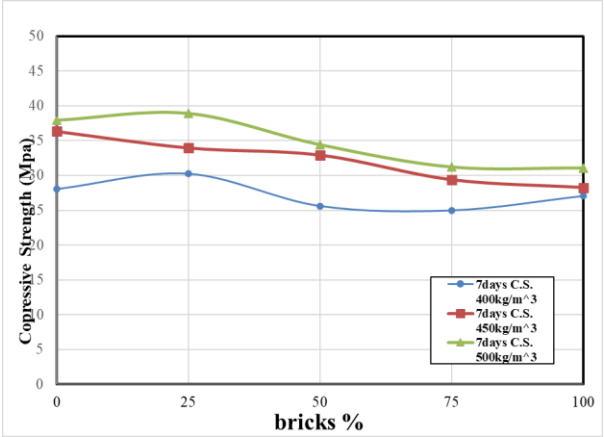

Fig. 5. Early compressive strength for G1

D. *28 days compressive strength*

The percentage improvement in the 28-day compressive strength resulting from the partial replacement of natural aggregates with crushed bricks is illustrated in Fig.6. For mixtures with a cement content of 400 kg/m³, replacing 25% of natural aggregate with crushed bricks led to an increase in compressive strength from approximately 35 MPa to 37 MPa, corresponding to an improvement of approximately 5.7%. However, further increasing the replacement level

DOI: https://doi.org/XXXX.XXXX

to 50% resulted in a strength reduction of nearly 8.6%, whereas a more pronounced decrease of approximately 14.3% was observed at 75% replacement. At full replacement (100%), the compressive strength partially recovered, showing a reduction of only 2.9% compared with the reference mix.

For mixtures containing 450 kg/m³ cement, the beneficial effect of crushed brick replacement was evident. A 25% replacement level increased the compressive strength from approximately 42 MPa to 44 MPa, representing an improvement of approximately 4.8%. In contrast, strength reductions of approximately 7.1% and 11.9% were recorded at 50% and 75% replacement levels, respectively. At 100% brick replacement, the compressive strength decreased by approximately 4.8%, indicating better strength retention than that of mixtures with lower cement contents.

The mixtures with the highest cement content (500 kg/m³) exhibited the most stable behavior. A 25% crushed brick replacement increased the compressive strength from nearly 45 MPa to 47 MPa, achieving an improvement of approximately 4.4%. Even at higher replacement levels, the strength loss remained relatively limited, with reductions of approximately 2.2%, 11.1%, and 6.7% at 50%, 75%, and 100% replacement levels, respectively. These results confirm that a moderate crushed brick replacement level of approximately 25% provides optimum mechanical performance, whereas higher cement contents significantly mitigate the adverse effects of increased brick aggregate incorporation.

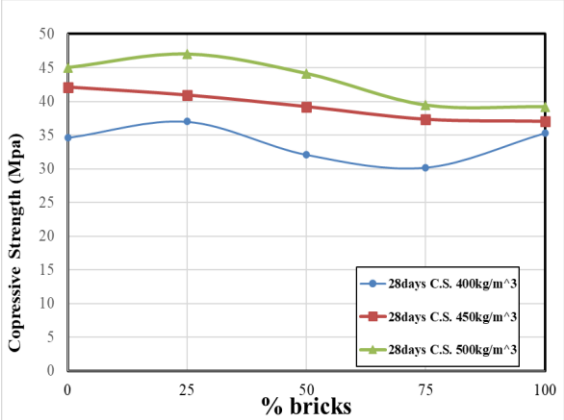

Fig. 6. 28 days compressive strength for G1

E. Early tensile strength

Fig. 7 shows tensile strength of the lightweight concrete mixtures with cement contents of 400 and 450 kg/m³. For mixtures containing 400 kg/m³ cement, the tensile strength gradually increased with increasing normal aggregate content. The reference mixture with 0% normal aggregates recorded a tensile strength of approximately 2.0 MPa. Increasing the normal aggregate content to 25% resulted in a slight reduction of approximately 1.95 MPa, corresponding to a marginal decrease of approximately 2.5%, which may be attributed to local heterogeneity at low replacement levels. However, at 50% replacement, the tensile strength increased to approximately 2.2 MPa, representing an improvement of approximately 10.0% compared to the reference mixture. A significant enhancement was observed at 75% normal aggregate content, where the tensile strength reached approximately 3.0 MPa, corresponding to an improvement of nearly 50.0%. At full replacement (100%), the tensile strength further increased to approximately 3.2 MPa, achieving a maximum improvement of approximately 60.0% relative to the lightweight aggregate mixture.

Similarly, mixtures with a higher cement content of 450 kg/m³ demonstrated consistently higher tensile strength values at all replacement levels. The reference mixture

DOI: https://doi.org/XXXX.XXXX

recorded a tensile strength of approximately 2.8 MPa, which increased slightly to approximately 2.85 MPa at 25% replacement, corresponding to an improvement of approximately 1.8%. At 50% normal aggregate content, the tensile strength increased to approximately 3.1 MPa, representing an improvement of approximately 10.7%. Further increases to 75% and 100% normal aggregates resulted in tensile strengths of approximately 3.25 MPa and 3.35 MPa, corresponding to improvements of approximately 16.1% and 19.6%, respectively. The observed enhancement in tensile strength with increasing normal aggregate content can be attributed to the higher stiffness and lower porosity of normal aggregates, which improve the crack resistance and strengthen the interfacial transition zone, particularly at early curing ages.

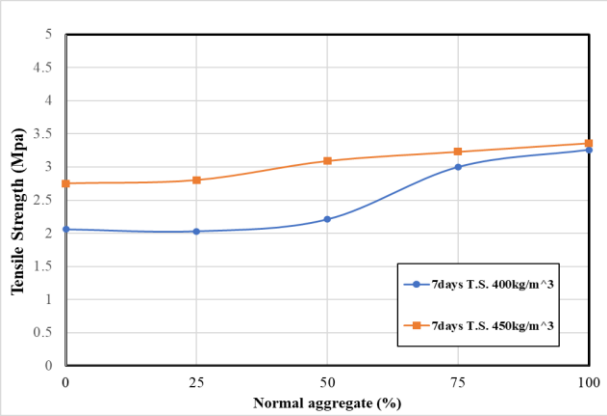

Fig. 7. Early tensile strength for G1

F. 28 days tensile strength

Fig.8 illustrates the variation in splitting tensile strength of lightweight concrete as a function of normal aggregate percentage for mixtures with cement contents of 400 and 450 kg/m³ at 28 d and 7 d, respectively. The results revealed a clear and consistent improvement in the tensile strength with increasing normal aggregate content, indicating the significant role of aggregate stiffness and bond quality in controlling the tensile behavior. For mixtures with a cement content of 400 kg/m³ tested at 28 d, increasing the normal aggregate content from 0% to 25% resulted in a marginal increase in tensile strength from approximately 2.9 MPa to 2.95 MPa, corresponding to an improvement of approximately 1.7%. A more noticeable enhancement was observed at 50% normal aggregate content, where the tensile strength increased to approximately 3.2 MPa, representing an improvement of approximately 10.3% compared with the reference mix. Further increasing the normal aggregate content to 75% led to a significant increase in the tensile strength to nearly 3.9 MPa, corresponding to an improvement of approximately 34.5%. At full replacement (100%), the tensile strength reached approximately 4.0 MPa, achieving a maximum improvement of approximately 37.9% relative to the mixture containing only lightweight aggregates.

Similarly, for mixtures with a cement content of 450 kg/m³ tested at 7 d, a continuous increase in tensile strength was observed with increasing normal aggregate percentage. The tensile strength increased from approximately 3.6 MPa at 0% normal aggregate to approximately 3.7 MPa at 25%, indicating an improvement of approximately 2.8%. At 50% normal aggregate content, the tensile strength reached nearly 3.9 MPa, corresponding to an improvement of approximately 8.3%. Further increases to 75% and 100% normal aggregates resulted in tensile strengths of approximately 4.0 MPa and 4.3 MPa, representing improvements of approximately 11.1% and 19.4%, respectively. These results confirm that incorporating higher proportions of normal aggregates enhances tensile resistance by improving crack-bridging capacity and strengthening the interfacial transition zone, while mixtures with lower normal aggregate content exhibit reduced tensile performance owing to the higher porosity and lower stiffness of the lightweight aggregates.

DOI: https://doi.org/XXXX.XXXX

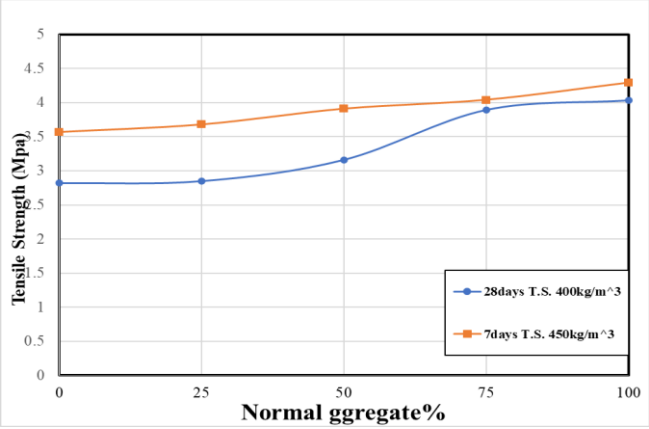

Fig. 8. 28 daya tensile strength for G1

Conclusion

This study demonstrates that incorporating crushed waste brick aggregates as a partial replacement for natural coarse aggregates in lightweight concrete can enhance its mechanical performance and sustainability. The optimal mixing proportions, including the silica fume content and superplasticizer dosage, are critical for achieving improved compressive and tensile strengths. Moderate replacement levels (approximately 25%) and higher cement contents effectively balanced strength gains with the benefits of reduced density. These findings support the practical use of recycled brick aggregates in lightweight concrete, contributing to resource efficiency and environmental sustainability in construction.

References

[1] K.H. Mo, U.J. Alengaram, M.Z. Jumaat, M.Y.J. Liu, J. Lim, Assessing some durability properties of sustainable lightweight oil palm shell concrete incorporating slag and manufactured sand, Journal of Cleaner Production 112 (2016) 763-770.

[2] D. Bouvard, J.M. Chaix, R. Dendievel, A. Fazekas, J.M. Létang, G. Peix, D. Quenard, Characterization and simulation of microstructure and properties of EPS lightweight concrete, Cement and Concrete Research 37(12) (2007) 1666-1673.

[3] M. Maaroufi, K. Abahri, C.E. Hachem, R. Belarbi, Characterization of EPS lightweight concrete microstructure by X-ray tomography with consideration of thermal variations, Construction and Building Materials 178 (2018) 339-348.

[4] U. Anggarini, S. Pratapa, V. Purnomo, N.C.J.O.C. Sukmana, A comparative study of the utilization of synthetic foaming agent and aluminum powder as pore-forming agents in lightweight geopolymer synthesis, 17(1) (2019) 629-638.

[5] V. Vaganov, M. Popov, A. Korjakins, G. Šahmenko, Effect of CNT on microstructure and minearological composition of lightweight concrete with granulated foam glass, (2017).

[6] E. Mohseni, M. Jafar Kazemi, M. Koushkbaghi, B. Zehtab, B. Behforouz, Corrigendum to "Evaluation of mechanical and durability properties of fiber-reinforced lightweight geopolymer composites based on rice husk ash and nanoalumina" [Constr. Build. Mater. 209 (2019) 532–540], Construction and Building Materials 232 (2020) 117262.

[7] Z. Bian, Y. Huang, J.-X. Lu, G. Ou, S. Yang, C.S. Poon, Development of self-foaming cold-bonded lightweight aggregates from waste glass powder and incineration bottom ash for lightweight concrete, Journal of Cleaner Production 428 (2023).

[8] O.A. Abdulkareem, A.M. Mustafa Al Bakri, H. Kamarudin, I. Khairul Nizar, A.e.A. Saif, Effects of elevated temperatures on the thermal behavior and mechanical performance of fly ash geopolymer paste, mortar and lightweight concrete, Construction and Building Materials 50 (2014) 377-387.

[9] M.Y.J. Liu, U.J. Alengaram, M.Z. Jumaat, K.H. Mo, Evaluation of thermal conductivity, mechanical and transport properties of lightweight aggregate foamed geopolymer concrete, Energy and Buildings 72 (2014) 238-245.

[10] O. Youssf, J.E. Mills, M. Elchalakani, F. Alanazi, A.M.J.P. Yosri, Geopolymer concrete with lightweight fine aggregate: material performance and structural application, 15(1) (2022) 171.

[11] R. Rawat, D.J.J.o.S.C.-B.M. Pasla, Mix design of FA-GGBS based lightweight geopolymer concrete incorporating sintered fly ash aggregate as coarse aggregate, 13(8) (2024) 1164-1179.

[12] M.T. Selvi, A. Dasarathy, S.P.J.M.T.P. Ilango, Mechanical properties on light weight aggregate concrete using high density polyethylene granules, 81 (2023) 926-930.

[13] A. Wongsa, V. Sata, P. Nuaklong, P. Chindaprasirt, Use of crushed clay brick and pumice

DOI: https://doi.org/XXXX.XXXX

aggregates in lightweight geopolymer concrete, Construction and Building Materials 188 (2018) 1025-1034.
[14] Z.C. Yong, M.K. Yew, M.C. Yew, J.H. Beh, F.W. Lee, S.K. Lim, L.H. Saw, Utilizing bio-based and industrial waste aggregates to improve mechanical properties and thermal insulation in lightweight foamed macro polypropylene fibre-reinforced concrete, Journal of Building Engineering 91 (2024).
[15] M.Y.J. Liu, U.J. Alengaram, M. Santhanam, M.Z. Jumaat, K.H. Mo, Microstructural investigations of palm oil fuel ash and fly ash based binders in lightweight aggregate foamed geopolymer concrete, Construction and Building Materials 120 (2016) 112-122.
[16] P. Shen, L. Lu, F. Wang, Y. He, S. Hu, J. Lu, H. Zheng, Water desorption characteristics of saturated lightweight fine aggregate in ultra-high performance concrete, Cement and Concrete Composites 106 (2020) 103456.
[17] A.İ. Uğurlu, M.B. Karakoç, A. Özcan, Effect of binder content and recycled concrete aggregate on freeze-thaw and sulfate resistance of GGBFS based geopolymer concretes, Construction and Building Materials 301 (2021).
[18] Sunita, Effect of biomass Ash, foundry sand and recycled concrete aggregate over the strength aspects of the concrete, Materials Today: Proceedings 50 (2022) 2044-2051.
[19] I.S. Agwa, S.A. Mostafa, M.H. Abd-Elrahman, M.J.J.o.B.E. Amin, Effect of Recycled Aggregate Treatment Using Fly Ash, Palm Leaf Ash, and Silica Fume Slurries on the Mechanical and Transport Properties of High-Strength Concrete, (2025) 113292.
[20] P. Rattanachu, P. Toolkasikorn, W. Tangchirapat, P. Chindaprasirt, C. Jaturapitakkul, Performance of recycled aggregate concrete with rice husk ash as cement binder, Cement and Concrete Composites 108 (2020) 103533.
[21] J. de-Prado-Gil, R. Martínez-García, P. Jagadesh, A. Juan-Valdés, M.-I. Gónzalez-Alonso, C.J.A.S.E.J. Palencia, To determine the compressive strength of self-compacting recycled aggregate concrete using artificial neural network (ANN), 15(2) (2024) 102548.
[22] C.J. Zega, Á.A.J.W.m. Di Maio, Use of recycled fine aggregate in concretes with durable requirements, 31(11) (2011) 2336-2340.

DOI: https://doi.org/XXXX.XXXX

Advanced Multidisciplinary Engineering Journal (AMEJ)
ISSN: XXXX-XXXX

Journal Homepage:
https://pub.scientificirg.com/index.php/AMEJ/en

Cite this: AMEJ, xxxx (xx), xxx

Comparative Analysis of Nano Zinc Oxide, Nano Silica Fume, and Nano Marble Powder as Cement Replacements in Self-Compacting Concrete

Sahar A. Mostafa*[1], and *Nasser Alanazi*[2]

[1] Department of Civil Engineering, Faculty of Engineering, Beni-Suef University, Beni-Suef, Egypt,
sahar_abdelsalam2010@yahoo.com

Civil Engineering Department, College of Engineering, University of Ha'il, Ha'il 55474, Saudi Arabia
n.alanazi@uoh.edu.sa

**Corresponding Author: sahar_abdelsalam2010@yahoo.com*

Abstract - Self-compacting concrete (SCC) is an advanced class of concrete that offers significant advantages in terms of constructability and quality. However, achieving an optimal balance between mechanical performance and durability remains challenging. This study investigated the effects of incorporating nano zinc oxide, nano silica fume, and nano marble powder as partial replacements of cement on the fresh, mechanical, and durability properties of SCC. Ten SCC mixtures were prepared, including a control mix and nine nano-modified mixes with varying replacement levels. Nano zinc oxide was used at replacement ratios of 0.5%, 1.0%, and 1.5%, whereas nano silica fume and nano marble powder were incorporated at 1%, 2%, and 3% replacement levels. The fresh properties of SCC were evaluated to ensure compliance with self-compacting requirements, whereas the hardened performance was assessed through compressive strength (CS), splitting tensile strength (TS), and flexural strength (FS) tests at 7 and 28 days. In addition, sorptivity was measured at 28 days to evaluate the durability-related performance. The results demonstrated that the incorporation of nanomaterials significantly influenced the performance of SCC depending on the type and dosage of the nanomaterial. Nano silica fume exhibited the most pronounced improvement in both mechanical strength and durability, with an optimum replacement level of 2%, achieving notable enhancements in compressive, tensile, and FSs, and the lowest sorptivity values. Nano zinc oxide provided moderate but consistent improvements in mechanical properties; however, it increased sorptivity at higher dosages. In contrast, the nano marble powder primarily acted as an inert filler, resulting in moderate strength enhancement and improved durability at low replacement levels, whereas excessive replacement led to marginal performance gains. Overall, the findings highlight the critical role of nanomaterial selection and dosage optimization in enhancing SCC performance.

Received: *19 August 2025*
Revised: *28 September 2025*
Accepted: *29 November 2025*
Available online: *25 December 2025*

Keywords:

-Self-compacting concrete;
-Nanotechnology
-Nano silica fume
-Nano zinc oxide
-Nano marble powder -

DOI: https://doi.org/XXXX.XXXX

Introduction

Self-compacting concrete (SCC) has gained significant attention in recent decades as an advanced class of concrete, characterized by its ability to flow under its own weight, fill formwork, and pass through congested reinforcement without the need for mechanical vibration [1]. This unique behavior results in improved construction efficiency, enhanced surface finish, reduced labor requirements, and minimized noise pollution at construction sites. However, achieving an optimal balance between flowability, segregation resistance, and mechanical performance remains a major challenge in SCC mix design. These challenges have driven extensive research on modifying the binder system and incorporating advanced materials to improve the fresh and hardened properties of SCC [2].

In parallel with the development of SCC, nanotechnology has emerged as a promising approach for enhancing cementitious material performance. Nanosized particles possess extremely high specific surface areas and unique physicochemical characteristics, which enable them to significantly influence cement hydration, microstructural development, and pore structure refinement [3]. When incorporated into concrete, nanomaterials can act as nucleation sites for hydration products, fill nanoscale voids, and enhance the interfacial transition zone (ITZ) between cement paste and aggregates. Consequently, improvements in mechanical strength, durability, and transport properties have been widely reported [4]. Consequently, the application of nanotechnology in SCC has attracted increasing research interest because of the sensitivity of SCC properties to microstructural modifications.

Nano silica fume is one of the most extensively studied nanomaterials in cement-based composites owing to its high pozzolanic reactivity and ultra-fine particle size. Previous studies have demonstrated that nanosilica fume can significantly enhance compressive, tensile, and FSs by promoting the formation of additional C–S–H gel and refining the pore structure [5]. In SCC mixtures, nano silica fume has been shown to improve both mechanical performance and durability-related properties, such as water absorption and permeability, particularly when used at optimized replacement levels. However, excessive incorporation may lead to particle agglomeration and increased water demand, highlighting the importance of optimizing the dosage [6].

Nano-ZnO has also been investigated as a functional nanomaterial in cementitious systems [7]. Research has indicated that nano-Zn particles can influence hydration kinetics, improve early age strength development, and enhance microstructural densification [8]. In SCC, nano-ZnO has been reported to improve the mechanical performance through filler effects and hydration acceleration, particularly at low replacement levels. Nevertheless, some studies have noted that improper dispersion or higher dosages may adversely affect durability-related properties owing to changes in pore connectivity, emphasizing the need for careful evaluation of its performance when used as a partial cement replacement [9].

In contrast, nano marble powder has received comparatively less attention despite its potential as a sustainable and cost-effective nanofiller [10]. Derived from marble waste, nano marble powder primarily acts as an inert material that enhances particle packing and matrix densification in cementitious materials [11]. Previous studies have reported moderate improvements in the mechanical properties and durability of concrete when nano marble powder is used at low replacement levels. In SCC applications, its fine particle size may contribute to improved flowability and reduced porosity; however, excessive replacement of cement can lead to binder dilution and reduced hydration product. Therefore, understanding the combined effects of the nano marble powder on the fresh, mechanical, and durability properties of SCC remains an important research gap [12].

Based on the above considerations, the present study aims to investigate the influence of nano-ZnO, nano-silica fume, and nano marble powder as partial replacements of cement on the fresh, mechanical, and durability properties of SCC. Different

DOI: https://doi.org/XXXX.XXXX

replacement levels were adopted to identify the optimum dosage of each nanomaterial. The performance of the nanomodified SCC mixtures was evaluated in terms of CS, TS, FS, and sorptivity at different curing ages. This comprehensive experimental approach provides valuable insights into the effectiveness of various nanomaterials in enhancing SCC performance and contributes to the development of optimized, high-performance, and durable SCC mixtures [13].

The significance of this research lies in its comprehensive evaluation of the combined mechanical and durability performance of SCC incorporating different nano materials as partial replacements of cement. While previous studies have extensively examined individual nanomaterials in conventional concrete, limited research has systematically compared the effects of nano-ZnO, nano silica fume, and nano marble powder within the same SCC framework and under identical testing conditions. This study addresses this gap by providing a direct comparison of the influence of nanomaterial type and dosage on compressive, tensile, and FSs, as well as sorptivity as a key durability indicator. Moreover, the use of nano marble powder derived from waste materials introduces an environmentally beneficial perspective by promoting sustainable construction practices through waste valorization and cement reduction. The findings of this study contribute to a deeper understanding of the role of nanoscale modifications in SCC, identify optimal replacement levels for each nanomaterial, and offer practical guidance for designing high-performance and durable SCC mixtures. Consequently, this study provides valuable insights for researchers and practitioners seeking to enhance SCC performance using advanced and sustainable nanobased approaches.

Experimental program

A. Raw materials

Ordinary Portland cement (OPC) was used as the primary binder in this study, with a cement content of 550 kg/m³ to provide sufficient paste volume and ensure the flowability and stability required for the SCC. The cement was obtained from a local cement manufacturer and complied with ASTM C150/C150M requirements. Silica fume was incorporated as a supplementary cementitious material at a dosage of 27.5 kg/m³ to enhance particle packing, reduce pore connectivity, and improve the fresh and hardened properties of the concrete. The silica fume consisted mainly of amorphous silicon dioxide, met the specifications of ASTM C1240, and was supplied by a certified commercial source.

Natural aggregates were used in both the coarse and fine fractions. Coarse aggregates with a maximum nominal size suitable for SCC mixtures were used at a content of 762 kg/m³ to achieve adequate flow without blocking or segregation. Fine aggregates were incorporated at the same dosage (762 kg/m³) and had a well-graded particle size distribution to enhance homogeneity and passing ability. Both coarse and fine aggregates were sourced from local quarries and satisfied the grading, cleanliness, and physical property requirements specified in ASTM C33/C33M standard.

Potable water conforming to ASTM C1602/C1602M [14] was used for mixing at a content of 184.8 L/m³, ensuring compatibility with cement hydration and durability. A high-range water-reducing admixture (HRWRA) was added at a dosage of 6.93 L/m³ to achieve self-compacting characteristics without increasing the water-to-binder ratio. The superplasticizer was a polycarboxylate-ether-based admixture supplied by a commercial manufacturer and complied with ASTM C494/C494M Type F **[15]**. The optimized combination of cementitious materials, aggregate grading, and chemical admixture resulted in an SCC mixture exhibiting a slump flow diameter exceeding 65 cm in accordance with ASTM C1611/C1611M **[16]**, adequate passing ability, and a characteristic cube CS of 73.6 MPa. **Tab. 1** summarizes the mix proportions

Tab. 1. Mix proportions

Item	Value
Cement (kg/m³)	550
Silica fume (kg/m³)	27.5
Coarse aggregate (kg/m³)	762
Fine aggregate (kg/m³)	762
Water (L/m³)	184.8

DOI: https://doi.org/XXXX.XXXX

Superplasticizer (L/m³)	6.93
Slump flow diameter (cm)	≥ 65
Time to reach 50 cm slump, T_{50} (s)	4.2
J-ring height difference (cm)	0.4
Characteristic cube strength (MPa)	73.6

A. Preparation of Nano Materials

Nano-sized zinc oxide, nano silica fume, and nano marble powder were prepared using a mechanical grinding technique to achieve particle sizes in the nanometer range that are suitable for SCC applications. The raw materials were initially dried to remove any residual moisture and then subjected to high-energy mechanical milling using a laboratory ball mill. The grinding process was performed for a controlled duration to ensure sufficient particle size reduction while avoiding excessive agglomeration [17]. The milling parameters, including the rotation speed and grinding time, were carefully selected to obtain uniformly fine particles with a high specific surface area. The produced nanomaterials were subsequently sieved and stored in airtight containers to prevent moisture absorption and particle agglomeration before use. Mechanical grinding was selected because of its simplicity, scalability, and effectiveness in producing nanoscale powders for cementitious systems [18].

B. Dispersion of Nano Materials in SCC

The dispersion of n-ZnO, n-SF, and n-MP within the SCC matrix was performed to ensure a homogeneous distribution and prevent particle agglomeration, which could negatively affect the fresh and hardened properties of the concrete. The nanomaterials were first dispersed in a portion of the mixing water using mechanical stirring to promote particle separation and uniform suspension using a magnetic stirrer shown in **Fig. 1** The dispersed suspension was then introduced into the concrete mixture during mixing, followed by the addition of a polycarboxylate-ether-based superplasticizer to further enhance dispersion through electrostatic repulsion and steric hindrance mechanisms. This dispersion approach improved the stability of fresh SCC, enhanced particle packing, and facilitated better interaction between the nanoparticles and cement hydration products. Consequently, flowability, reduced segregation, and enhanced mechanical performance of the hardened SCC were achieved [19].

Fig. 1. Raw materials

C. Mixing procedures

The mixing procedures for the SCC mixtures were carefully designed to ensure uniformity, proper dispersion of nanomaterials, and consistent fresh properties. Initially, all dry constituents, including cement, aggregates, and the designated amount of nanomaterial (nano zinc oxide, nano silica fume, or nano marble powder) used as a partial replacement of cement, were dry-mixed in a pan mixer for approximately 2–3 min to achieve a homogeneous blend. This step was essential to prevent the localized concentration of nanoparticles and ensure an even distribution within the binder matrix. Subsequently, approximately two-thirds of the mixing water was gradually added, while mixing continued to initiate cement hydration and improve workability. The remaining mixing water, pre-mixed with the required dosage of polycarboxylate-ether-based superplasticizer, was then introduced slowly to enhance flowability and promote further dispersion of nanoparticles through electrostatic repulsion and steric hindrance mechanisms. Mixing was continued for an additional 3–5 min until a uniform, highly flowable, and stable SCC mixture was obtained. Special attention was given to the mixing time and sequence to minimize nanoparticle agglomeration and segregation, ensuring that all SCC mixtures exhibited consistent fresh properties before casting. Immediately after

DOI: https://doi.org/XXXX.XXXX

mixing, the fresh concrete was subjected to SCC workability tests before casting it into molds for subsequent curing and testing

D. Testing

An experimental testing program was conducted to assess the performance of the formulated SCC combination. Ten concrete mixtures were formulated, comprising one control mixture devoid of nanomaterials and nine modified mixtures integrating three distinct dosage levels of each nanomaterial (nano-ZnO, nano-SF, and nano-MP). The fresh and hardened characteristics of all mixtures were evaluated under uniform curing and testing settings to ensure the uniformity and reliability of the outcomes. CS tests were conducted on the cube specimens at curing ages of 7 and 28 days in accordance with ASTM C39/C39M. The TS was assessed at identical ages in accordance with ASTM C496/C496M, whereas FS tests were performed on prism specimens according to ASTM C78/C78M. To assess the durability characteristics of the SCC mixtures, water sorptivity was quantified at 28 days of curing in line with ASTM C1585 [20]. All specimens were immersed in water under regulated laboratory conditions until they attained the specified testing age as shown in **Fig.2**. The test findings were used to evaluate the impact of nanomaterial type and dosage on the mechanical and transport properties of SCC[21].

Fig.2: Mixing and testing procedures

Results and discussion

A. Compressive strength at 7 days

Fig. 3 illustrates the CS results of the SCC mixtures incorporating different nanomaterials as partial replacements for cement, compared with the control mix. The control mix (CT00), which contained no nanomaterials, achieved a CS of approximately 39.47 MPa. The incorporation of nano zinc oxide at replacement levels of 0.5%, 1.0%, and 1.5% resulted in a gradual improvement in CS, reaching approximately 40.41, 41.60, and 42.90 MPa, respectively. This corresponds to an enhancement of approximately 2.4%, 5.4%, and 8.7% relative to the control mix, respectively. The observed improvement can be attributed to the filler effect of the nano-Zn particles and their ability to accelerate cement hydration by providing additional nucleation sites for the hydration products [7].

A more pronounced enhancement was observed for mixes incorporating nano silica fume at replacement levels of 1%, 2%, and 3%. The CS increased significantly to approximately 44.13, 47.53, and 45.43 MPa. The mix containing 2% nano silica fume exhibited the highest CS among all the tested mixes, with an improvement of nearly 20.4% compared with the control mix. This superior performance is mainly attributed to the high pozzolanic reactivity of the nano silica fume, which enhances the formation of secondary C–S–H gel and significantly refines the pore structure. However, a slight reduction in strength was observed at 3% replacement, likely due to particle agglomeration and an increase in water demand, which may have negatively affected dispersion efficiency and matrix homogeneity [22]

In contrast, the incorporation of nano marble powder at replacement levels of 1%, 2%, and 3% showed a marginal improvement at lower dosages, followed by a reduction in CS at higher percentages of replacement. The CS values were approximately 39.57, 40.05, and 38.04 MPa for NM10, NM20, and NM30, respectively. While the nanomarbles primarily act as an inert filler that enhances particle packing and matrix densification at low replacement levels, excessive replacement of cement reduces the available binder content and limits the formation of hydration products, resulting in lower strength development [12, 23].

Overall, the results demonstrate that replacing cement with nanomaterials significantly influences the CS of SCC, depending on both the type and dosage of the nanomaterial. Nano silica fume was the most effective additive, particularly at an optimum replacement level of 2%, whereas nano zinc oxide provided moderate but consistent strength enhancement.

DOI: https://doi.org/XXXX.XXXX

Conversely, the nano marble powder exhibited limited effectiveness and should be used at low replacement levels to avoid adverse effects on mechanical performance. These findings highlight the importance of optimizing the nanomaterial dosage to balance the benefits of the nanomaterial-scale effects with the overall binder chemistry and rheology of SCC.

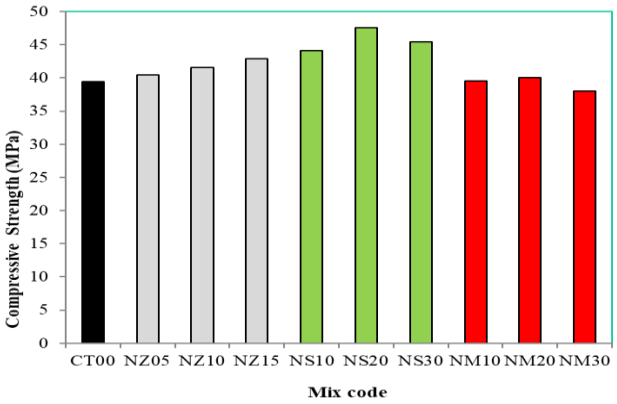

Fig. 3. Compressive strength for SCC with different types of nanoparticles

B. Compressive strength at 28 days

Fig. 4 presents the CS results of the SCC mixtures at 28 days of curing for the control mix and mixes incorporating different nanomaterials as partial replacements for cement. As expected, all mixtures exhibited a noticeable increase in CS compared to their corresponding 7-day results, reflecting the continued hydration process and progressive densification of the cementitious matrix. The control mix (CT00) achieved a CS of approximately 52.01 MPa at 28 days, which served as the reference for evaluating the effectiveness of incorporating the nanomaterial.

The inclusion of nano-ZnO at replacement levels of 0.5%, 1.0%, and 1.5% led to a consistent enhancement in CS, with values of approximately 53.88 MPa, 55.65 MPa, and 57.20 MPa, respectively. These results correspond to strength improvements of approximately 3.6%, 7.0%, and 10.0% compared to the control mix. The continued strength gain at 28 d suggests that nano-ZnO not only accelerates early hydration but also contributes to long-term strength development by improving microstructural refinement and enhancing the interfacial transition zone (ITZ) between the cement paste and aggregates.

A more pronounced improvement was observed in the mixes incorporating nanosilica fume. Replacement levels of 1%, 2%, and 3% resulted in CSs of approximately 58.77, 65.50, and 63.21 MPa, respectively. The mixture containing 2% nano silica fume (NS20) exhibited the highest CS among all tested mixes, with an enhancement of nearly 26% relative to the control mix. This superior performance is primarily attributed to the high pozzolanic reactivity and extremely fine particle size of the nano silica fume, which promotes the formation of additional C–S–H gel, significantly reduces porosity, and refines the pore structure. The slight reduction in strength observed at the 3% replacement level may be attributed to particle agglomeration and increased water demand, which can negatively affect the dispersion efficiency and limit further strength development.

In contrast, the incorporation of nano-marble powder showed moderate improvements at 28 d. The CSs of NM10, NM20, and NM30 were approximately 57.00, 59.36, and 59.14 MPa, respectively. While the nano marble powder primarily acts as an inert filler, its fine particle size enhances the packing density and contributes to matrix densification at moderate replacement levels. However, increasing the replacement ratio beyond the optimum level reduces the effective cement content, which limits hydration product formation and restricts further strength enhancement.

Overall, the 28-day results confirmed that the effectiveness of nanomaterials in SCC is strongly dependent on both the material type and dosage. Nano silica fume demonstrated the most significant contribution to long-term CS, particularly at an optimum replacement level of 2%, followed by nano zinc oxide, which provided a steady and sustained improvement. The nano marble powder exhibited limited effectiveness and should be carefully optimized to balance the filler benefits against the cement dilution effects. These findings highlight the importance of dosage optimization when incorporating

DOI: https://doi.org/XXXX.XXXX

nanomaterials as cement replacements in high-performance SCC mixtures.

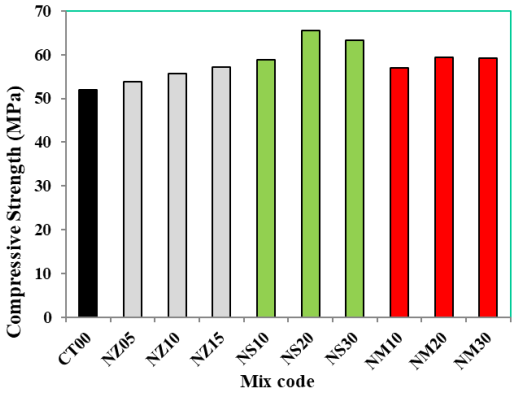

Fig. 4. Compressive strength for SCC with different types of nanoparticles

C. Early tensile strength

Fig. 5 illustrates the TS results of the SCC mixtures at 7 days of curing for the control mix and mixes incorporating different nanomaterials as partial replacements of cement. The control mix (CT00) recorded TS of approximately 6.32 MPa, which was used as a benchmark to assess the influence of nanomaterial incorporation at early ages. In general, all modified mixes exhibited comparable or improved tensile strength values relative to the control mix, indicating the positive role of nanomaterials in enhancing early-age tensile performance.

For mixes incorporating nano-ZnO at replacement levels of 0.5%, 1.0%, and 1.5%, the TS increased gradually to approximately 6.49, 6.66, and 6.86 MPa, respectively. These values represent improvements of approximately 2.7%, 5.4%, and 8.5% compared to the control mix. The enhancement in tensile strength can be attributed to the nano zinc particles acting as micro-fillers that improve particle packing and reduce microcrack initiation, in addition to their contribution to accelerating cement hydration at early ages, which improves the matrix cohesion.

A more significant improvement was observed in the mixes containing nanosilica fume. Replacement levels of 1%, 2%, and 3% resulted in TS values of approximately 7.20, 7.60, and 7.30 MPa, respectively. The mix with 2% nano silica fume (NS20) exhibited the highest tensile strength among all tested mixes, achieving an enhancement of nearly 20% relative to the control mix. This pronounced improvement is mainly attributed to the high pozzolanic activity and extremely fine particle size of the nano silica fume, which promotes the formation of additional C–S–H

gel and significantly strengthens the interfacial transition zone (ITZ). The slight reduction observed at the 3% replacement level may be related to particle agglomeration and reduced dispersion efficiency at higher nanofiller contents.

In contrast, the mixes incorporating nano-marble powder showed limited improvement in TS. The values of NM10, NM20, and NM30 were approximately 6.23, 6.45, and 6.12 MPa, respectively. While the nano marble powder contributes to matrix densification through a filler effect at lower dosages, its largely inert nature and the dilution of cement content limit its effectiveness in enhancing tensile resistance, particularly at higher replacement levels.

Overall, the 7-day tensile strength results demonstrate that nanosilica fume is the most effective nanomaterial in improving the early age tensile performance of SCC, followed by nanozinc oxide, which provides moderate but consistent enhancement. The nano marble powder exhibited minimal influence and should be used cautiously to avoid compromising the tensile behavior. These results highlight the sensitivity of tensile strength to nanomaterial type, dosage, and dispersion efficiency at early curing ages.

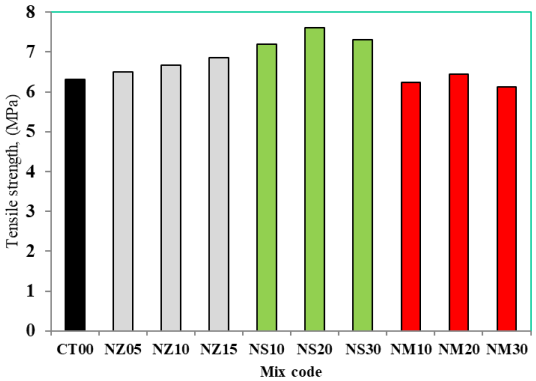

DOI: https://doi.org/XXXX.XXXX

Fig. 5. Early tensile strength for SCC with different types of nanoparticles

D. 28 days tensile strength

Fig. 6 shows the TS results of the SCC mixtures at 28 days of curing for the control and nanomodified mixes. A general increase in tensile strength was observed for all mixtures compared to the corresponding 7-day results, reflecting the continuous hydration process and the progressive development of a denser and more cohesive cementitious matrix. The control mix (CT00) exhibited aTS of approximately 8.45 MPa at 28 d, which served as the reference value for assessing the effectiveness of the incorporation of the nanomaterial.

The incorporation of nano-ZnO as a partial replacement of cement resulted in a steady enhancement in tensile strength with increasing dosage. The mixes NZ05, NZ10, and NZ15 achieved tensile strength values of approximately 8.67 MPa, 8.90 MPa, and 9.32 MPa, respectively, corresponding to improvements of approximately 2.6%, 5.3%, and 10.3% relative to the control mix. This behavior indicates that nano-ZnO contributes not only to early age strength enhancement but also to sustained tensile performance at later ages, mainly through improved particle packing, reduced microcrack propagation, and refinement of the interfacial transition zone (ITZ).

A more pronounced improvement was observed in the mixes incorporating nano silica fume. At replacement levels of 1%, 2%, and 3%, the tensile strength increased significantly to approximately 9.70 MPa, 10.33 MPa, and 10.05 MPa, respectively. The mix containing 2% nano silica fume (NS20) demonstrated the highest tensile strength among all tested mixtures, with an enhancement of nearly 22% compared with the control mix. This superior performance can be attributed to the high pozzolanic reactivity and ultrafine particle size of the nano silica fume, which promotes the formation of additional C–S–H gel, strengthens the paste–aggregate bond, and significantly improves the resistance to tensile cracking. The slight reduction observed at the 3% replacement level suggests that excessive nano silica fume may lead to particle agglomeration and increased water demand, which can adversely affect the dispersion efficiency.

In contrast, the mixes incorporating nano marble powder showed moderate improvements in the tensile strength at 28 days. The tensile strengths of NM10, NM20, and NM30 were approximately 9.12, 9.56, and 9.46 MPa, respectively. Although the nano marble powder mainly acts as an inert filler, its fine particle size enhances matrix densification and contributes to improved tensile behavior at moderate replacement levels. However, increasing the replacement ratio beyond the optimum level limits cement hydration owing to binder dilution, resulting in marginal gains or slight reductions in tensile strength.

Overall, the 28-day tensile strength results confirmed that the nano silica fume is the most effective nano material for enhancing the tensile performance of SCC, particularly at an optimum replacement level of 2%, followed by nano zinc oxide, which provides consistent and gradual improvement. The nano marble powder exhibited limited effectiveness and should be carefully optimized to avoid compromising the tensile resistance. These findings emphasize the strong dependence of the tensile behavior on the nanomaterial type, dosage, and dispersion efficiency in SCC mixtures.

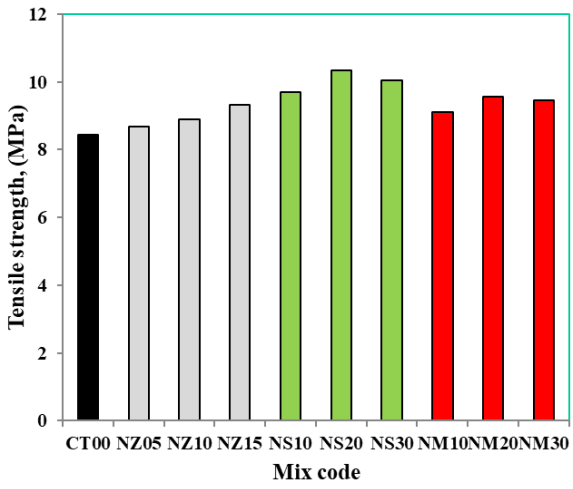

Fig. 6. 28-days tensile strength for SCC with different types of nanoparticles

E. Early flexural strength

Fig.7 presents the FS results of the SCC mixtures at 7 days of curing for the control and nanomodified mixes. The control mix

DOI: https://doi.org/XXXX.XXXX

(CT00) exhibited an FS of approximately 8.53 MPa, which was adopted as the reference value to evaluate the influence of nanomaterial incorporation on the early age flexural performance. In general, all nanomodified mixtures demonstrated equal or improved FS compared to the control mix, indicating the beneficial role of nanomaterials in enhancing crack resistance and load-carrying capacity at early ages.

For mixes incorporating nano ZnO at replacement levels of 0.5%, 1.0%, and 1.5%, the FS increased gradually to approximately 8.67 MPa, 9.00 MPa, and 9.37 MPa, respectively. These values corresponded to improvements of approximately 1.6%, 5.5%, and 9.8% relative to the control mix. The enhancement in FS can be attributed to the ability of the nano-Zn particles to improve matrix homogeneity and reduce microcrack initiation, particularly under bending stresses, where tensile cracking governs the failure behavior.

A more pronounced improvement was observed in the mixes incorporating nanosilica fume. Replacement levels of 1%, 2%, and 3% resulted in FS values of approximately 9.38, 9.74, and 9.63 MPa, respectively. The mix containing 2% nano silica fume (NS20) achieved the highest FS among all tested mixes, with an enhancement of nearly 14% compared with the control mix. This improvement is mainly attributed to the high pozzolanic reactivity and ultra-fine particle size of the nano silica fume, which enhances the formation of secondary C–S–H gel and significantly strengthens the interfacial transition zone (ITZ), thereby improving the resistance to flexural cracking. The slight reduction observed at the 3% replacement level suggests that excessive nano silica fume may result in particle agglomeration, reducing its effectiveness at early ages [24, 25].

In contrast, the incorporation of nano marble powder showed limited improvement in FS at 7 d. The FSs of NM10, NM20, and NM30 were approximately 8.83, 9.16, and 8.72 MPa, respectively. While nanomarbles mainly act as inert fillers that improve particle packing and matrix densification at low dosages, higher replacement levels reduce the effective cement content, limiting early age strength development.

Overall, the 7-day FS results demonstrate that nanosilica fume is the most effective nanomaterial for enhancing the early age flexural performance of SCC, followed by nano-ZnO, which provides gradual and consistent improvement. The nano marble powder exhibited modest effectiveness and should be optimized carefully to avoid compromising the early age flexural resistance. These findings highlight the sensitivity of FS to nanomaterial type, dosage, and dispersion efficiency during the early curing stages.

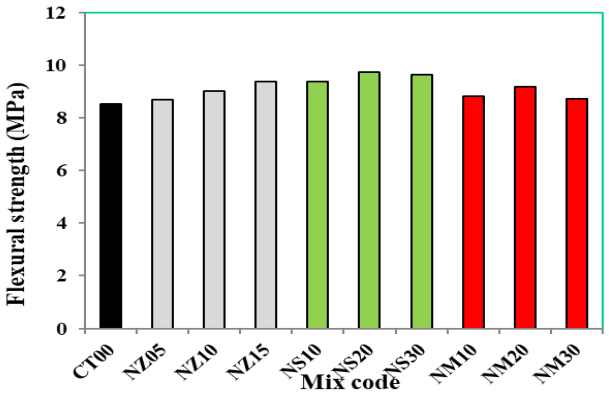

Fig. 7. Flexural strength for SCC with different types of nanoparticles

F. flexural strength at 28 days

Fig. 8 shows the FS results of the SCC mixtures at 28 days of curing for the control mix and mixes incorporating different nanomaterials as partial replacements of cement. As expected, all mixtures exhibited a significant increase in FS compared to the corresponding 7-day results, indicating a continuous hydration process and progressive improvement in the microstructure of the cementitious matrix. The control mix (CT00) achieved an FS of approximately 12.75 MPa at 28 d, which was considered the reference value for evaluating the influence of nanomaterial incorporation.

The addition of nano zinc oxide at replacement levels of 0.5%, 1.0%, and 1.5% resulted in noticeable enhancements in FS, reaching approximately 14.62, 15.42, and 16.37 MPa,

DOI: https://doi.org/XXXX.XXXX

respectively. These values correspond to improvements of approximately 14.7%, 21.0%, and 28.3% compared to the control mix. The observed enhancement can be attributed to the ability of the nano Zn particles to refine the pore structure, improve matrix continuity, and enhance crack-bridging capacity under bending stresses, particularly at later curing ages [26].

A more pronounced improvement was observed in mixtures incorporating nanosilica fume. Replacement levels of 1%, 2%, and 3% resulted in FS values of approximately 17.62, 18.00, and 16.94 MPa, respectively. The mixture containing 2% nano silica fume (NS20) achieved the highest FS among all the tested mixtures, with an improvement of nearly 41% relative to the control mix. This superior performance is mainly attributed to the high pozzolanic activity and ultrafine particle size of the nano silica fume, which promotes the formation of C–S–H gel, significantly densifies the matrix, and strengthens the interfacial transition zone (ITZ). The slight reduction in FS at 3% replacement may be related to particle agglomeration and increased water demand, which negatively affect dispersion efficiency and crack resistance.

In contrast, the incorporation of the nano marble powder led to moderate improvements in the FS at 28 d. The FSs of NM10, NM20, and NM30 were approximately 13.50, 13.87, and 12.95 MPa, respectively. While the nano marble powder primarily acts as an inert filler that enhances particle packing and matrix densification at low to moderate replacement levels, excessive replacement of cement reduces the amount of hydration products, thereby limiting further enhancement in flexural performance [27, 28].

Overall, the 28-day FS results confirm that nanosilica fume is the most effective nanomaterial for improving the flexural behavior of SCC, particularly at an optimum replacement level of 2%, followed by nano ZnO, which provides consistent and substantial strength gains with increasing dosage. The nano marble powder exhibited limited effectiveness and should be carefully optimized to avoid adverse effects on flexural performance. These findings emphasize the strong dependence of FS on nanomaterial type, dosage, and curing age in SCC mixtures [21].

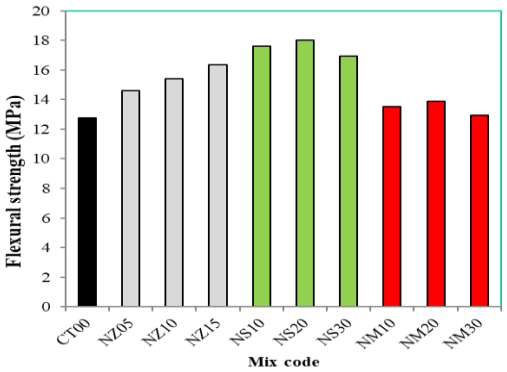

Fig. 8. Flexural strength for SCC with different types of nanoparticles

G. Sorptivity

Fig. 9 presents the sorptivity results of the SCC mixtures at 28 days of curing for the control mix and mixes incorporating different nanomaterials as partial replacements of cement. Sorptivity is a key durability indicator that reflects the capillary water absorption behavior and pore connectivity within the concrete matrix. The control mix (CT00) exhibited a sorptivity value of approximately 2.057×10^{-6} m/s$^{1/2}$, which served as a reference for evaluating the influence of nanomaterial incorporation on the transport properties of SCC.

The incorporation of nano zinc oxide led to an increase in the sorptivity values compared to the control mix. At replacement levels of 0.5%, 1.0%, and 1.5%, the sorptivity values increased to approximately 2.449×10^{-6}, 2.254×10^{-6}, and 2.223×10^{-6} m/s, respectively. This increase suggests that nano-ZnO, despite its positive effect on mechanical properties, may alter pore continuity or introduce microstructural heterogeneity at higher dosages, potentially due to incomplete dispersion or localized agglomeration, which can increase capillary suction pathways [29].

In contrast, mixes incorporating nano silica fume exhibited a significant reduction in sorptivity values compared to the control mix. Replacement levels of 1%, 2%, and 3% resulted in sorptivity values of approximately 1.715×10^{-6}, 1.617×10^{-6}, and 1.656×10^{-6} m/s$^{1/2}$, respectively. The mix containing 2%

DOI: https://doi.org/XXXX.XXXX

nano silica fume (NS20) achieved the lowest sorptivity value among all tested mixes, representing a reduction of approximately 21% compared with the control mix. This pronounced improvement is attributed to the high pozzolanic reactivity and ultra-fine particle size of the nano silica fume, which promotes the formation of additional C–S–H gel, significantly refines the pore structure, and reduces capillary pore connectivity. The slight increase observed at 3% replacement may be associated with particle agglomeration and reduced dispersion efficiency.

The incorporation of nano marble powder resulted in moderate reductions in sorptivity compared with the control mix. The sorptivity values for NM10, NM20, and NM30 were approximately 1.911×10^{-6}, 1.890×10^{-6}, and 1.763×10^{-6} m/s², respectively. Although the nano marble powder is largely inert, its fine particle size contributes to pore filling and matrix densification, thereby reducing water absorption at moderate replacement levels. However, its effectiveness remains lower than that of nanosilica fume because of the absence of significant pozzolanic activity.

Overall, the 28-day sorptivity results clearly demonstrated that the nano silica fume is the most effective nano material for enhancing the durability performance of SCC by reducing capillary water absorption. Nano marble powder provides moderate improvement through a filler effect, whereas nano zinc oxide may negatively influence sorptivity when used as a cement replacement. These findings highlight the importance of optimizing the nanomaterial type and dosage to achieve a balanced improvement in both the mechanical and durability properties of SCC.

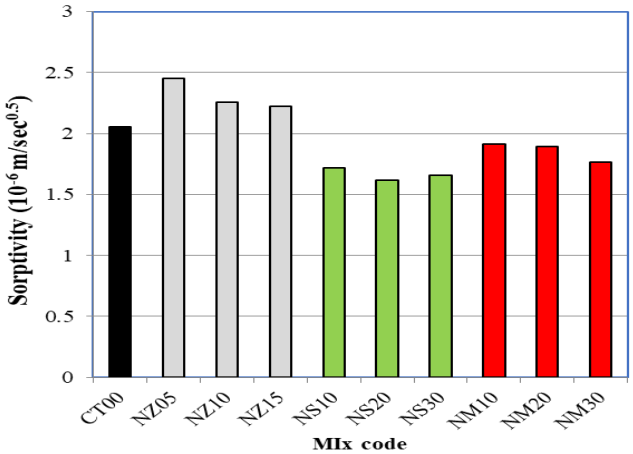

Fig. 9. Sorptivity for SCC with different types of nanoparticles

Conclusion

This study evaluated the influence of different nanomaterials as partial replacements of cement on the fresh, mechanical, and durability properties of SCC. Based on the experimental results and comparative analysis, the incorporation of nanomaterials significantly affects the performance of SCC, with the observed behavior strongly dependent on the type and replacement level of the nanomaterial. Among the investigated nanomaterials, nano silica fume proved to be the most effective, particularly at an optimum replacement level of 2%, resulting in the greatest improvements in compressive, splitting tensile, and FSs at both 7 and 28 days. The use of nanosilica fume also led to a substantial reduction in sorptivity at 28 d, indicating a denser microstructure and improved durability performance owing to enhanced pozzolanic activity and pore refinement. Nano zinc oxide provided moderate and consistent improvements in the mechanical properties, particularly at higher replacement levels. However, it exhibited increased sorptivity, suggesting a potential negative impact on durability when used as a cement replacement. The nano marble powder primarily acted as an inert filler, contributing to improved particle packing and matrix densification at low to moderate replacement levels, whereas excessive replacement resulted in limited mechanical enhancement owing to cement dilution effects. The results highlight that improper dosage or excessive incorporation of nanomaterials may lead to particle agglomeration, reduced dispersion efficiency, and diminished performance benefits.

DOI: https://doi.org/XXXX.XXXX

The combined evaluation of mechanical and durability properties emphasizes the importance of optimizing the nanomaterial type and dosage to achieve balanced and high-performance SCC mixtures. The findings of this study support the potential application of nano-based cement replacements in SCC for developing high-performance and more sustainable concrete, while also promoting the utilization of industrial waste materials such as marble powder.

References

[1] B. Cheng, L. Mei, W.-J. Long, S. Kou, L. Li, S. Geng, Ai-guided proportioning and evaluating of self-compacting concrete based on rheological approach, Construction and Building Materials 399 (2023).
[2] Z. Salari, B. Vakhshouri, S. Nejadi, Analytical review of the mix design of fiber reinforced high strength self-compacting concrete, Journal of Building Engineering 20 (2018) 264-276.
[3] I.S. Agwa, O.M. Omar, B.A. Tayeh, B.A. Abdelsalam, Effects of using rice straw and cotton stalk ashes on the properties of lightweight self-compacting concrete, Construction and Building Materials 235 (2020).
[4] A.S. Aadi, N.H. Sor, A.A. Mohammed, The behavior of eco-friendly self – compacting concrete partially utilized ultra-fine eggshell powder waste, Journal of Physics: Conference Series 1973(1) (2021).
[5] Z. Guo, Q. Sun, L. Zhou, T. Jiang, C. Dong, Q. Zhang, Mechanical properties, durability and life-cycle assessment of waste plastic fiber reinforced sustainable recycled aggregate self-compacting concrete, Journal of Building Engineering 91 (2024).
[6] Z. Algin, M. Ozen, The properties of chopped basalt fibre reinforced self-compacting concrete, Construction and Building Materials 186 (2018) 678-685.
[7] T. Vulic, M. Hadnadjev-Kostic, O. Rudic, M. Radeka, R. Marinkovic-Neducin, J. Ranogajec, Improvement of cement-based mortars by application of photocatalytic active Ti–Zn–Al nanocomposites, Cement and Concrete Composites 36 (2013) 121-127.
[8] A. Adesina, Durability Enhancement of Concrete Using Nanomaterials: An Overview, Materials Science Forum 967 (2019) 221-227.
[9] A. P. P, D.K. Nayak, B. Sangoju, R. Kumar, V. Kumar, Effect of nano-silica in concrete; a review, Construction and Building Materials 278 (2021) 122347.
[10] M.A.B. Martins, L.R.R. Silva, B.H.B. Kuffner, R.M. Barros, M.L.N.M. Melo, Behavior of high strength self-compacting concrete with marble/granite processing waste and waste foundry exhaust sand, subjected to chemical attacks, Construction and Building Materials 323 (2022).
[11] A. Essam, S.A. Mostafa, M. Khan, A.M.J.C. Tahwia, B. Materials, Modified particle packing approach for optimizing waste marble powder as a cement substitute in high-performance concrete, 409 (2023) 133845.
[12] M.A. Abouelnour, M.A. Abd EL-Aziz, K.M. Osman, I.N. Fathy, B.A. Tayeh, M.E.J.C. Elfakharany, B. Materials, Recycling of marble and granite waste in concrete by incorporating nano alumina, 411 (2024) 134456.
[13] <2016_Book_InCIEC2015.pdf>.
[14] ASTM C 1602: standard specification for mixing water used in the production of hydraulic cement concrete. 2006.
[15] ASTM C494/C494M–11. Standard specification for chemical admixtures for concrete.
[16] Y. Su, J. Li, C. Wu, P. Wu, Z.-X. Li, Influences of nano-particles on dynamic strength of ultra-high performance concrete, Composites Part B: Engineering 91 (2016) 595-609.
[17] B.A. Tayeh, A.A. Hakamy, M.S. Fattouh, S.A. Mostafa, The effect of using nano agriculture wastes on microstructure and electrochemical performance of ultra-high-performance fiber reinforced self-compacting concrete under normal and acceleration conditions, Case Studies in Construction Materials 18 (2023).
[18] A.S. Faried, S.A. Mostafa, B.A. Tayeh, T.A. Tawfik, The effect of using nano rice husk ash of different burning degrees on ultra-high-performance concrete properties, Construction and Building Materials 290 (2021) 123279.
[19] C.M. Kansal, R. Goyal, Effect of nano silica, silica fume and steel slag on concrete properties, Materials Today: Proceedings 45 (2021) 4535-4540.
[20] ASTM C1585-13: Standard Test Method for Rate of Absorption of Water (Sorptivity) of Concrete. ASTM International. ASTM International, West Conshohocken (2013).
[21] A. Joshaghani, M. Balapour, M. Mashhadian, T. Ozbakkaloglu, Effects of nano-TiO2, nano-Al2O3, and nano-Fe2O3 on rheology, mechanical and durability properties of self-consolidating concrete (SCC): An experimental study, Construction and Building Materials 245 (2020) 118444.
[22] R. Ma, L. Guo, W. Sun, J. Liu, J. Zong, Strength-enhanced ecological ultra-high performance fibre-reinforced cementitious composites with nano-silica, Materials and Structures 50(2) (2017).
[23] A.A. Mahmoud, A.A. El-Sayed, A.M. Aboraya, I.N. Fathy, M.A. Abouelnour, I.M.J.S.R. Nabil, Influence of sustainable waste granite, marble and nano-alumina additives on ordinary concretes: a physical, structural, and radiological study, 14(1) (2024) 22011.

DOI: https://doi.org/XXXX.XXXX

[24] T. Luo, C. Hua, L. Li, T. Zhang, X. Lu, L.G. Li, S.A. Mostafa, The effect of micro silica fume (MSF) content on pore fractal dimension (PFD) and mechanical properties of self-consolidating concrete, Case Studies in Construction Materials 21 (2024).
[25] I.S. Agwa, S.A. Mostafa, M.H. Abd-Elrahman, M.J.J.o.B.E. Amin, Effect of Recycled Aggregate Treatment Using Fly Ash, Palm Leaf Ash, and Silica Fume Slurries on the Mechanical and Transport Properties of High-Strength Concrete, (2025) 113292.
[26] I.H. Yang, J. Park, A Study on the Thermal Properties of High-Strength Concrete Containing CBA Fine Aggregates, Materials (Basel) 13(7) (2020).
[27] G. Kaplan, A. Öz, B. Bayrak, A.C. Aydın, The effect of geopolymer slurries with clinker aggregates and marble waste powder on embodied energy and high-temperature resistance in prepacked concrete: ANFIS-based prediction model, Journal of Building Engineering 67 (2023).
[28] S. Zhang, K. Cao, C. Wang, X. Wang, J. Wang, B.J.C. Sun, B. Materials, Effect of silica fume and waste marble powder on the mechanical and durability properties of cellular concrete, 241 (2020) 117980.
[29] P. Murthi, V. Lavanya, K. Poongodi, Effect of eggshell powder on structural and durability properties of high strength green concrete for sustainability: A critical review, Materials Today: Proceedings (2022).

DOI: https://doi.org/XXXX.XXXX

Advanced Multidisciplinary Engineering Journal (AMEJ)
ISSN: XXXX-XXXX

Journal Homepage:
https://pub.scientificirg.com/index.php/AMEJ/en

Cite this: AMEJ xxxx (xx), xxx

Towards Sustainable Ultra-High-Performance Concrete: Role of Nano Rice Husk Ash and Nano Sugarcane Bagasse Ash

Sahar A. Mostafa [1*]

[1]*Department of Civil Engineering, Faculty of Engineering, Beni-Suef University, Beni-Suef, Egypt, sahar_abdelsalam2010@yahoo.com*

**Corresponding Author: sahar_abdelsalam2010@yahoo.com*

Abstract - Ultra-high-performance concrete (UHPC) has gained considerable attention owing to its superior mechanical properties and durability; however, its performance can be further enhanced by incorporating nanoscale supplementary cementitious materials. This study investigates the effects of nano rice husk ash (NRHA) and nano sugarcane bagasse ash (NSCBA) on the mechanical and durability performance of ultra-high-performance concrete (UHPC) incorporating end-hooked steel fibers. Both nanomaterials were produced through controlled calcination at 700 °C for 3 h, followed by ball milling to achieve nano-sized particles, ensuring high pozzolanic reactivity and effective dispersion. UHPC mixtures were prepared with varying nano contents, and a comprehensive experimental program was conducted to evaluate the compressive strength, splitting tensile strength, flexural strength, and sorptivity at different curing ages. The results demonstrated that the incorporation of NRHA and NSCBA significantly enhanced the mechanical performance of UHPC at both early and later ages. At 7 and 28 d, the compressive, splitting tensile, and flexural strengths showed notable improvements compared to those of the control mixture, with optimum nano contents yielding the highest strength gains. In particular, mixtures containing an intermediate dosage of NRHA exhibited the highest enhancements in tensile and flexural performance, indicating improved crack-bridging efficiency and fiber–matrix interaction. Durability assessment based on sorptivity measurements at 28 days revealed a substantial reduction in capillary water absorption for nano-modified UHPC, with NRHA-based mixtures showing the greatest improvement owing to pronounced pore refinement and matrix densification. Overall, the findings confirm that the use of agricultural waste-derived nanomaterials can effectively improve both the mechanical and durability properties of UHPC. Among the investigated mixtures, NRHA at the optimum dosage demonstrated superior overall performance, highlighting its potential as a sustainable and high efficiency nanoadditive for advanced UHPC applications.

Received: *13 July 2025*
Revised: *20 September 2025*
Accepted: *30 November 2025*
Available online: *25 December 2025*

Keywords:

-UHPC;
-Nano rice husk ash;
-Nano sugarcane bagasse ash
-Mechanical properties
-Durability;
-Sorptivity

DOI: https://doi.org/XXXX.XXXX

Introduction

Ultra-high-performance concrete (UHPC) is one of the most advanced classes of cement-based materials owing to its exceptional mechanical strength, superior durability, and refined microstructure compared with conventional and high-strength concretes [1]. Typically characterized by compressive strengths exceeding 120, UHPC achieves outstanding performance through optimized particle packing, low water-to-binder ratios, high cementitious content, and the incorporation of supplementary cementitious materials and steel fibers [2]. Previous studies have demonstrated that UHPC exhibits remarkable resistance to chloride penetration, abrasion, and chemical attacks, making it suitable for demanding structural applications, such as long-span bridges, precast elements, and protective structures [3]. However, despite these advantages, UHPC production faces several challenges, including high cement consumption, increased costs, and environmental concerns related to carbon dioxide emissions associated with cement manufacturing. Consequently, recent research has focused on enhancing the performance of UHPC while simultaneously improving sustainability through the partial replacement of cement with highly reactive supplementary materials [4]. Researchers have emphasized that optimizing the UHPC composition at the micro- and nanoscale plays a critical role in achieving superior mechanical and durability properties [5]. The incorporation of fine and ultrafine materials has been shown to refine the pore structure, improve the interfacial transition zone, and enhance hydration efficiency [6]. Therefore, the development of UHPC mixtures incorporating alternative and sustainable materials has become an essential research direction in the field of concrete technology [7].

Nanotechnology has emerged as a promising approach to improve the performance of cementitious composites by modifying their behavior at the nanoscale. Nanomaterials possess extremely high specific surface areas, which significantly enhance their pozzolanic reactivity and interaction with hydration products. Previous studies have reported that nanosilica, nanoalumina, and nanoclay can accelerate cement hydration, increase calcium silicate hydrate (C–S–H) formation, and reduce porosity, leading to enhanced mechanical strength and durability [8]. In UHPC systems, the effect of nanomaterials is even more pronounced because of the dense matrix and low water content. Researchers have shown that the inclusion of nanoscale additives can improve early age strength, refine pore connectivity, and reduce permeability [9]. However, the effectiveness of nanomaterials strongly depends on their dispersion and dosage, as excessive nano content may lead to particle agglomeration and reduced performance [10]. Therefore, identifying optimum nano dosages and effective dispersion techniques is crucial. Recent experimental investigations have emphasized that nanoscale pozzolanic materials derived from industrial and agricultural waste can offer comparable or superior performance to conventional nanosilica while also contributing to sustainability and cost reduction [11].

Agricultural waste materials, such as rice husk ash (RHA) and sugarcane bagasse ash (SCBA) [12], have attracted considerable attention as sustainable supplementary cementitious materials owing to their high silica content and wide availability [13]. Numerous studies have demonstrated that properly processed RHA contains a high percentage of amorphous silica, often exceeding 85%, which contributes to its strong pozzolanic activity [14]. Similarly, SCBA reportedly contains significant amounts of reactive silica and alumina, enabling effective participation in secondary hydration reactions [15]. Previous research has shown that incorporating RHA and SCBA into conventional and high-strength concrete can improve compressive strength, reduce water absorption, and enhance resistance to chemical attacks. Recently, nanosized RHA and SCBA have been investigated, with results indicating substantial improvements in mechanical properties and durability compared to their microscale counterparts. Studies have reported strength improvements ranging from 10% to 30%, depending on the processing methods and replacement levels [16]. The transformation of agricultural waste into high-value nanomaterials aligns with global sustainability goals and

DOI: https://doi.org/XXXX.XXXX

offers a viable approach for reducing cement consumption while enhancing UHPC performance [17].

Steel fiber reinforcement is a key component of UHPC mixtures, playing a crucial role in improving the tensile strength, flexural performance, and post-cracking behavior. End-hooked steel fibers, in particular, have been shown to provide superior mechanical anchorage within the cementitious matrix, resulting in improved load transfer and ductility. Previous studies have demonstrated that the synergistic interaction between steel fibers and supplementary cementitious materials significantly influences the performance of UHPC [18]. The incorporation of nanomaterials has been reported to improve the fiber–matrix bonding by refining the interfacial transition zone and increasing the matrix compactness [19]. This enhancement leads to improved crack-bridging efficiency and higher tensile and flexural strength. Research has also shown that UHPC mixtures incorporating both fibers and nano-additives exhibit reduced crack widths and improved energy absorption capacity. However, the combined effect of agricultural waste-derived nanomaterials and end-hooked steel fibers in UHPC remains relatively underexplored, particularly with respect to durability indicators such as sorptivity and long-term water absorption behavior [20].

Durability performance is a critical consideration for UHPC applications, particularly in aggressive environments, where exposure to moisture, chlorides, and chemical agents can compromise structural integrity. Sorptivity is widely recognized as an effective indicator of concrete durability because it reflects the capillary absorption behavior and pore connectivity of the cementitious matrix [21]. Previous research has established a strong correlation between reduced sorptivity and improved resistance to chloride ingress and chemical attacks [22]. Studies have reported that the incorporation of nanomaterials significantly reduces sorptivity by refining the pore structure and blocking capillary channels through additional C–S–H formation. Nano RHA, in particular, has been shown to outperform conventional pozzolanic materials in reducing water absorption due to its high silica content and nano-scale particle size [23].Despite these findings, few studies have systematically evaluated the combined effects of nano RHA and nano SCBA on the mechanical and durability performance of UHPC reinforced with end-hooked steel fibers. This research gap highlights the need for a comprehensive experimental investigation to quantify the strength enhancement, durability improvement, and optimal nanomaterial dosage [24].

The significance of this research lies in its comprehensive evaluation of UHPC incorporating agricultural waste-derived nanomaterials and end-hooked steel fibers. Unlike previous studies that focused primarily on conventional nano-additives or single performance indicators, this study systematically investigated the compressive, splitting tensile, flexural, and sorptivity properties at different curing ages. This study provides quantitative evidence of the optimum nanomaterial dosage required to achieve maximum mechanical and durability performance while avoiding particle agglomeration. Furthermore, the utilization of nano rice husk ash and nano sugarcane bagasse ash contributes to sustainable construction practices by recycling agricultural waste and reducing cement consumption. The findings of this study offer valuable insights for the development of high-performance, durable, and environmentally friendly UHPC mixtures suitable for advanced structural applications.

Experimental program

A. Raw materials

The ultra-high-performance concrete (UHPC) mixtures investigated in this study were produced using carefully selected raw materials to achieve superior mechanical performance, enhanced durability, and optimized rheological properties of the UHPC. Ordinary Portland cement (OPC) was used as the primary binder, conforming to the ASTM C150 specifications [25]. It is characterized by a high calcium silicate content, mainly tricalcium silicate (C_3S) and dicalcium silicate (C_2S), which are responsible for the early and long-term strength development. Silica fume was incorporated as a supplementary cementitious material owing to its extremely fine particle size and high amorphous silicon dioxide (SiO_2)

DOI: https://doi.org/XXXX.XXXX

content exceeding 90%. The high pozzolanic reactivity of silica fume contributes to pore refinement, densification of the cement matrix, and improved interfacial transition zones (ITZ), which are essential characteristics of UHPC systems.

Fine sand with a controlled particle size distribution was employed as the main aggregate to ensure dense packing and minimize the internal voids [26]. In addition, waste glass powder was used as a partial fine aggregate replacement, sourced from recycled glass and ground to a fine size. Glass powder is rich in amorphous silica (SiO_2), which enhances pozzolanic activity and contributes to sustainable concrete production by recycling industrial waste materials. Potable water was used for all the mixtures to ensure consistency and avoid adverse chemical reactions [27].

End-hooked steel fibers were incorporated at a volumetric fraction of 1% to enhance the mechanical performance and crack resistance of the UHPC. These fibers provide effective crack bridging, improve post-cracking behavior, and significantly enhance the tensile and flexural strengths. The hooked ends ensure improved mechanical anchorage within the cementitious matrix, leading to better stress transfer and improved ductility [13, 28].

Nano rice husk ash (NRHA) and nano sugarcane bagasse ash (NSCBA) were used as nano-scale pozzolanic additives in different proportions (1–3%). Rice husk ash is predominantly composed of amorphous silica (typically 85–95% SiO_2), whereas sugarcane bagasse ash contains significant amounts of SiO_2 along with minor proportions of Al_2O_3, Fe_2O_3, and CaO. After nanosizing, both ashes exhibited a high specific surface area, which accelerated hydration reactions, promoted the formation of additional calcium silicate hydrate (C–S–H) gel, and refined the pore structure, resulting in improved strength and reduced permeability [29].

A high-range water-reducing admixture based on polycarboxylate ether (PCE), commercially known as Viscocrete, was used as a superplasticizer to achieve the required flowability and self-compacting characteristics of UHPC at a low W/B ratio. The dispersing mechanism of Viscocrete relies on electrostatic repulsion and steric hindrance, ensuring uniform particle dispersion, improved workability, and the prevention of fiber agglomeration [30]. This combination of carefully selected raw materials ensures the production of UHPC with enhanced mechanical properties, durability, and sustainability of the UHPC. The mixing procedures are shown in **Tab. 1** and **Fig. 1.**

Tab. 1. Mix proportions

Item	Value
Cement (kg/m³)	800
Silica fume (kg/m³)	80
sande (kg/m³)	1200
waste glass	300
Water (L/m³)	184.8
Superplasticizer (L/m³)	6.93
steel fiber r (Vf)	1%
NRHA	1-3%
NSCBA	1-3%

Fig. 1. Mixing proportions

B. Preparation of Nano Materials

The preparation of nano rice husk ash (NRHA) and nano sugarcane bagasse ash (NSCBA) was carried out through a controlled thermal and mechanical treatment process to ensure high pozzolanic activity and uniform particle dispersion. Initially, rice husks and sugarcane bagasse were collected, cleaned to remove impurities, and air-dried. The raw materials were then subjected to controlled calcination in an electric

DOI: https://doi.org/XXXX.XXXX

furnace at 700 °C for 3 h [31]. This calcination temperature was carefully selected to eliminate organic matter while preserving the amorphous structure of silica, which is essential for achieving high pozzolanic reactivity and preventing the formation of undesirable crystalline phases in the ash. After calcination, the obtained ashes were naturally cooled to room temperature and subsequently ground using a ball milling process to achieve nanosized particles. The milling parameters were optimized to obtain a particle size predominantly in the range of approximately 50–100 nm with a narrow size distribution. Careful control of the milling time and rotational speed was applied to minimize excessive heat generation and avoid particle agglomeration. The milling process was conducted under controlled conditions to ensure effective dispersion and prevent the formation of clusters or hard agglomerates. The preparation steps are summarized in **Fig. 2.**

The resulting nanosized NRHA and NSCBA exhibited a high specific surface area and enhanced pozzolanic reactivity, which significantly promoted the formation of additional C–S–H gel, refined the pore structure, and improved the mechanical and durability performance of UHPC mixtures [32].

Fig. 2. Preparation of nano ashes

C. Dispersion of Nano Materials in UHPC

To ensure the effective dispersion of nano rice husk ash (NRHA) and nano sugarcane bagasse ash (NSCBA) and to prevent particle agglomeration, a magnetic stirrer was employed before their incorporation into the UHPC mixtures. The required amount of nanomaterial was first dispersed in a portion of the mixing water and subjected to continuous stirring using a magnetic stirrer at a controlled rotational speed for a predetermined duration [33]. This process promoted a uniform suspension of nanosized particles and enhanced their stability within the liquid medium. The application of magnetic stirring facilitates the breakdown of weak agglomerates formed owing to Van der Waals forces, thereby improving particle separation and distribution, as shown in **Fig. 3.**

The resulting nanosuspension was then gradually introduced into the concrete mixture during the water and superplasticizer addition stages. This dispersion technique significantly enhanced the homogeneity of the cementitious matrix, improved the interaction between the nanoparticles and hydration products, and promoted the formation of a denser microstructure. Consequently, the use of a magnetic stirrer contributed to improved pozzolanic reactivity, refined pore structure, and enhanced mechanical and durability properties [34].

Fig. 3. Dispersion of nano materials using a magnetic stirrer

DOI: https://doi.org/XXXX.XXXX

D. Mixing procedures

The mixing procedure of the ultra-high-performance concrete (UHPC) was carefully designed to ensure the homogeneous dispersion of all constituents, particularly the nanomaterials and steel fibers, and to achieve optimal rheological and mechanical performance. Initially, all dry materials, including cement, silica fume, fine sand, waste glass powder, and the required proportion of nano rice husk ash (NRHA) or nano sugarcane bagasse ash (NSCBA), were dry mixed for approximately 3–5 min using a high-shear laboratory mixer. This step was essential for achieving a uniform distribution and minimizing particle segregation. Subsequently, potable water was gradually added while mixing continued, followed by the incorporation of the polycarboxylate-based superplasticizer (Viscocrete), which was introduced in stages to enhance the dispersion efficiency and avoid sudden loss of workability as presented in **Fig. 4.**

After achieving a homogeneous and flowable cementitious matrix, end-hooked steel fibers were gradually introduced into the mixture while maintaining continuous mixing at low-to-moderate speeds. This controlled addition prevented fiber balling and ensured a uniform fiber distribution throughout the matrix [35]. The mixing process was continued until a consistent, self-compacting UHPC mixture with high cohesiveness and stability was achieved. The total mixing duration was carefully controlled to avoid excessive air entrainment and maintain the desired rheological properties. This optimized mixing procedure ensured the effective dispersion of nanosized materials, enhanced fiber–matrix bonding, and contributed significantly to the improved mechanical strength and durability characteristics of the UHPC mixtures.

Fig. 4. Mixing procedures

E. Testing

To evaluate the mechanical performance and durability characteristics of UHPC mixtures incorporating nano rice husk ash (NRHA) and nano sugarcane bagasse ash (NSCBA), a comprehensive experimental testing program was conducted. Compressive strength tests were performed at curing ages of 7 and 28 d to assess both early age and long-term strength development of the UHPC mixes as shown in **Fig.5.** In addition, splitting tensile strength tests were conducted at the same curing ages to evaluate the tensile performance and effectiveness of the nanomaterials and steel fiber reinforcement in enhancing crack resistance.

Furthermore, flexural strength tests were conducted at 7 and 28 days to investigate the bending behavior and post-cracking performance of the UHPC mixtures, particularly reflecting the contribution of end-hooked steel fibers and nano-additives to load transfer and ductility. To assess the durability-related properties, sorptivity tests were performed at 28 days to

DOI: https://doi.org/XXXX.XXXX

evaluate the water absorption characteristics and pore structure refinement of the UHPC matrix. Sorptivity measurements provide valuable insights into the influence of nanomaterials on capillary suction and permeability reduction.

All test results were systematically recorded and analyzed to quantify the percentage improvement of each UHPC mixture relative to the control. The combined assessment of the compressive, tensile, flexural, and sorptivity results enabled a comprehensive evaluation of the mechanical efficiency and durability enhancement achieved through the incorporation of NRHA and NSCBA.

Fig. 5. Mixing and testing procedures

Results and discussion

A. Compressive strength at 7 days

The 7-day compressive strength results clearly demonstrated the significant influence of nano rice husk ash (NRHA) and nano sugarcane bagasse ash (NSCBA) on the early age mechanical performance of UHPC mixtures. As illustrated in **Fig.6**, the control mixture achieved a compressive strength of approximately 98.68 MPa, which was used as the reference baseline. All modified mixtures exhibited higher compressive strength values, confirming the effectiveness of nanomaterial incorporation in enhancing early hydration reactions and matrix densification.

For the NSCBA-based mixtures, a gradual improvement in compressive strength was observed with increasing nano content up to an optimum level. NSCBA1 and NSCBA3 achieved compressive strengths of approximately 101.03 MPa and 107.25 MPa, corresponding to improvement ratios of about +2.38% and +8.69%, respectively. The maximum enhancement was recorded for NSCBA2, which reached approximately 118.83 MPa, representing an improvement of approximately 20.42% compared to the control mixture. This optimum performance indicates that the intermediate NSCBA dosage provided the most effective balance between pozzolanic reactivity and particle dispersion [15, 36].

Similarly, UHPC mixtures incorporating NRHA exhibited a marked increase in early-age compressive strength. NRHA1, NRHA2, and NRHA3 demonstrated strength improvements of approximately +11.81%, +20.42%, and +15.10%, respectively, compared to the Among these mixtures, NRHA2 exhibited the highest compressive strength, confirming the presence of an optimal nano content beyond which marginal strength reduction may occur owing to the particle agglomeration effects [37].

The relatively low standard deviation values observed for all UHPC mixtures indicated good repeatability and consistency of the experimental results. The limited scatter in the compressive strength measurements reflects the effectiveness of the adopted mixing and dispersion procedures, particularly the use of magnetic stirring and controlled fiber addition. Moreover, the slightly lower standard deviation recorded for the optimum mixtures (NSCBA2 and NRHA2) suggests improved homogeneity and a more uniform microstructure than the control and higher-dosage mixes.

Overall, the results confirm that both nano materials significantly enhance the early-age compressive strength of UHPC; however, NSCBA2 can be identified as the optimum mixture at 7 days, combining the highest strength gain with stable performance and minimal variability

DOI: https://doi.org/XXXX.XXXX

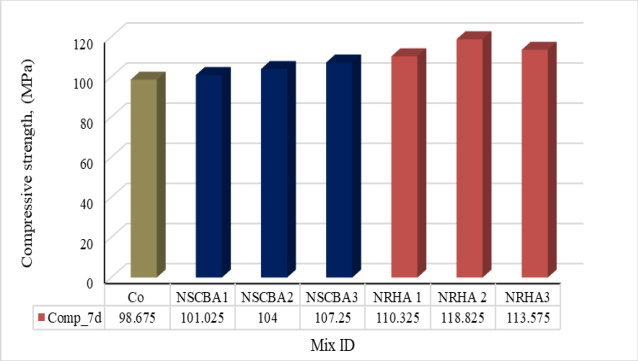

Fig. 6. Compressive strength for UHPC with different types of nanoparticles

B. Compressive strength at 28 days

The 28-day compressive strength results provide a clear assessment of the long-term mechanical performance of UHPC mixtures incorporating nano rice husk ash (N-RHA) and nano sugarcane bagasse ash (N-SCBA). As shown in **Fig. 7**, the control mixture achieved a compressive strength of approximately 130.03 MPa, which was considered the reference value for evaluating the strength enhancement at later curing ages. Compared to the 7-day results, all mixtures exhibited a noticeable increase in compressive strength at 28 d, reflecting the continued hydration and pozzolanic reactions promoted by the nanomaterials.

For the NSCBA-modified mixtures, a consistent increase in compressive strength was observed with increasing nano content. NSCBA1 and NSCBA3 achieved compressive strengths of approximately 134.70 MPa and 143.00 MPa, corresponding to improvement ratios of about +3.60% and +9.98%, respectively, relative to the control mix. The highest strength within this group was recorded for NSCBA2, which reached approximately 163.75 MPa, representing a substantial improvement of approximately 25.94%. This result confirms that the optimum NSCBA dosage significantly enhances the long-term strength by contributing to sustained pozzolanic activity, increased C–S–H gel formation, and improved microstructural compactness [38].

Similarly, the UHPC mixtures incorporating NRHA exhibited a pronounced long-term strength enhancement. NRHA1, NRHA2, and NRHA3 recorded compressive strengths of approximately 146.93 MPa, 163.75 MPa, and 158.03 MPa, corresponding to improvement ratios of +13.00%, +25.94%, and +21.53%, respectively. Among these, NRHA2 exhibited the highest 28-day compressive strength, indicating that the intermediate NRHA dosage provided the most efficient balance between silica availability and particle dispersion, whereas higher contents led to slightly reduced gains owing to possible agglomeration effects [39].

The low standard deviation values observed at 28 d indicate the high repeatability and reliability of the test results. The reduced scatter in compressive strength, particularly for the optimum mixtures (NSCBA2 and NRHA2), suggests a more homogeneous microstructure and improved uniformity in nanoparticle dispersion and fiber–matrix interaction. This behavior highlights the effectiveness of the adopted dispersion and mixing procedures in achieving a stable long-term performance.

Overall, the 28-day results confirmed that both nanomaterials significantly enhanced the long-term compressive strength of UHPC. However, NRHA2 and NSCBA2 were identified as the optimum mixtures, providing the highest strength improvement combined with consistent performance and minimal variability.

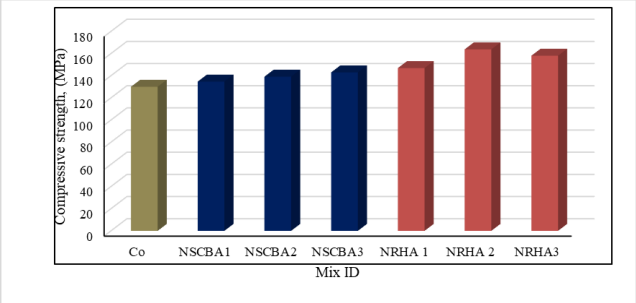

Fig. 7. compressive strength for UHPC with different types of nanoparticles

C. Early tensile strength

The splitting tensile strength results at 7 days provide valuable insights into the early age cracking resistance and tensile performance of UHPC mixtures incorporating nano rice husk ash (NRHA) and nano sugarcane bagasse ash (NSCBA). As illustrated in **Fig. 8**, the control mixture exhibited a splitting tensile strength of approximately 14.54 MPa, which was used as a reference value to assess the effectiveness of the

DOI: https://doi.org/XXXX.XXXX

incorporation of nanomaterials. Compared with the control mix, all modified UHPC mixtures demonstrated improved tensile strength, confirming the beneficial role of nano additives and steel fiber reinforcement in enhancing early age tensile behavior [40].

For the NSCBA-modified mixtures, a gradual increase in splitting tensile strength was observed with an increase in the nano content. NSCBA1 achieved a tensile strength of approximately 14.93 MPa, corresponding to an improvement ratio of about +2.69% relative to the control mix. A more pronounced enhancement was recorded for NSCBA2, which reached approximately 15.32 MPa, representing an improvement of approximately +5.38%. The highest tensile strength within this group was observed for NSCBA3, with a value of approximately 15.78 MPa, corresponding to an improvement ratio of approximately +8.54%. This progressive enhancement indicates that the nano-SRBA effectively contributes to matrix densification and improves stress transfer at the fiber–matrix interface during early age loading [41].

Similarly, UHPC mixtures incorporating NRHA exhibited a superior splitting tensile strength at 7 d. NRHA1, NRHA2, and NRHA3 recorded tensile strength values of approximately 16.56 MPa, 17.48 MPa, and 16.79 MPa, corresponding to improvement ratios of approximately +13.92%, +20.25%, and +15.51%, respectively. Among these mixtures, NRHA2 exhibited the highest splitting tensile strength, indicating that the intermediate NRHA dosage provided the most effective balance between nanoscale reactivity and particle dispersion. The slight reduction observed for NRHA3 suggests the onset of nanoparticle agglomeration at higher contents, which may reduce the stress distribution efficiency.

The relatively low standard deviation values recorded for all the mixtures reflect the good repeatability and consistency of the tensile test results. The reduced scatter observed for the optimum mixtures, particularly NRHA2, indicates the enhanced homogeneity and uniform dispersion of the nanoparticles and steel fibers within the UHPC matrix. Overall, the results confirm that both NRHA and NSCBA significantly enhanced early age splitting tensile strength; however, NRHA2 can be identified as the optimum mixture at 7 d, achieving the highest tensile improvement combined with stable and reliable performance [42].

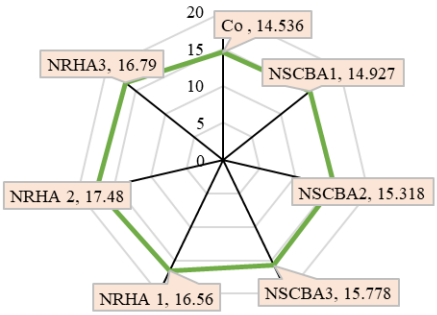

Fig. 8. Early tensile strength for UHPC with different types of nanoparticles

D. 28 days tensile strength

The 28-day splitting tensile strength results provide a comprehensive evaluation of the long-term tensile behavior and crack resistance of UHPC mixtures incorporating nano rice husk ash (NRHA) and nano sugarcane bagasse ash (NSCBA). As illustrated in **Fig. 9**, the control mixture exhibited a splitting tensile strength of approximately 19.44 MPa, which was considered the reference value for assessing tensile enhancement at later curing ages. Compared with the control mix, all UHPC mixtures containing nanomaterials demonstrated noticeable improvements, highlighting the sustained contribution of nanoscale pozzolanic reactions and improved fiber–matrix interactions over time.

For the NSCBA-modified mixtures, moderate but consistent enhancements in the splitting tensile strength were observed. NSCBA1 recorded a tensile strength of approximately 19.94 MPa, corresponding to an improvement ratio of about +2.60%. A higher enhancement was achieved by NSCBA2, which reached approximately 20.47 MPa, representing an improvement of approximately +5.33%. The highest tensile strength within this group was observed for NSCBA3, with a value of approximately 21.44 MPa, corresponding to an improvement ratio of approximately +10.30%. This trend

DOI: https://doi.org/XXXX.XXXX

suggests that increasing the NSCBA content promotes further matrix densification and enhances the stress transfer mechanisms at the fiber–matrix interface, particularly at later ages [43].

In contrast, the UHPC mixtures incorporating NRHA exhibited more pronounced tensile strength gains at 28 days. NRHA1, NRHA2, and NRHA3 achieved splitting tensile strength values of approximately 22.31 MPa, 23.76 MPa, and 23.12 MPa, corresponding to improvement ratios of approximately +14.79%, +22.25%, and +18.93%, respectively. Among these mixtures, NRHA2 exhibited the highest splitting tensile strength, confirming the presence of an optimal NRHA dosage that maximized pozzolanic efficiency and microstructural refinement. The slight reduction in strength observed for NRHA3 may be attributed to partial nanoparticle agglomeration at higher contents, which can reduce the effective stress distribution.

The relatively low standard deviation values recorded at 28 days indicate high test repeatability and reliable tensile performance. The reduced scatter associated with the optimum mixtures, particularly NRHA2, reflects improved homogeneity, effective nanoparticle dispersion, and stronger fiber–matrix bonding. Overall, the results demonstrate that both NRHA and NSCBA significantly enhance the long-term splitting tensile strength; however, NRHA2 can be identified as the optimum mixture at 28 d, combining the highest tensile improvement with stable and consistent performance [44].

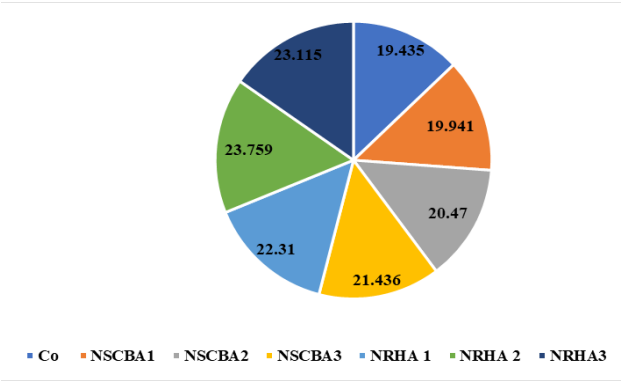

Fig. 9. 28 days tensile strength for UHPC with different types of nanoparticles

E. Early flexural strength

The flexural strength results at 7 days provide important insights into the early age bending performance and crack-bridging efficiency of UHPC mixtures incorporating nano rice husk ash (NRHA) and nano sugarcane bagasse ash (NSCBA). As illustrated in **Fig. 10**, the control mixture exhibited a flexural strength of approximately 20.05 MPa, which was adopted as the reference value for evaluating the influence of nanomaterial incorporation. All modified mixtures demonstrated enhanced flexural performance compared to the control mix, highlighting the combined contribution of nanomaterials and end-hooked steel fibers in improving the early age load-carrying capacity under bending.

For the NSCBA-modified mixtures, a gradual increase in the flexural strength was observed with increasing nano content. NSCBA1 achieved a flexural strength of approximately 20.37 MPa, corresponding to an improvement ratio of about +1.64%. A more noticeable enhancement was recorded for NSCBA2, which reached approximately 21.15 MPa, representing an improvement of approximately +5.51% relative to the control mix. The highest flexural strength within this group was observed for NSCBA3, with a value of approximately 22.02 MPa, corresponding to an improvement ratio of approximately +9.85%. This progressive improvement indicates that increasing the NSCBA content effectively enhances matrix densification and improves the fiber–matrix interfacial bond, which plays a critical role in the flexural behavior at early ages.

In contrast, UHPC mixtures incorporating NRHA exhibited more pronounced improvements in flexural strength at 7 d. NRHA1, NRHA2, and NRHA3 recorded flexural strength values of approximately 22.04 MPa, 22.89 MPa, and 22.63 MPa, corresponding to improvement ratios of approximately +9.96%, +14.19%, and +12.90%, respectively. Among these mixtures, NRHA2 exhibited the highest flexural strength, indicating that the intermediate NRHA dosage provided the most effective enhancement of the early age bending resistance. The slight reduction observed for NRHA3 suggests the onset of

DOI: https://doi.org/XXXX.XXXX

nanoparticle agglomeration at higher contents, which may reduce the stress transfer efficiency despite increased silica availability [45].

The relatively low standard deviation values observed for all mixtures reflect good test repeatability and consistency. The reduced scatter associated with the optimum mixtures, particularly NRHA2, indicates improved homogeneity, uniform nanoparticle dispersion, and effective fiber distribution within the UHPC matrix. Overall, the results confirmed that both NRHA and NSCBA significantly enhanced the early age flexural strength; however, NRHA2 was identified as the optimum mixture at 7 d, providing the highest flexural strength improvement combined with stable and reliable performance.

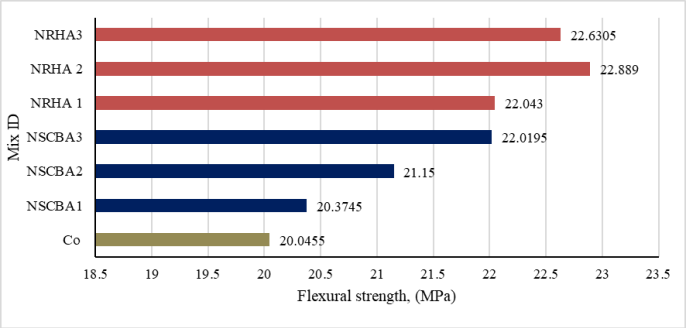

Fig. 10. Flexural strength for UHPC with different types of nanoparticles

F. flexural strength at 28 days

The flexural strength results at 28 days provide a clear indication of the long-term bending performance and post-cracking behavior of UHPC mixtures incorporating nano rice husk ash (NRHA) and nano sugarcane bagasse ash (NSCBA). As shown in **Fig. 11**, the control mixture exhibited a flexural strength of approximately 26.78 MPa, which was adopted as the reference value for evaluating the effectiveness of the nanomaterial incorporation at later curing ages. Compared to the control mix, all UHPC mixtures containing nanomaterials demonstrated substantial improvements, reflecting the sustained contribution of pozzolanic reactions and enhanced fiber–matrix interaction over time.

For the NSCBA-based mixtures, a pronounced increase in flexural strength was observed with increasing nano content. NSCBA1 and NSCBA2 achieved flexural strength values of approximately 30.70 MPa and 32.38 MPa, corresponding to improvement ratios of about +14.67% and +20.94%, respectively. The highest flexural strength within this group was recorded for NSCBA3, which reached approximately 34.38 MPa, representing a significant improvement of approximately +28.39% compared to the control mixture. This trend highlights the effectiveness of NSCBA in enhancing the long-term flexural performance by promoting matrix densification, refining the interfacial transition zone, and improving stress transfer across microcracks bridged by steel fibers.

In contrast, the UHPC mixtures incorporating NRHA exhibited even greater enhancements in flexural strength at 28 d. NRHA1, NRHA2, and NRHA3 recorded flexural strength values of approximately 37.00 MPa, 37.80 MPa, and 35.57 MPa, corresponding to improvement ratios of approximately +38.20%, +41.18%, and +32.86%, respectively. Among these mixtures, NRHA2 exhibited the highest flexural strength, indicating that the intermediate NRHA dosage provided the most effective enhancement of the bending resistance. The slight reduction observed for NRHA3 suggests that excessive nano content may lead to partial agglomeration, which can reduce the stress redistribution efficiency despite the increased availability of reactive silica [46].

The relatively low standard deviation values recorded for the flexural strength results indicate the good repeatability and consistency of the experimental program. The reduced scatter associated with the optimum mixtures, particularly NRHA2 and NSCBA3, reflects improved homogeneity, effective nanoparticle dispersion, and strong fiber–matrix bonding within the UHPC matrix. Overall, the results confirmed that both nanomaterials significantly enhanced the long-term flexural performance of UHPC; however, NRHA2 was identified as the optimum mixture at 28 d, providing the highest flexural

DOI: https://doi.org/XXXX.XXXX

strength improvement combined with stable and reliable performance.

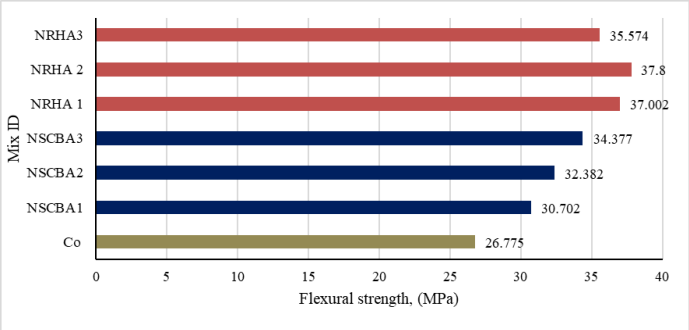

Fig. 11. Flexural strength for UHPC with different types of nanoparticles

G. Sorptivity

The sorptivity results at 28 days provide a clear assessment of the durability performance and capillary water absorption behavior of UHPC mixtures incorporating nano rice husk ash (NRHA) and nano sugarcane bagasse ash (NSCBA). As shown in **Fig. 12**, the control mixture exhibited a sorptivity value of approximately 2.26%, which was considered the reference for evaluating the effectiveness of nanomaterial incorporation in reducing water absorption and refining the pore structure. Lower sorptivity values indicate improved resistance to capillary suction and enhanced durability of the concrete.

For the NSCBA-modified mixtures, a noticeable reduction in sorptivity was observed with an increase in the nano content. NSCBA1 and NSCBA3 recorded sorptivity values of approximately 2.69% and 2.45%, respectively. Compared to the control mixture, NSCBA3 achieved a reduction of approximately 8.07%, whereas NSCBA2, with a value of approximately 2.48%, showed a reduction of approximately 9.58%. These results indicate that NSCBA contributes to partial pore refinement and matrix densification; however, its effectiveness in reducing capillary absorption is relatively moderate compared to that of NRHA [8, 47].

In contrast, the UHPC mixtures incorporating NRHA exhibited a more pronounced reduction in sorptivity at 28 d. NRHA1, NRHA2, and NRHA3 achieved sorptivity values of approximately 1.89%, 1.78%, and 1.82%, corresponding to reductions of approximately 16.63%, 21.39%, and 19.49%, respectively, relative to the control mix. Among these mixtures, NRHA2 exhibited the lowest sorptivity, indicating the highest resistance to capillary water absorption. This superior performance can be attributed to the high amorphous silica content and nanoscale particle size of NRHA, which promote extensive pozzolanic reactions and result in the formation of additional C–S–H gel that effectively blocks capillary pores [48].

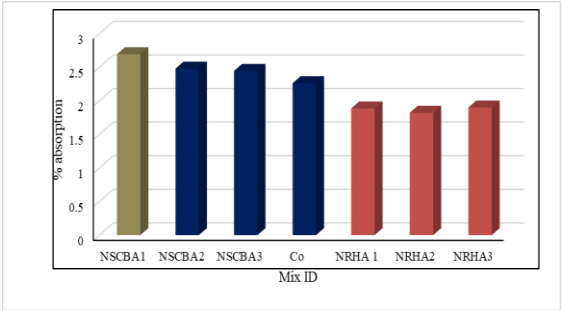

Fig. 12. Sorptivity for UHPC with different types of nanoparticles

Conclusion

The experimental investigation conducted in this study clearly demonstrated the effectiveness of incorporating nano rice husk ash (N-RHA) and nano sugarcane bagasse ash (N-SCBA) in enhancing the mechanical and durability performance of UHPC. The compressive strength of UHPC was significantly enhanced by incorporating nanomaterials. At 7 days, strength improvements reached up to ≈20.4%, while at 28 days, the maximum improvement increased to approximately ≈25.9%, confirming the sustained contribution of nanoscale pozzolanic reactions over time. The splitting tensile strength showed notable enhancement with nanomaterial incorporation. At 7 days, the tensile strength increased by up to ≈20.3%, whereas at 28 days, the improvement reached approximately ≈22.3%, indicating improved crack resistance and fiber–matrix interaction. The flexural strength exhibited the most pronounced enhancement among all the mechanical properties. At 7 days, the flexural strength increased by up to ≈14.2%, whereas at 28 days, the improvement reached approximately ≈41.2%, highlighting the strong synergistic effect between nanomaterials and end-hooked steel fibers under bending loads.

DOI: https://doi.org/XXXX.XXXX

Durability assessment based on sorptivity measurements at 28 days revealed a significant reduction in the water absorption. UHPC mixtures incorporating NRHA achieved a maximum sorptivity reduction of approximately 21.4%, whereas NSCBA-based mixtures showed a moderate reduction of up to 9.6%, demonstrating enhanced pore refinement and matrix densification. Among all investigated mixtures, the UHPC containing an intermediate dosage of NRHA consistently achieved the highest overall performance, combining maximum improvements in compressive, tensile, and flexural strengths with the greatest reduction in sorptivity. The relatively low standard deviation values observed across all test results confirmed good repeatability, uniform dispersion of nanomaterials, and consistent behavior of the UHPC mixtures. The use of agricultural waste-derived nanomaterials, particularly NRHA, offers a sustainable and efficient approach for producing high-performance UHPC with superior mechanical properties and enhanced durability.

References

[1] S.A. Mostafa, I.N. Fathy, A.A. Mahmoud, M.A. Abouelnour, K. Mahmoud, S.M. Shaaban, S.A. Elhameed, I.M.J.A.o.N.E. Nabil, Optimization of UHPC with basil plant ash: Impacts on strength, durability, and gamma-ray attenuation, 226 (2026) 111825.
[2] M.A. Bajaber, I.Y. Hakeem, UHPC evolution, development, and utilization in construction: a review, Journal of Materials Research and Technology 10 (2021) 1058-1074.
[3] G. Liao, Y. Xu, D. Wang, L.J.M. Wu, Influence of Steel Fiber Content on the Long-Term Stability of Slag-Containing UHPC Under Different Environments, 18(5) (2025) 1068.
[4] X. Wang, D. Wu, Q. Geng, D. Hou, M. Wang, L. Li, P. Wang, D. Chen, Z. Sun, Characterization of sustainable ultra-high performance concrete (UHPC) including expanded perlite, Construction and Building Materials 303 (2021).
[5] D. Xu, J. Tang, X. Hu, Y. Zhou, C. Yu, F. Han, J.J.C. Liu, B. Materials, Influence of silica fume and thermal curing on long-term hydration, microstructure and compressive strength of ultra-high performance concrete (UHPC), 395 (2023) 132370.
[6] H. Huang, X. Gao, Y. Li, A. Su, SPH simulation and experimental investigation of fiber orientation in UHPC beams with different placements, Construction and Building Materials 233 (2020) 117372.
[7] M.S.M. Norhasri, M.S. Hamidah, A.M. Fadzil, Inclusion of nano metaclayed as additive in ultra high performance concrete (UHPC), Construction and Building Materials 201 (2019) 590-598.
[8] Z. Yu, L. Wu, Z. Yuan, C. Zhang, T. Bangi, Mechanical properties, durability and application of ultra-high-performance concrete containing coarse aggregate (UHPC-CA): A review, Construction and Building Materials 334 (2022).
[9] S. Ahmad, K.O. Mohaisen, S.K. Adekunle, S.U. Al-Dulaijan, M. Maslehuddin, Influence of admixing natural pozzolan as partial replacement of cement and microsilica in UHPC mixtures, Construction and Building Materials 198 (2019) 437-444.
[10] M. Ozawa, S. Subedi Parajuli, Y. Uchida, B. Zhou, Preventive effects of polypropylene and jute fibers on spalling of UHPC at high temperatures in combination with waste porous ceramic fine aggregate as an internal curing material, Construction and Building Materials 206 (2019) 219-225.
[11] Y. Lin, J. Yan, Z. Wang, F. Fan, C. Zou, Effect of silica fumes on fluidity of UHPC: Experiments, influence mechanism and evaluation methods, Construction and Building Materials 210 (2019) 451-460.
[12] B. Ribeiro, T. Uchiyama, J. Tomiyama, T. Yamamoto, Y. Yamashiki, Development of Interlocking Concrete Blocks with Added Sugarcane Residues, Fibers 8(10) (2020) 61.
[13] S.A. Mostafa, M.M. El-Deeb, A.A. Farghali, A.S. Faried, Evaluation of the nano silica and nano waste materials on the corrosion protection of high strength steel embedded in ultra-high performance concrete, Sci Rep 11(1) (2021) 2617.
[14] I. Asadi, P. Shafigh, M. Hashemi, A.R. Akhiani, M. Maghfouri, B. Sajadi, N. Mahyuddin, M. Esfandiari, H. Rezaei Talebi, H.S.C. Metselaar, Thermophysical properties of sustainable cement mortar containing oil palm boiler clinker (OPBC) as a fine aggregate, Construction and Building Materials 268 (2021).
[15] S.N. Minnu, A. Bahurudeen, G. Athira, Comparison of sugarcane bagasse ash with fly ash and slag: An approach towards industrial acceptance of sugar industry waste in cleaner production of cement, Journal of Cleaner Production 285 (2021) 124836.
[16] R.K. Sandhu, R. Siddique, Influence of rice husk ash (RHA) on the properties of self-compacting concrete: A review, Construction and Building Materials 153 (2017) 751-764.
[17] M.A. Mosaberpanah, O. Eren, A.R. Tarassoly, The effect of nano-silica and waste glass powder on mechanical, rheological, and shrinkage properties of UHPC using response surface methodology, Journal of Materials Research and Technology 8(1) (2019) 804-811.
[18] M.F. Md Jaafar, H. Mohd Saman, N.F. Ariffin, K. Muthusamy, S. Wan Ahmad, N. Ismail, Corrosion monitoring on steel reinforced nano metaclayed-UHPC towards strain modulation using fiber Bragg grating sensor, IOP Conference Series: Materials Science and Engineering 431 (2018) 122006.
[19] G.M. Kamil, Q.Q. Liang, M.N.S. Hadi, Numerical analysis of axially loaded rectangular concrete-filled steel tubular short columns at elevated temperatures, Engineering Structures 180 (2019) 89-102.
[20] S.D. Salahaddin, J.H. Haido, G.J.A.S.E.J. Wardeh, Rheological and mechanical characteristics of basalt fiber UHPC incorporating waste glass powder in lieu of cement, 15(3) (2024) 102515.

DOI: https://doi.org/XXXX.XXXX

[21] E. Ghafari, M. Arezoumandi, H. Costa, E. Júlio, Influence of nano-silica addition on durability of UHPC, Construction and Building Materials 94 (2015) 181-188.
[22] S.A. Mostafa, A.S. Faried, A.A. Farghali, M.M. El-Deeb, T.A. Tawfik, S. Majer, M. Abd Elrahman, Influence of Nanoparticles from Waste Materials on Mechanical Properties, Durability and Microstructure of UHPC, Materials (Basel) 13(20) (2020).
[23] M. Alkaysi, S. El-Tawil, Z. Liu, W. Hansen, Effects of silica powder and cement type on durability of ultra high performance concrete (UHPC), Cement and Concrete Composites 66 (2016) 47-56.
[24] A. Joshaghani, M.A. Moeini, Evaluating the effects of sugar cane bagasse ash (SCBA) and nanosilica on the mechanical and durability properties of mortar, Construction and Building Materials 152 (2017) 818-831.
[25] A. ASTM, C150/C150M-17, Standard Specifcation for Portland Cement, American Society for Testing and Materials, West Conshohocken, PA, USA, 2017.
[26] Z. Dong, G. Wu, X.-L. Zhao, H. Zhu, X. Shao, Behaviors of hybrid beams composed of seawater sea-sand concrete (SWSSC) and a prefabricated UHPC shell reinforced with FRP bars, Construction and Building Materials 213 (2019) 32-42.
[27] A. Rezzoug, A.H. AlAteah, M. Alqurashi, S.A.J.B. Mostafa, Development of Ultra High-Performance Concrete with Artificial Aggregates from Sesame Ash and Waste Glass: A Study on Mechanical Strength and Durability, 15(11) (2025) 1942.
[28] L. Abosrra, A.F. Ashour, M. Youseffi, Corrosion of steel reinforcement in concrete of different compressive strengths, Construction and Building Materials 25(10) (2011) 3915-3925.
[29] X. Yuan, W. Xu, A.H. AlAteah, S.A.J.C. Mostafa, B. Materials, Evaluation of the performance of high-strength geopolymer concrete prepared with recycled coarse aggregate containing eggshell powder and rice husk ash cured at different curing regimes, 434 (2024) 136722.
[30] M. Courtial, M.N. de Noirfontaine, F. Dunstetter, M. Signes-Frehel, P. Mounanga, K. Cherkaoui, A. Khelidj, Effect of polycarboxylate and crushed quartz in UHPC: Microstructural investigation, Construction and Building Materials 44 (2013) 699-705.
[31] I.S. Agwa, A.M. Zeyad, B.A. Tayeh, M. Amin, Effect of different burning degrees of sugarcane leaf ash on the properties of ultrahigh-strength concrete, Journal of Building Engineering 56 (2022).
[32] A.S. Faried, S.A. Mostafa, B.A. Tayeh, T.A. Tawfik, The effect of using nano rice husk ash of different burning degrees on ultra-high-performance concrete properties, Construction and Building Materials 290 (2021) 123279.
[33] N.D.K.R. Chukka, B.S. Reddy, K. Vasugi, Y.B.S. Reddy, L. Natrayan, S.J.A.S. Thanappan, Technology, Experimental testing on mechanical, durability, and adsorption dispersion properties of concrete with multiwalled carbon nanotubes and silica fumes, 2022 (2022) 4347753.
[34] K. Kishore, M.N. Sheikh, M.N.J.J.o.B.E. Hadi, Functionalization of Carbon Nanotubes for Enhanced Dispersion and Improved Properties of Geopolymer Concrete: A Review, (2025) 113096.
[35] Y. Zhang, Y. Zhu, S. Qu, A. Kumar, X. Shao, Improvement of flexural and tensile strength of layered-casting UHPC with aligned steel fibers, Construction and Building Materials 251 (2020) 118893.
[36] S.A. Khawaja, U. Javed, T. Zafar, M. Riaz, M.S. Zafar, M.K. Khan, Eco-friendly incorporation of sugarcane bagasse ash as partial replacement of sand in foam concrete, Cleaner Engineering and Technology 4 (2021).
[37] R. Hari, Y.J.C. Zhuge, B. Materials, Performance assessment of pervious concrete incorporated with calcium silicate hydrates (CSH) cultivated on rice husk ash substrates–A trend surface analysis interpretation, 446 (2024) 138050.
[38] X. Wang, S. Ding, A. Ashour, H. Ye, V.K. Thakur, L. Zhang, B.J.J.o.C.P. Han, Back to basics: Nanomodulating calcium silicate hydrate gels to mitigate CO2 footprint of concrete industry, 434 (2024) 139921.
[39] M. Gesoglu, E. Güneyisi, D.S. Asaad, G.F. Muhyaddin, Properties of low binder ultra-high performance cementitious composites: Comparison of nanosilica and microsilica, Construction and Building Materials 102 (2016) 706-713.
[40] D.-Y. Yoo, S. Kim, J.-J. Kim, B. Chun, An experimental study on pullout and tensile behavior of ultra-high-performance concrete reinforced with various steel fibers, Construction and Building Materials 206 (2019) 46-61.
[41] I. Lopez Boadella, F. Lopez Gayarre, J. Suarez Gonzalez, J.M. Gomez-Soberon, C. Lopez-Colina Perez, M. Serrano Lopez, J. de Brito, The Influence of Granite Cutting Waste on The Properties of Ultra-High Performance Concrete, Materials (Basel) 12(4) (2019).
[42] P. Ganesh, A.R. Murthy, Tensile behaviour and durability aspects of sustainable ultra-high performance concrete incorporated with GGBS as cementitious material, Construction and Building Materials 197 (2019) 667-680.
[43] Q. Ma, Y. Zhu, Experimental research on the microstructure and compressive and tensile properties of nano-SiO 2 concrete containing basalt fibers, Underground Space 2(3) (2017) 175-181.
[44] D. Zhu, S. Liu, Y. Yao, G. Li, Y. Du, C. Shi, Effects of short fiber and pre-tension on the tensile behavior of basalt textile reinforced concrete, Cement and Concrete Composites 96 (2019) 33-45.
[45] L. Gemi, E. Madenci, Y.O. Ozkilic, S. Yazman, A. Safonov, Effect of Fiber Wrapping on Bending Behavior of Reinforced Concrete Filled Pultruded GFRP Composite Hybrid Beams, Polymers (Basel) 14(18) (2022).
[46] Z. Mo, R. Wang, X. Gao, Hydration and mechanical properties of UHPC matrix containing limestone and different levels of metakaolin, Construction and Building Materials 256 (2020) 119454.
[47] W. Xu, T.Y. Lo, W. Wang, D. Ouyang, P. Wang, F. Xing, Pozzolanic Reactivity of Silica Fume and Ground Rice Husk Ash as Reactive Silica in a Cementitious System: A Comparative Study, Materials (Basel) 9(3) (2016).
[48] A. Rajasekar, K. Arunachalam, M. Kottaisamy, V. Saraswathy, Durability characteristics of Ultra High Strength Concrete with treated sugarcane bagasse ash, Construction and Building Materials 171 (2018) 350-356.

DOI: https://doi.org/XXXX.XXXX

Advanced Multidisciplinary Engineering Journal

Published and typeset in Scientific Innovation Research Group (SIRG) is a USA academic publisher, established as an LLC company in 2025 at 2222 W. GRAND RIVER AVE STE A, Okemos, INGHAM COUNTY, MI 48864 USA.
SIRG publishes online scholarly journals that are free of submission charges.

Scientific Innovation Research Group (SIRG) LLC,
Michigan, USA

Mailing Address: 2222 W. GRAND RIVER AVE STE A,
Okemos, INGHAM COUNTY, MI 48864 USA

e-mail: manager@pub.scientificirg.com

https://pub.scientificirg.com/index.php/index/en

SIRG
Scientific Innovation Research Group